The emerging role of the α4(+)/α4(-) interface as a determinant of functional signatures of α4β2 nicotinic acetylcholine receptors

Simone Mazzaferro

A thesis submitted in partial fulfilment of the requirement of Oxford Brookes University for the degree of Doctor of Philosophy

PhD Thesis
June 2013

3RD PARTY COPYRIGHT MATERIAL EXCLUDED FROM DIGITISED THESIS

PLEASE REFER TO THE ORIGINAL TEXT TO SEE THIS MATERIAL

Cju scuru da menzanotti non ndavi nenti.
Voju a lana da pecura mia.

[Calabrian dialect proverbs]

To my family and to all the people

that have been close to

me even in the difficult moments.

List of Publications

Mazzaferro S, Benallegue N, Carbone A, Gasparri F, Vijayan R, Biggin PC, Moroni M and Bermudez I (2011) Additional acetylcholine (ACh) binding site at alpha4/alpha4 interface of (alpha4beta2)$_2$alpha4 nicotinic receptor influences agonist sensitivity. *The Journal of Biological Chemistry*.

Mantione E, Micheloni S, Alcaino C, New K, **Mazzaferro S** and Bermudez Isabel (2012) Allosteric modulators of $\alpha4\beta2$ nicotinic acetylcholine receptors: A new direction for antidepressant drug discovery. *Future Medicinal Chemistry*.

Manuscripts accepted:

Benallegue N, **Mazzaferro S**, Alcaino C, and Bermudez I (2013). The additional acetylcholine binding site at the $\alpha4(+)/\alpha4(-)$ interface of the $(\alpha4\beta2)_2\alpha4$ nicotinic acetylcholine receptor contributes to desensitisation. *British Journal of Pharmacology*.

Manuscript in preparation:

Mazzaferro S, Gasparri F, New K, Alcaino C, Faundez-Parraguez M, Iturriaga-Vásquez P, Biggin PC and Bermudez I. The ligand selectivity of the agonist site at the $\alpha4(+)/\alpha4(-)$ interface of the $(\alpha4\beta2)_2\alpha4$ nAChR revealed by cysteine substitution accessibility method.

Oral presentations

Welcome Trust Nicotinic Receptor Research, Conference Centre at Hinxton, Cambridge (2011). The $\alpha4(+)/\alpha4(-)$ interface of the $(\alpha4\beta2)_2\alpha4$ nicotinic receptor contains an agonist binding site that contributes to receptor activation.

International School of Neuroscience, Catholic University of Buenos Aires (2012). Substituted-Cysteine accessibility method (SCAM) applied to concatamers.

Poster presentations

American Neuroscience Society (SFN) Annual Meeting. Washington, USA (2011). Additional acetylcholine (ACh) binding site at $\alpha4/\alpha4$ interface of $(\alpha4\beta2)_2\alpha4$ nicotinic receptor influences agonist sensitivity.'

Berlin Neuroscience Forum 2012. Berlin Germany (2012).

Federation of European Neuroscience Societies (FENS) Annual Meeting. Barcelona, Spain (2012). Pharmacological characterization of the Acetylcholine binding site at the $\alpha4/\alpha4$ interface of the $(\alpha4\beta2)_2\alpha4$ nicotinic acetylcholine receptors.

List of tables

List of figures

CHAPTER 1 _____ 1

Figure. 1.1. Cholinergic synapse. _____ 5

Figure 1.2. Ribbon diagrams of the tridimensional structure of the whole Torpedo nAChR at a 4Å resolution._____ 7

Figure. 1.3. Ribbon diagrams of the Torpedo α1-subunit. _____ 9

Figure. 1.4. nAChR subunit combinations _____ 11

Figure. 1.5. Central section of the whole (A) extracellular (B) and intracellular (C) vestibules of Torpedo nAChR. _____ 14

Figure. 1.6. The flipped state. _____ 16

Figure. 1.7. Multiple states of the muscle nAChR. _____ 17

Figure. 1.8. Top view of the AChBP. AChBP pentamers in presence of agonist (left) and antagonist (right)._____ 20

Figure. 1.9. ECD-TMD interfaces of nAChR at 4 Å resolutions and contact residues between Cys-Loop, β1-2 Loop and M2-3 Loop. _____ 21

Figure 1.10. α4β2 concatenated receptors._____ 45

CHAPTER 2 _____ 47

Figure. 2.1. Diagram showing β2_α4_β2_α4_α4 cRNA injection into Xenopus oocytes. _____ 54

Figure 2.2. Covalent MTS modification of substituted cysteine in an identified subunit interface. _____ 59

Figure 2.3. Protection assay experiment for the partial agonist Cyt at the α4(+)/α4(-) interface of the β2_α4_β2_α4^{T152C}_α4 mutant._____ 63

CHAPTER 3 _____ 65

Figure 3.1. ACh binding sites at the (α4β2)2α4 nAChR._____ 69

Figure 3.2. Position of the potentiating Zn^{2+} binding site in the concatenated (α4β2)2α4 nAChR. _____ 70

Figure 3.3. Agonist sensitivity of a chimeric β2_α4_β2_α4_β2/α4 nAChR. ____ 73

Figure. 3.4. Effect of α4W182A subunit on the ACh sensitivity of β2_α4_β2_α4_α4 nAChR._____ 76

Figure 3.5. Activation of β2_α4_β2_α4_α4 receptors containing two α4W182A mutant subunits._____ 78

Figure 3.6. Effects of the antagonist DhβE on mutant β2_α4_β2_α4_α4 nAChRs. _____ 81

List of abbreviations

5-HT$_3$	Serotonin
5-HT$_3$R	Serotonin receptor
A-85380	3-[(2S)-2-Azetidinylmethoxy pyridine dihydrochloride
ACh	Acetylcholine
AChBP	Acetylcholine binding protein
AD	Alzheimer's desease
ADNFLE	Autosomal dominant nocturnal frontal lobe epilepsy
ANOVA	Analysis of variance
ASA	Accessible surface area
C-terminus	Carboxy-terminus
cDNA	complementary deoxyribose nucleic acid
CI	Confidence interval
CNS	Central nervous system
CRC	Concentration response curve
cRNA	Complementary ribonucleic acid
Cyt	Cytisine
DA	Dopamine
dFBr	Desformylflustrabromine
dNTP	Deoxyribonucleotide triphosphate
DhβE	Dihydro-β-erythroidine
DMSO	Dimethylsulphoxide
DTT	Dithioerythritol
EC$_{50}$	Concentration producing half maximal effect
EC$_{50\_1}$	Concentration producing half-maximal high sensitivity stimulatory effect in a biphasic CRC
EC$_{50\_2}$	Concentrations producing half-maximal low sensitivity stimulatory effects in a biphasic CRC
ECD	Extracellular domain

ELIC	Prokaryotic pentameric ligand-gated ion channels from *Erwinia chrysanthemi*
Epi	Epibatidine
GABA	γ-aminobutyric acid
GLIC	Prokaryotic pentameric ligand-gated ion channels from *Gloeobacter violaceus*
GluCl	Glutamate-gated chloride channels
GlyR	Glycine receptor
HEK	Human Embryonic Kidney 293
HEPES	N-2-hydroxyethylpiperazine-N'-2-ethansulphonic acid
HS	High sensitivity
IC_{50}	Concentration producing half maximal inhibition
KAB-18	Biphenyl-2-carboxylic acid 1-(3-phenyl-propyl)-piperidin-3-ylmethyl ester
LS	Low sensitivity
MCL	Maximum compounds length
Mec	Mecamylamine
MMTS	Methyl methanesulfonothioate
MTS	Methenosulphatee reagents
MTSEA	Aminoethyl methanethiosulfonate
MTSET	[2-(Trimethylammonium)ethyl] methanethiosulfonate
N-terminus	Amino-terminus
NA	Noradrenaline
NAc	Nucleus accumbens
nAChR	Nicotinic acetylcholine receptors
nH	Hill coefficient
NAMs	Negative allosteric modulators
Nic	Nicotine
NMDA	n-methyl-D-aspartic acid
NS9283	3-[3-(3-pyridyl)-1,2,4-oxadiazol-5-yl]benzonitrile
PAMs	Positive allosteric modulators
PCR	Polymerase chain reaction

PFC	Prefrontal cortex
pLGIC	Pentameric ligand-gated ion channel
PNS	Peripheral nervous system
PNU-120596	(5-Chloro-2,4-dimethoxyphenyl)-N-(5-methyl-3-isoxazolyl)-urea)
REFER	Rate-equilibrium free energy relationships
Saz-A	Sazetidine-A
SCAM	Substituted Cysteine Accessibility Method
SEM	Standard error of the mean
TC-2559	4-(5-ethoxy-3-pyridinyl)-N-methyl-($3E$)-3-buten-1-amine difumarate
TMD	Transmembrane domain
TPP	Tegmental pedunculopontine nucleus
UCI-30002	[N-(1,2,3,4-tetrahydro- 1-naphthyl)-4-nitroaniline]
Var	Varenicline
VTA	Ventral tegmental area

Abstract

The α4β2 nicotinic acetylcholine receptor (nAChR) assembles in two alternate forms, (α4β2)$_2$α4 and (α4β2)$_2$β2, which display stoichiometry-specific agonist sensitivity. Being heteromeric pentameric ligand-gated ion channels (pLGIC), α4β2 receptors are activated by binding of agonist to sites located at the α4(+)/β2(-) interfaces. These interfaces are present in both stoichiometries they are unlikely to contain structural differences conferring specific properties to (α4β2)$_2$α4 and (α4β2)$_2$β2 receptors. In contrast, the auxiliary subunit can be either α4 or β2, leading to stoichiometry-specific β2(+)/β2(-) and α4(+)/α4(-) interfaces. Using fully concatenated (α4β2)$_2$α4 nAChRs in conjunction with structural modelling, chimeric receptors and functional mutagenesis, this study identified an additional agonist site at the α4(+)/α4(-) interface that accounts for the stoichiometry-specific agonist sensitivity of the (α4β2)$_2$α4 receptor. The additional agonist site occupies a region that also contains a potentiating Zn^{2+} binding site. However, unlike Zn^{2+}, the agonist binding influences agonist responses by directly contributing to channel gating. By engineering a receptor with a C226S mutation to provide a free cysteine in loop C in the + side of the α4(+)/α4(-) interface, this study found that the acetylcholine (ACh) responses of the additional agonist site are modified following modification of the substituted cysteine with sulfhydryl reagents. These findings suggested that agonist occupation of the site at the α4(+)/α4(-) interface leads to channel gating through a coupling mechanism involving a conformational switch in loop C. The sulfhydryl reagents had similar effects on substituted cysteines in the α4(+)/β2(-) interfaces. Further studies showed that the additional agonist site is less sensitive to desensitisation than the sites at the α4(+)/β2(-) interfaces, suggesting that the agonist sites are functionally non-equivalent. Non-functional equivalency was also indicated by the finding that the agonist selectivity of the site at the α4(+)/α4(-) differs from that of the sites at the α4(+)/β2(-) interface. The findings may have important consequences for drug discovery programs and the manner by which α4β2 receptor signalling in the brain can be modified in brain pathologies.

CHAPTER 1

Introduction

Introduction

The spectacular progress in the field of molecular biology in the last 30 years has made it possible to identify and clone the genes coding for pentameric Ligand-gated ion channels (pLGIC). Subsequent expression of pLGIC cDNAs (complementary deoxyribose nucleic acids) in artificial expression systems has permitted the characterization of the functional properties of these ion channels without the ambiguities often encountered in native cells. Heterologous expression of pLGIC has also facilitated assays of the functional consequences of single point mutations positioned in various regions of these proteins, giving invaluable insights into the architecture and function of the agonist binding site, allosteric sites and the ion pore. More recently, the availability of structural data at the atomic level has given insights of how these proteins exert their functions at the molecular level. However, as the functional properties of these proteins and the mechanisms underlying them are elucidated, more questions arise regarding how the different structural and functional components of these proteins such as non-agonist binding subunit interfaces or allosteric sites contribute to generate global signals. This thesis explores the role of the auxiliary subunit in an ACh-gated pLGIC, the $(\alpha4\beta2)_2\alpha4$ nicotinic acetylcholine receptor (nAChR).

1.1 Nicotinic Acetylcholine Receptors

nAChRs are integral membrane ion channels gated by the neurotransmitter ACh. They transmit neuronal signals in the central (CNS) and peripheral (PNS) systems, where they broadly contribute to regulate an assortment of physiological functions and pathophysiological processes associated with cognition, mood, reward, skeletal muscle function, motor control, arousal, analgesia and inflammation (Corringer et al., 2000; Gotti et al., 2009; Taly et al., 2009; Hurst et al., 2013 for comprehensive reviews). The nAChRs belong to the broader gene superfamily of Cys-loop pLGIC's, which also includes ion channels gated by glycine (GlyR), γ-aminobutyric acid ($GABA_A$ and $GABA_C$), serotonin (5-HT_3) and in invertebrates glutamate receptors (Lester et al., 2004).

Like all cell-surface pLGIC's, nAChRs regulate the flow of ions across the plasma membrane. In the case of nAChRs, the net influx of cations that occurs upon receptor gating depolarises the plasma membrane and increases cell excitability. Calcium entry through nAChRs such as the homomeric $\alpha7$ nAChRs leads to additional effects on multiple intracellular signaling cascades (Dajas-Bailador & Wonnacott, 2004). Like all other chemical synapses the nicotinergic synapse consists of a pre-synaptic terminal, a post-synaptic terminal and a synaptic gap, in between the terminals **(Fig. 1.1)**. The presynaptic terminal contains the synaptic vesicles, which store ACh. The transmitter is synthesized in the presynaptic terminal from acetyl Coenzyme A and choline in a reaction catalyzed by the enzyme choline acetyltransferase. The newly synthesized ACh is then transported into the vesicles by vesicular ACh transporters. When the pre-synaptic terminal is depolarized by the arrival of action potentials synaptic vesicles fuse with the pre-synaptic membrane facing the synaptic gap and the post-synaptic membrane causing ACh release. This produces a sharp rise in ACh concentration at the post-synaptic membrane such that many post-synaptic nAChRs become occupied with ACh and then open within a few milliseconds to produce synaptic signals. Like all fast ligand-gated ion channels, nAChRs have low affinity for agonists, which allows for fast dissociation from the binding site and thus a rapid termination of the post-synaptic signals. The transient nature of the ACh-postsynaptic signals is further achieved by removal of ACh from the synaptic gap by diffusion and, more critically, by hydrolysis into choline and acetate in a reaction catalyzed by acetylcholinesterase. Choline is transported into the presynaptic terminal by a Na^+/choline transporter and once in the presynaptic terminal it is used for the synthesis of ACh. Fast synaptic nicotinergic transmission occurs at excitatory autonomic ganglia and at the neuromuscular junction.

In the CNS, however, nAChRs are predominantly located in pre-, peri- or extra-synaptic regions, from where they modulate the release of other neurotransmitters such as dopamine, GABA, glutamate, noradrenalin and $5-HT_3$, which makes nAChR-signalling one of the most important modulatory systems in the CNS (see reviews by Wonnacott, 1997; Gotti et al., 2009). Some nAChR-mediated synaptic signalling has been reported in the brain (Dani, 2001;

Mansvelder & McGehee, 2002) but an overwhelming degree of nicotinergic transmission in the CNS is extra-synaptic. In this type of transmission, nAChRs are exposed to lower concentrations of ACh and for longer periods than at synaptic transmission, mainly because the receptors are at a greater distance from the source of ACh release than their synaptic counterparts. In addition, because non-synaptic regions display lower levels of acetylcholinesterase activity, removal of ACh from non-synaptic regions is probably less efficient than at synapses.
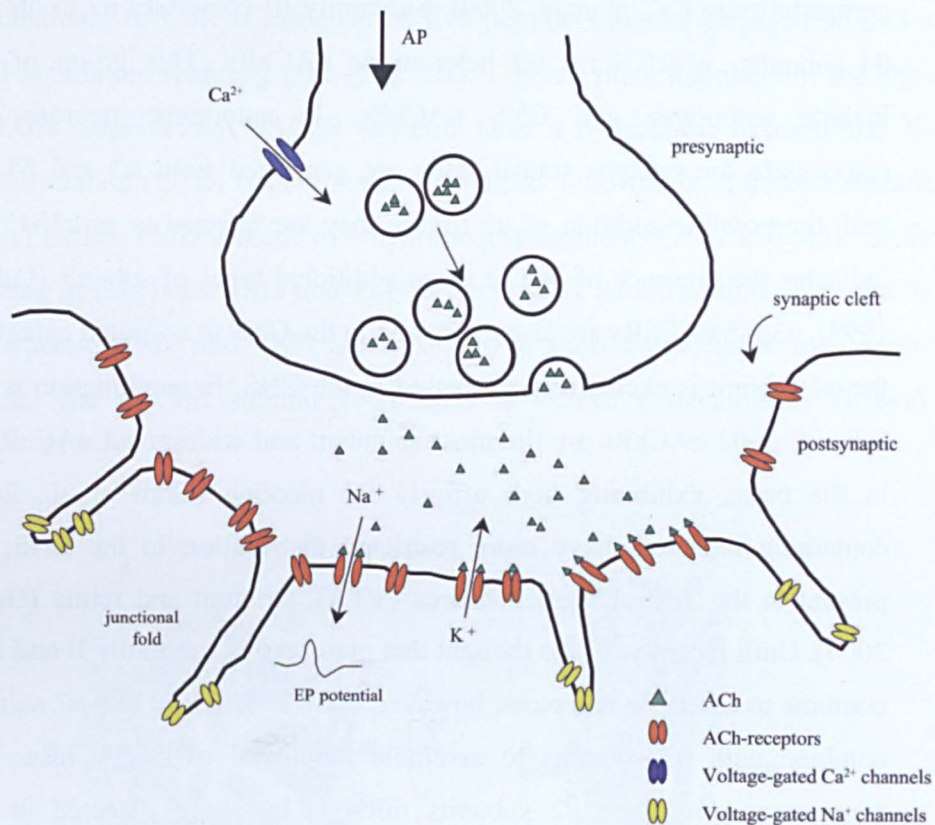
Figure. 1.1. Cholinergic synapse. Diagram of the cholinergic synapse depicting vesicle fusion, ACh hydrolysis, choline uptake and ACh metabolism.

1.2 Classification of nAChR subunits

So far, 16 genes coding for nAChR subunits have been identified and cloned from vertebrates (Albuquerque et al., 2009). The subunits have been grouped into two different classes, the α subunits (α1-α10) and non-α subunits (β1-β4 γ, δ and ε). On the basis of their distribution in the body, gene structure and protein sequence, α and non-α nAChR subunits have been classified into four subfamilies (I-IV) (Corringer et al., 2000; Novère et al., 2002). The subunits of the subfamilies I and II are considered ancestral, whereas subfamily IV evolved later than the other subfamilies. Subfamily I contains the α9 and α10 subunits, subunits mostly found in epithelial tissues. Subfamily II contains the neuronal subunits α7, α8, both of which form homomeric nAChRs. So far, subunit α8 has only been found in avian neurons (Lukas et al., 1999). Homomeric α7 nAChRs

are prevalent in the mammalian CNS and are distinguished by their high relative permeability to Ca^{2+} (Fucile, 2004). Subfamily III comprises α2 to α6 and β2 to β4 subunits, which form αβ heteromeric nAChRs. This group of receptors include autonomic and CNS nAChRs. In autonomic neurons, nAChRs responsible for synaptic transmission are generated from α3 and β4 subunits, with the possible addition of α5 (hence they are referred to as α3β4*, where * indicates the presence of one or more additional types of subunit (Lukas et al., 1999). α3β4* nAChRs are also expressed in the CNS to a limited extent, whereas the α4 subunit is exclusively expressed in the CNS. In combination with the β2 subunit, α4β2 nAChRs are the most abundant and widespread nAChR subtypes in the brain, exhibiting high affinity for nicotine (Gotti et al., 2009). α6-containing receptors have more restricted distribution in the CNS; they are present in the ventral tegmental area (VTA), striatum and retina (Gotti et al., 2009). Until recently, it was thought that members of subfamily II and III did not combine to assemble receptors, however, there is evidence that α7 subunits may combine with β2 subunits to assemble functional α7β2 nAChRs. Thus, co-expression of α7 and β2 subunits mRNAs has been detected in rat brain cholinergic neurons (Azam et al., 2003) and heterologous co-expression of these two subunits in oocytes or brain slices yields receptors that display slower desensitisation than that of α7 homomers (Khiroug et al., 2002; Murray et al., 2012). Although subunit α9 can form homomeric receptors, it specifically assembles with subunit α10 to form α9α10 nAChRs (Sgard et al., 2002). These receptors display a unique pharmacology, somewhere between that of nicotinic and muscarinic receptors (Verbitsky et al., 2000). They are found in the organ of Corti in the inner ear (Elgoyhen et al., 2001) but also in the pain perception pathway, specifically in dorsal root ganglion neurons (Lips et al., 2002) and in epithelial tissue (Kummer et al., 2008). Subfamily IV comprises α1, β1, δ, γ and ε subunits, which interact only between themselves to assemble the muscle α1γα1δβ1 (fetal muscle) or in the α1εα1δβ1 (adult skeletal muscle) nAChRs (Corringer et al., 2000).

1.3 The Structure of nAChRs

The functional nAChR is made up of five peptide subunits arranged around a central membrane-spanning pore **(Fig. 1.2)**. Like all other members of the Cys-loop LGIC superfamily, nAChR subunits have a hydrophilic extracellular N-terminal domain (ECD) largely made of β-sheets followed by a transmembrane domain (TMD). TMD is made of 4 hydrophobic segments (TM1 to TM4) mostly consisting of α-helices. TM3 and TM4 are linked by an intracellular hydrophilic loop, whereas TM2 and TM3 are linked by a short extracellular hydrophilic segment. The nAChR subunit C-terminus is located extracellularly (Unwin, 2005).
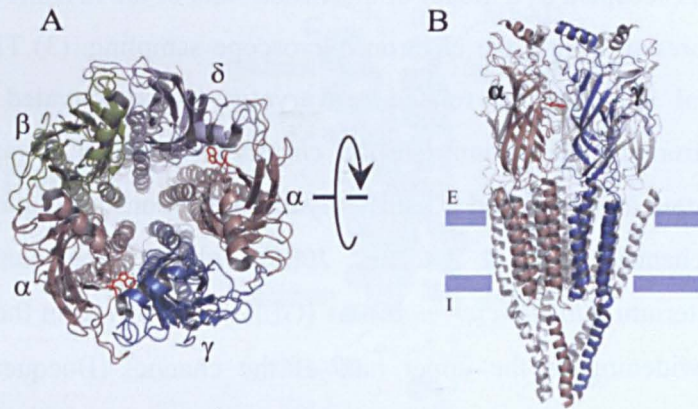
Figure 1.2.   Ribbon diagrams of the tridimensional structure of the whole Torpedo nAChR at a 4Å resolution. (A) Anti-clockwise organization viewed from the extracellular side. **(B)** Parallel side view with the membrane plane. (Subunits: α brown; β, green; γ, blue δ light blue; in red the locations of Trp149; E and I, show the extracellular an intracellular side respectively). (Adapted from Unwin, 2005).

In the last twelve years, breakthrough structural studies have led to a better understanding of the structure of Cys-loop LGIC and the events that trigger receptor gating following agonist binding in Cys-loop LGIC and nAChRs in particular. These breakthroughs are as follows. (1) Resolution of the X-ray crystal structures of ACh binding protein (AChBP) from various fresh water snails, which is a homolog of the nAChR extracellular domain, illuminated how an agonist binds to the receptor, and crucially that a peripheral loop, called loop C, closes when agonist occupies the binding site (Brejc et al., 2001; Hansen et al., 2005; Celie et al., 2004). (2) The 4 Å resolution structure of the nAChR has provided a picture of the agonist binding site, the pore and intracellular region of the nAChR in near-physiological conditions (Unwin, 2005). Currently, this structure is accepted as a model of the closed state of the nAChR because agonist was not present during the electron microscope sampling. (3) The resolution of the crystal structures of related prokaryotic proton-activated channels. The channel from the bacterium *Erwinia chrysanthemi* (ELIC) was solved in the inactive state and exhibited a narrow hydrophobic constriction at the upper half of the channel (Hilf & Dutzler, 2008), whereas the channel from the cyanobacterium *Gloeobacter violaceus* (GLIC) was solved in the open state and showed widening in the upper half of the channel (Bocquet et al., 2009). Together, these experimental data have led to the views on the structure and function of Cys-loop LGIC and nAChRs in particular that are discussed in the next sections.

1.3.1 The ECD

ECD of nAChRs contains the structural elements that form the ACh binding site **(Fig. 1.3)**. The ECD contains a hydrophobic β-sandwich core of 8 (GLIC) or 10 (AChBPs, *Torpedo* nAChR, ELIC) anti-parallel β strands that define the inner and the outer sheets of this region. This region also contains loops linking the various β-sheets that are critical for receptor activation (Celie et al., 2004; Hansen et al., 2005; Unwin, 2005; Dellisanti et al., 2007; Bocquet et al., 2009; Hilf & Dutzler, 2009). In α subunits these loops are loops A, B, C, Cys-loop and the β1–β2 loop, whereas in non-α subunits, i.e., β, γ, δ, ε subunits, the loops are D, E, F. The ECD has a short α-helix, also conserved in the AChBPs that

contains glycosylation sites and antigenic regions (Dellisanti et al., 2007; Unwin, 2005; Hansen et al., 2005; Celie et al., 2004).
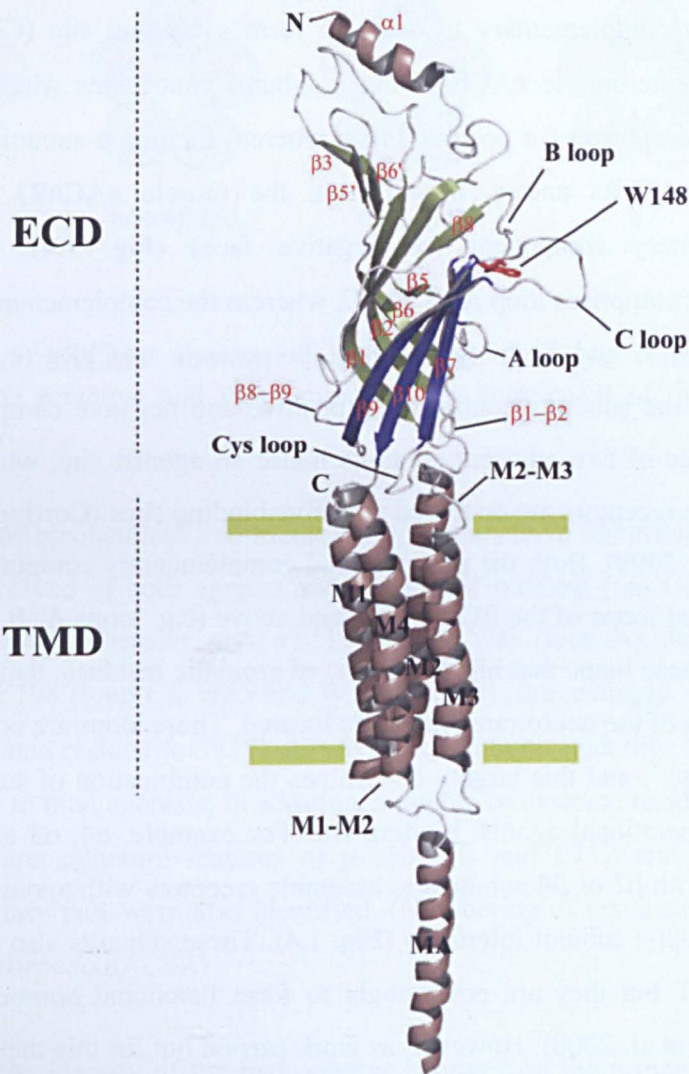
Figure. 1.3.   Ribbon diagrams of the Torpedo α1-subunit. Regions with α-helices are shown in brown; the β-strands composing the β-sandwich are in blue (inner) and green (outer). (Adapted from Unwin, 2005).

1.3.2 The ACh Binding Site

The ACh binding site is a hydrophobic pocket that lies at the interface between the ECD of two adjacent subunits (Corringer et al., 2000). The two ECD must be structurally complementary in order to form a binding site (Corringer et al., 2000). In heteromeric nAChRs, the α-subunit contributes what is termed the principal component (or positive face), whereas the non α-subunit ($\beta2$ and $\beta4$ in neuronal nAChRs and γ, ϵ and δ in the muscle nAChR) contribute the complementary component (or negative face) **(Fig. 1.4)**. The principal component comprises loop A, B and C, whereas the complementary face consists of loops D, E and F. In the case of homomeric nAChRs (e.g., $\alpha7$ and $\alpha9$ receptors), the subunits contain both positive and negative components so that the interface of two adjacent subunits house an agonist site, which means that homomeric receptors are endowed with five binding sites (Corringer et al., 2000; Taly et al., 2009). Both the principal and complementary components lie within the so called loops of the ECD mentioned above (e.g. loops A, B, C, D, E, F). It is within these loops that highly conserved aromatic residues, that are critical for the binding of the neurotransmitter, are located. These loops are not conserved by all subunits, `, and this largely determines the combination of subunits that can form an operational agonist binding site. For example, $\alpha4$, $\alpha3$ and $\alpha6$ subunits combine with $\beta2$ or $\beta4$ subunits to assemble receptors with agonist binding sites at the $\alpha(+)/\beta(-)$ subunit interfaces **(Fig. 1.4)**. These subunits also conserve loops D, E and F but they are not thought to form functional homomeric receptors (Corringer et al. 2000). However, as work carried out for this thesis (Mazzaferro et al., 2011; **Chapters 3** to **4**) and by other researchers (Harpsøe et al., 2011) shows, the interface between this type of subunit can house an operational agonist site.

Heteropentameric receptors   Homopentameric receptors

α4β2   α6α4β2β3   α6β2β3   α7   α9
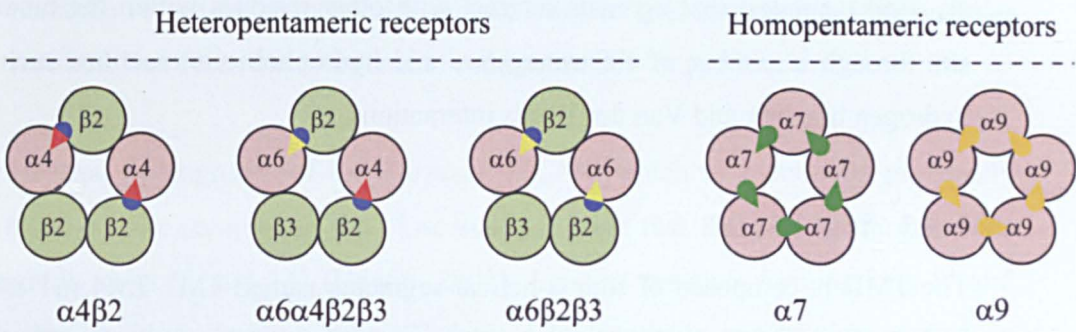
Figure. 1.4.   nAChR subunit combinations Triangles and semi-circles represent the principal and the complementary component of the binding site respectively.

A number of biochemical and mutagenesis studies have identified key residues that are involved in both agonist and antagonist binding (see Corringer et al., 2000 for a comprehensive review). These are: Y93 (loop A), W149 (loop B), Y190 and Y198 (loop C), W55 and W57 (loop D). Interestingly, substitution of an aspartic acid residue for Y198 in nAChR α1 subunit underlies the inability of this subunit to bind agonists. In addition, a couple of cysteine residues, C192 and C193 that are signature features of α subunits and L112 and M114 on the complementary face were also identified. (Numbering of residues correspond to that of the *Torpedo* nAChR) .

Generally, the identity of the hydrophobic residues on the principal component defines ligand affinity, whereas the residues contributed by the complementary face appear to determine ligand selectivity. Typically, nicotinic agonists carry a positively charged nitrogen moiety that is stabilized by electronegative interactions with the conserved aromatic residues of the ligand binding site (Srinivasan et al., 2012). Thus, the positive charged nitrogen moiety of ACh and nicotine (Nic) are stabilised by π-cation interactions with the electron rich aromatic side chains of the conserved amino acids, specifically W149 (Xiu et al., 2009). In addition, analysis of AChBP (Hansen et al., 2005) or α7-AChBP chimera (Li et al., 2011) crystal structures in complex with agonists and studies of the interaction of agonists with nAChRs by nuclear magnetic resonance

(NMR) (Williamson et al., 2007) or unnatural amino acid mutagenesis (Zhong et al., 1998), suggest that agonists interact with other residues within the binding site through a number of electronegative and hydrophobic interactions such as hydrogen bonding and Van der Waals interactions.

1.3.3 The TMD

The TMD is composed of four α-helical segments named TM1-TM4 (α1-α4 in ELIC). These hydrophobic regions are organized as a four-helix bundle **(see Figs. 1.2 and 1.3)**. The first region, TM1, links the outer sheet of the ECD to the TMD. The other segments follow TM1 and cross the plasma membrane in opposite directions ending with TM4. TM1, TM2 and TM3 are linked by the important loops M1–M2 and M2–M3. Interactions between loop M2–M3 and segment β1–β2 and the Cys-loop of the ECD play a key role in the transduction of agonist binding into gating of the ion channel; this region is critically important for coupling agonist binding with ion pore gating (Unwin, 2005; Hilf & Dutzler, 2008; Bocquet et al., 2009).

1.3.4 The ion Channel

In *Torpedo* nAChR the four segments that make the TMD of each subunit are packed around a hydrophilic central pore that is lined by residues of TM2 of each subunit. TM2 is surrounded by TM1, TM3 and TM4, with TM4 being farthest from the pore. TM4 of all the TMs is the one that has the highest interaction with the lipid bi-layer. TM1 and TM3 make several contacts with TM2 and these appear to be essential for the stabilization of TM2 (Miyazawa et al., 2003). Electron micrographs of the *Torpedo* nAChR have shown that TM2 has different dimensions across the membrane (Miyazawa et al., 2003). The upper part of TM2, which faces the extracellular compartment, is wider than the rest of the pore, whilst the narrowest part of M2 is found towards the middle of the region. The pore is lined by conserved residues that form concentric rings; these residues determine the ion selectivity of the pore and influence other functional properties such as conductance and receptor desensitisation (Yakel, 2010). By convention, the concentric rings are numbered from the cytoplasmic end of the pore, where a first positively-charged ring is defined as 0', whilst the last ring, at the

extracellular end of M2 represents ring 20'. Above this region there is an outer vestibule facing the extracellular milieu, whereas below there is an intracellular vestibule that faces the cytoplasmic compartment.

Electron micrographs of the *Torpedo* nAChR, which as mentioned previously represent the receptor in the close state, suggest that the gate of the pore lies within rings 9' and 14' (Unwin, 2005). Leucine residues forming ring 9' and valine residues forming ring 13' form a hydrophobic constriction of 6 Å in diameter that is small enough to block the hydrated Na^+ and K^+ ion fluxes (about 8 Å in diameter) (White & Cohen, 1992; Miyazawa et al., 2003; Arevalo et al., 2005; Unwin, 2005; reviewed by Miller & Smart, 2010). Comparisons of the pore region of T*orpedo* nAChR and ELIC reveal interesting differences. Unlike the pore in the *Torpedo* nAChR, the extracellular entrance in ELIC is occluded by bulky hydrophobic side chains. This occlusion is what has led to the view that ELIC was crystalized in a closed conformation. The hydrophobic occlusion could represent a physical gate that stops diffusion of ions in the closed conformation of ELIC (Hilf & Dutzler, 2008).

1.3.5 The Extracellular and Intracellular Vestibules of TM2

The vestibules of TM2 seem to play an important role in the ion selectivity and conductance of pLGIC. For instance, altering the charge of this region by single point mutations changes ion conductance in *Torpedo* nAChR (Imoto et al., 1988) or the ionic selectivity of the channel (Galzi et al., 1992). Both vestibules contain negatively charged residues (aspartate and glutamate) and it may be that this creates a negative electrostatic environment required for efficient cation-selective transport by pLGIC (**Fig. 1.5**) (Unwin, 2005; Hilf & Dutzler, 2008). Consistently with this view, in anion-selective LGIC such as $GABA_A$ receptors, GlyR or glutamate-gated chloride channels (GluCl) receptors these regions are electropositive, which provide an attractive environment for negatively charged Cl^- ions (Hibbs & Gouaux, 2011).
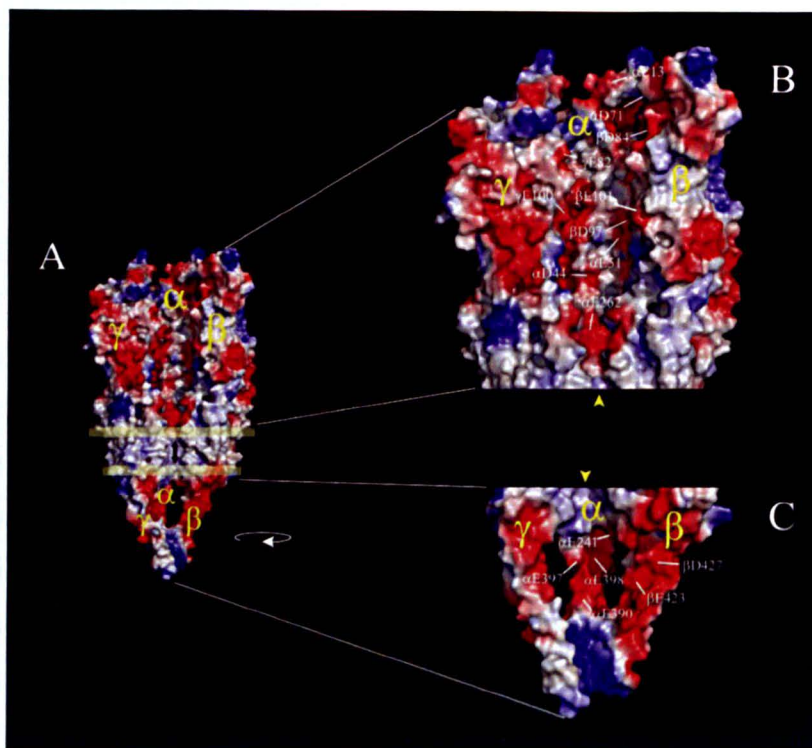
Figure 1.5. **Central section of the whole (A) extracellular (B) and intracellular (C) vestibules of Torpedo nAChR.** Aspartate and glutamate residues are present in the vestibules of the ion pore as shown. Colour differences show the variation in the electrostatic potential surface. (Adapted from Unwin, 2005).

1.4 nAChR Activation

Structural insights obtained from the superposition of crystal structures of AChBP with agonists or antagonists (Hansen et al., 2005; Dutertre & Lewis, 2006; Ulens et al., 2006) in conjunction with single channel studies of the activation of wild type and mutant pLGIC, particularly the muscle nAChR, have provided an overall view of the sequence of structural and energy changes triggered by agonist binding that lead to gating. These views are discussed next.

1.4.1 Functional States of the nAChR

In addition to the closed (resting), bound-active and bound-inactive (desensitised) states, a recent study with comparisons of the effects of partial and full agonists on channel gating has proposed a new functional state for the GlyR and muscle nAChR (Lape et al., 2008). This new state has been termed the flip state. The new state (a closed state) immediately precedes channel opening and displays a higher affinity for agonist than the closed receptors **(Fig.1.6)**. Interestingly, the ability to reach fully the flipped state determines the efficacy of the agonist.

A

Resting
(shut)

Flipped
(shut)

Open

B

$$R \underset{k_{-1}}{\overset{2k_{+1}}{\rightleftharpoons}} RA \underset{2k_{-2}}{\overset{k_{+2}}{\rightleftharpoons}} A_2R$$

$$\delta_1 \Big\Uparrow \gamma_1 \qquad \delta_2 \Big\Uparrow \gamma_2$$

$$AF \underset{2k_{F-2}}{\overset{k_{F+2}}{\rightleftharpoons}} A_2F$$

$$\beta_1 \Big\Uparrow \alpha_1 \qquad \beta_2 \Big\Uparrow \alpha_2$$

$$AR^* \qquad A_2R^*$$
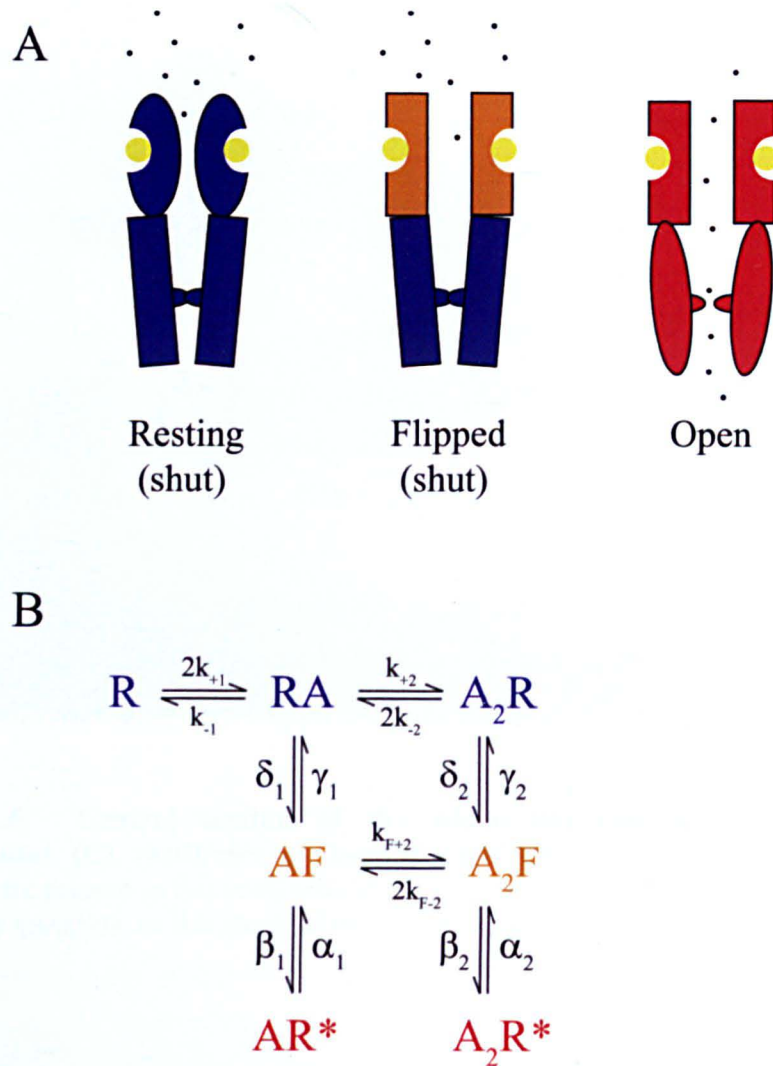
Figure. 1.6.   The flipped state. (A) The receptor at the resting state binds the agonist, then changes conformation to reach a flipped state. The flipped state has high affinity for the agonist but the channel is still closed. Next the flipped receptor transits to the open conformation. **(B)** The flip mechanism in muscle nAChR activated by tetramethylammonium (TMA). The agonist is represented by A while, R and R* are the receptor at the rest and activated states respectively. F represents the flipped conformation. (Adapted from Lape et al., 2008).

More recently, Sine and his team identified another two intermediate close states in muscle nAChRs that precede the transition to the open state (Mukhtasimova et al., 2009). These close states have been termed primed states and are comparable to the flipped state. The first priming leads the receptors to brief openings, whereas the second priming elicits long-lived openings of the receptor **(Fig. 1.7)**. By covalently locking the loop C in the closed conformation, which mimics the conformation of the bound binding site, has been found that priming of only one site elicits brief openings, whereas the priming of two sites triggers long openings (Mukhtasimova et al., 2009).
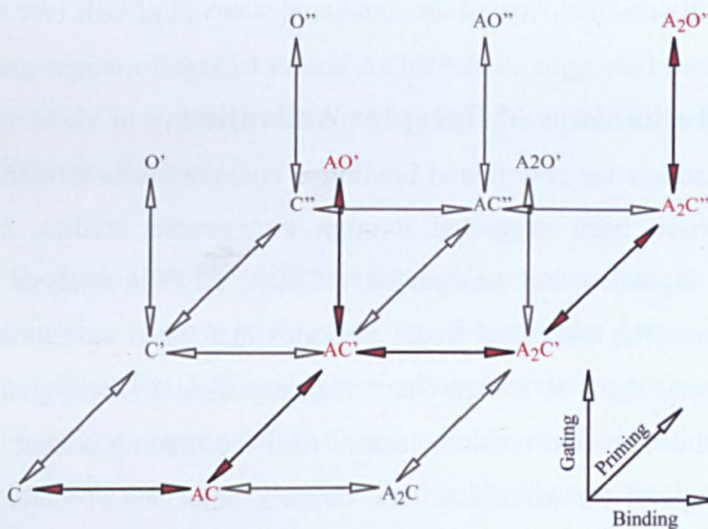
Figure. 1.7.   Multiple states of the muscle nAChR. Agonist binding, priming and channel gating steps are showed. C, C' and C'' are closed states, whereas O' and O'' represent open states. For the wild type nAChR in the absence of ACh, the C' and C'' states are negligible, suggesting that the first step in the activation process generates AC, from which there are three possible paths towards A2C''. Only the red pathway has been fitted to agonist-dependent dwell times, obtaining the rate constants. (Adapted from Mukhtasimova et al., 2009).

1.4.2 Energy Transitions in Gating

Measurements of the rate-equilibrium free energy relationships (REFER) in conjunction with single point mutations in the agonist binding and ion channel regions (Zhou et al., 2005) have given insights into how muscle nAChRs transit from the closed to the open, conducting state. Such studies have suggested that

agonist binding triggers blocks of coordinated motions starting with the β4-β5 linker, the β7-β8 linker, loop C, through the Cys-loop and the β1-β2 linker, to TM2 and gating of the ion channel (Grosman et al., 2000; Chakrapani et al., 2004; Purohit & Auerbach, 2008). This conformational wave propagates throughout the nAChR via Brownian motion in 1 μs (Grosman et al., 2000; Chakrapani & Auerbach, 2005). An interesting issue raised by these studies is that the receptor conformational transitions leading to gating are more complex and numerous than previously speculated from the classical view of receptor isomerisation (i.e., closed and open conformations corresponding to closed, open-bound receptor states). Such conformational complexity is in accord with the currently updated view of the functional states of pLGIC (see section 1.4.1).

1.4.3 Mechanisms of Receptor Activation

Current models for how ligand binding is converted into motion to activate the nAChR have been suggested through mutagenesis studies, comparisons of available liganded and unliganded AChBP, REFER analysis and computer stimulation. The emerging model indicates that when an agonist occupies the binding site, there is a significant rearrangement of hydrogen bonds among conserved amino acid residues located near the binding pocket, including E45, polar groups of the main chain and trapped molecules of water (Unwin, 2005; Lee & Sine, 2005; Price et al., 2007; Absalom et al., 2003; Xiu et al., 2005). The side chains of conserved amino acid residues from the primary and complementary subunits appear to converge towards the ligand, which interact via Van der Waals interactions. Loop C moves about 11 Å towards the receptor core, allowing the bridged cysteines in loop C (Cys190-Cys198) to interact with the ligand and loop F of the complementary subunit. This movement, termed loop C capping, perturbs an arginine residue (R209) located at the base of strands β9 and β10 and its salt bridge with loop 2 residue E45 (Lee & Sine, 2005). Studies using REFER analysis have suggested that the cascade of conformational transitions starts when α1W148 and the α1Y120 change position, providing binding energy to the ligand. This energy is then propagated along the interfaces, down to the coupling region and then to the M2 (Auerbach, 2010).

Capping of the binding site by loop C appears to trap the agonist within the binding site (Celie et al., 2004; Hansen et al., 2005; Billen et al., 2012; Rucktooa et al., 2012). Capping of the agonist site by loop C appears to be a universal event among pLGICs. For example, loop C appears contracted in crystals of the invertebrate GluCl receptor-glutamate complex (Hibbs & Gouaux, 2011) and $\beta9$-$\beta10$ loop in crystals of the proton activated GLIC appears in a capping conformation (Bocquet et al., 2009). In contrast uncapped loop C, which orientates away from the binding site, is typically observed in the presence of antagonists or in the absence of agonists (Celie et al., 2004; Hansen et al., 2005). In addition, comparisons of the binding site region of the *Torpedo* nAChR α subunit at 4Å resolution in its agonist-unbound conformations with the corresponding region of agonist bound AChBP have suggested that loop B also moves, most likely in synergy with the capping movement of loop C, towards bound ACh (Unwin, 2005).

When loop C capping occurs sufficient force is generated through the receptor via changes in the relative position of the β-barrel-like loops, to twist the extracellular surface **(Fig. 1.8)**, and in turn, alters the relative position of residues near the extracellular segment of TM2 and relocate residues critical to channel gating (Unwin, 2005). A key region involved in the changes in the extracellular segment of TM2 is the coupling region, which comprises the Cys-Loop, $\beta1$-2 loop and the M2-3loop (Kash et al., 2003; Bouzat et al., 2004; Xiu et al., 2005; Lee & Sine, 2005) **(Fig. 1.9)**. Studies of a chimera made of the AChBP and the TMD of the 5-HT$_3$ receptor (5-HT$_3$R) have suggested key conformational events that occur in the coupling region, in particular side-chain interactions have been observed between the $\beta1$- $\beta2$ loop and the Cys-loop of the ECD with the M2-M3 loop of the TMD (Unwin 2005; Lee & Sine 2005; Purohit & Auerbach 2008).
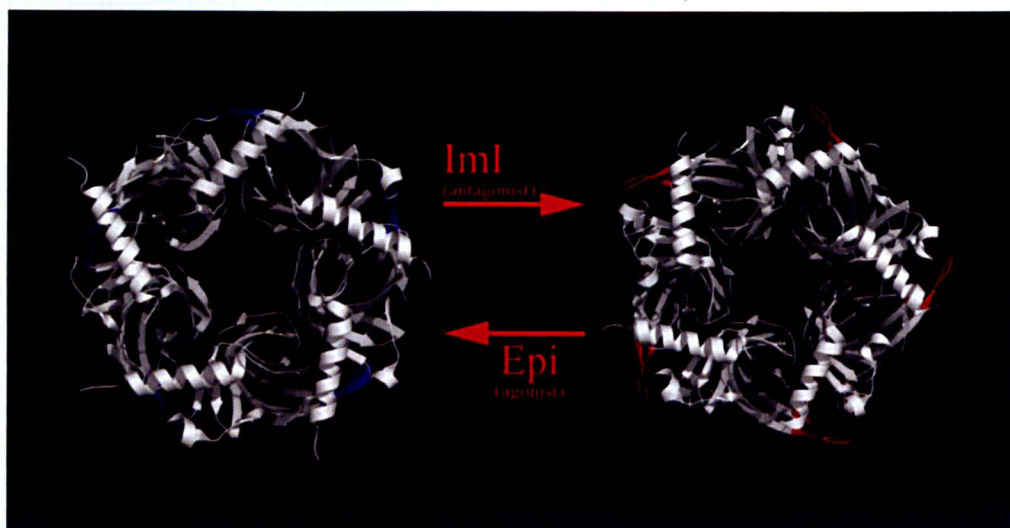
Figure. 1.8. Top view of the AChBP. AChBP pentamers in presence of agonist (left) and antagonist (right). Note the distinctive conformations for the antagonist (α-conotoxin ImI) and agonist (Epibatidine) complexes. The C-loop remains open in presence of antagonist (in red) and close with agonist (in blue). (Adapted from Hansen at al., 2005).

The interactions between residues at the ECD-TMD are mainly hydrophobic and electrostatic (Unwin, 2005; Lee & Sine, 2005; Price et al., 2007; Absalom et al., 2003; Xiu et al., 2005). The hydrophobic residues are highly conserved in the Cys-Loop family, whereas the charged residues can be in different positions. Rather than specific contact points it seems that the overall electrostatic environment is important in the interaction between ECD and TMD. In support of this view, findings from studies of the GABA$_A$ receptor have suggested that charged residues form salt bridges between them and that inverting their positions appears to have no impact on receptor function (Kash et al., 2003). Furthermore in 5-HT$_3$ receptors a trans to cis side-chain isomerisation of a proline (P303) in the M2-M3 loop appears to be critically involved in channel opening (Lummis et al., 2005). Interestingly, more recent mutagenesis studies of 5-HT$_3$A receptors have suggested that cis-trans isomerization of P303 is not involved in gating (Paulsen et al., 2009). Studies of the murine muscle nAChR using REFER approaches demonstrated that the M2 of α-subunits move before the non-α subunits, suggesting that the conformation change on M2 of alpha

subunits, act as a hub that allows gating isomerization (Purohit & Auerbach 2007).
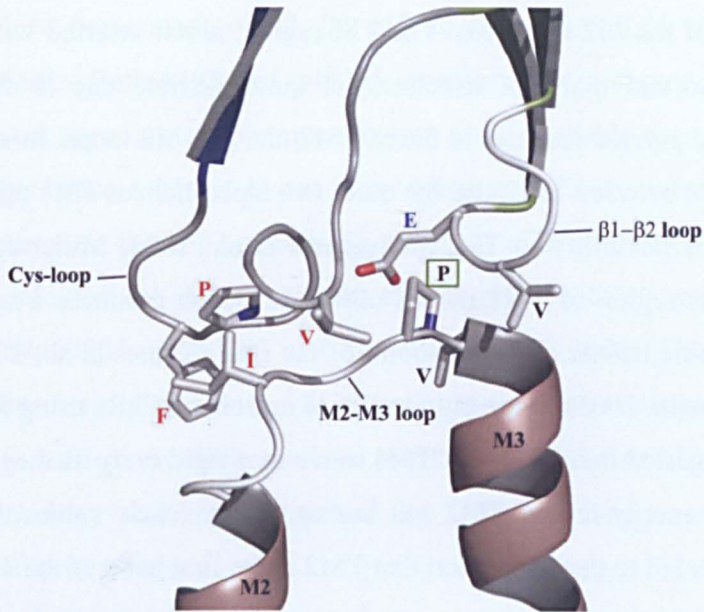
Figure. 1.9. ECD-TMD interfaces of nAChR at 4 Å resolutions and contact residues between Cys-Loop, β1-2 Loop and M2-3 Loop. Non-conserved hydrophobic residues are black and bold, conserved hydrophobic residues are red. The green box shows the proline 303 supposed to be implicated in the cis–trans isomerization during the activation of 5-HT₃A receptors (Adapted from Miller & Smart, 2010).

1.4.4 Opening of the channel gate

The consensus view on how the ion channel pore opens up is that the transduction process triggered following agonist binding leads to a sideways rotation of the M2 α-helices. The TM region, albeit inserted within the plasma membrane and made of α-helices, is quite flexible due to the presence of conserved glycine residues in the M1-M2 and M2-M3 loops. In addition, limited interaction between TM2 and the other two alpha-helices TM1 and TM4, confers movement flexibility to TM2 (Miyazawa et al., 2003; Miller & Smart, 2010). The upper region of TM2 moves outwards, which produces a separation of the hydrophobic barrier at the midpoint of the gate (Cymes et al., 2005; Paas et al., 2005; Unwin, 2005). Recently, studies of muscle nAChRs using REFER analysis have suggested that TM3 and TM4 move as a rigid body as they appear to have identical energy levels. TM2 has higher energy levels values than TM3/TM4, which has led to the suggestion that TM2 is the first helix of the TMD that moves as a consequence of the wave conformation transitions coming from the ECD (Auerbach, 2010).

More recently, electron microscopy studies of ACh-sprayed and freeze-trapped Torpedo post-synaptic membranes have suggested that gating is asymmetric (Unwin &Fujiyoshi, 2012). Binding of ACh to the α subunit in the agonist site located at the α/γ interface induces an outward displacement of the β subunit. Propagation of the outward movement down the protein structure perturbs the symmetrical side-to-side interactions within the ion pore, which leads to a more relaxed ion pore conformation typical of an open pore. The agonist site at the α/δ interface is also implicated in gating but conformational transitions in this agonist site are not associated with displacement of the β subunit conformational. It is likely that this agonist site influences breakup and reassembly of the gate-forming ring found in the ion pore.

1.5 α4β2 nAChRs

α4β2 nAChRs are the most abundant nAChR subtype in the brain where they form the high-affinity binding sites for nicotine (Picciotto et al., 2001). Pharmacological, immunocytochemical and molecular biological studies indicate

that the α4 and β2 can also combine with α5 subunits to form α4β2α5 nAChRs (Brown et al., 2007; Tapia et al., 2007; Kuryatov et al., 2008; Grady et al., 2010). Henceforth, receptors made of only α4 and β2 subunits will be referred as α4β2 nAChRs, whilst those made of α4, β2 and α5 subunits will be referred to as α4β2α5 nAChRs. Both α4β2 and α4β2α5 receptors are expressed in the brain, however as yet there are no pharmacological tools available that can separate them reliably, hence when it is not clear whether α4β2α5 receptors are also present in neurones, the α4β2-containing receptors will be referred to as α4β2* nAChRs. In addition, α4 and β2 subunits also combine with α6 and β3 subunits to generate α4α6β2β3 or α6β2β3 nAChRs (Gotti et al., 2009). These and other receptors containing α6 subunits will be referred to as α6-containing nAChRs. The latter are sufficiently different from α4β2 or α4β2α5 nAChRs in terms of their pharmacology and distribution in the CNS to justify a separate α6-containing receptor group.

Like most brain nAChRs, α4β2* nAChRs appear to be primarily localized presynaptically where they facilitate the release of various neurotransmitters (Dani, 2001; Wonnacott, 1997). Depending on the brain region, α4β2 nAChRs account for 90 to 60% of total presynaptic α4β2* nAChR present (Brown et al., 2007; Mao et al., 2008). α4β2* nAChRs have been implicated in learning and memory, nociception and nicotine dependence (Picciotto et al., 2001; Tapper et al., 2004; Maskos et al., 2005). Mutations in both the α4 (*CHRNA4*) and β2 (*CHRNB2*) subunit genes cause autosomal nocturnal frontal lobe epilepsy (ADNFLE) (Weiland et al., 2000). Losses in numbers of α4β2* nAChRs have been documented in age-related degenerative diseases such as Alzheimer's, suggesting possible pathological involvement (Zanardi et al., 2002) and a single-nucleotide polymorphism (D398N) in the α5 nAChR subunit gene, rs16969968, has been repeatedly associated with both susceptibility to nicotine addiction and respiratory health phenotypes (Berrettini et al., 2008; Grucza et al., 2008; Spitz et al., 2008; Weiss et al., 2008).

1.5.1 Recombinant α4β2 and α4β2α5 nAChRs

Pharmacological studies of functional α4β2 nAChRs expressed heterologously in *Xenopus* oocytes or Human Embryonic Kidney (HEK) 293 cells after transfection with equal amounts of α4 or β2 cDNA or cRNA show biphasic sensitivity to activation by ACh (Buisson & D Bertrand, 2001; Houlihan et al., 2001; Nelson et al., 2003). Typically, the ACh concentration response curve (CRC) comprises a high sensitivity component (EC_{50} 1 - 4 µM) that accounts for 10-20% of the max response. The second component displays approx. 100-fold lower sensitivity for ACh (EC_{50} 90 - 120 µM) and accounts for 80 – 90% of the CRC. Subsequent studies that used extreme transfection ratios of α4 and β2 subunits to obtain monophasic high- or low-sensitivity ACh CRC showed that the components of biphasic ACh CRC reflected the presence of two different types of α4β2 nAChR (Nelson et al., 2003; Moroni et al., 2006). Since then the two receptor types have been referred to as HS (high sensitivity α4β2 nAChR) or LS (low sensitivity α4β2 nAChR) (Moroni et al. 2006). Subsequent studies that used either biochemical (Nelson et al., 2003) or electrophysiological (Moroni et al. 2006) approaches to determine the stoichiometry of α4β2 nAChRs inferred that the stoichiometry of HS receptors is (α4β2)₂β2, whereas LS receptors are (α4β2)₂α4. To avoid confusion with the various terms used to refer to the α4β2 nAChRs, the terms HS and LS will not be used in this thesis. Although the stoichiometry of α4β2 nAChRs in neurones is not known, the pharmacological similarities between native and recombinant α4β2* nAChRs are remarkably pronounced to confidently assume that the stoichiometry of native α4β2 nAChRs is identical to that inferred for their recombinant counterparts.

α4 and β2 subunits when assembled with α5 subunits in cell expression systems generate α4β2α5 receptors (Tapia et al. 2007; Kuryatov 2008). Studies of avian α5-containing nAChR have shown that the subunit stoichiometry of this receptor type is (α4β2)₂α5 (Ramirez-Latorre et al., 1996). This subunit composition is likely replicated in mammalian α5-containing nAChRs, as suggested from the findings of pharmacological studies that have expressed tethered β2 and α4 subunits together with loose α5 subunits in artificial expression systems (Tapia et al. 2007; Kuryatov 2008).

1.5.2 Expression of α4β2* nAChRs in Neurones

Functional evidence from studies carried out on thalamic and cortical preparations suggest that both $(\alpha4\beta2)_2\beta2$ and $(\alpha4\beta2)_2\alpha4$ nAChRs co-exist in the brain. Thus, functional studies have shown biphasic agonist CRCs for stimulation of putative α4β2 nAChR function in mice thalamic and cortical preparations (Marks et al. 1999; Marks et al. 2008; Marks et al., 2010). Such function is not present in the thalamus or cortex of α4-/- or β2-/- knockout mice, which also lack high affinity binding sites for the agonists epibatidine (Epi) and Nic both of which are a signature property of α4β2 nAChRs (Picciotto et al., 1999; Picciotto et al., 2001). Furthermore, immunocytochemical studies show changes in high- and low-sensitivity function with partial deletion of the genes coding for either of the α4 or β2 subunits (Gotti et al., 2008). More recently, the use of 3-[3-(3-pyridyl)-1,2,4-oxadiazol-5-yl]benzonitrile (NS9283), a novel allosteric modulator selective for $(\alpha4\beta2)_2\alpha4$ nAChRs, on rodent brain neuronal preparations has confirmed that thalamo-cortical neurones express both $(\alpha4\beta2)_2\beta2$ and $(\alpha4\beta2)_2\alpha4$ nAChRs and that striatal neurones express solely α4β2 receptors of the high-sensitivity type (Timmermann et al., 2012; Rode et al., 2012). Thus, together, functional and immunocytochemical studies strongly support the presence of $(\alpha4\beta2)_2\beta2$ and $(\alpha4\beta2)_2\alpha4$ nAChRs in neurones. Although $(\alpha4\beta2)_2\beta2$ and $(\alpha4\beta2)_2\alpha4$ nAChRs can be distinguished with available pharmacological probes, $(\alpha4\beta2)_2\beta2$ nAChRs cannot be so easily separated from $(\alpha4\beta2)_2\alpha5$ nAChRs as they have remarkably similar pharmacological profiles (Kuryatov, 2008). This problem is exacerbated by the fact that the α5 subunit is found in the presence of α4 and β2 subunits (Gotti et al. 2006; Brown et al. 2007) in the brain, where it contributes about 10 – 40%, depending of the brain region, of all α4β2* nAChR activity (Brown et al. 2007; Grady et al. 2007). Thus, a question that needs to be answered if we are to elucidate α4β2* nAChR functions in the brain is whether the high- sensitivity α4β2* nAChR activity detected in areas such as the thalamus is due to signals generated by $(\alpha4\beta2)_2\beta2$ or $(\alpha4\beta2)_2\alpha5$, or a mixture of both receptor types. So far, the availability of stoichiometry-specific compounds such as NS9283 suggests a scenario in which some α4β2-modulated brain functions may be preferentially influenced by a particular α4β2 nAChR isoform, while others may be modulated by a mixture of two or three

α4β2 nAChR types (Rode et al., 2012; Timmermann et al., 2012). In this scenario, changes in the relative proportion of the α4β2 or α4β2* nAChRs may have important consequences for the physiological/therapeutic effects of α4β2–selective compounds.

It is well documented that chronic exposure to competitive ligands alters the expression and activity of nAChRs in neurones, particularly those of α4β2 nAChRs (Nelson et al. 2003; Moroni et al. 2006; Kuryatov et al. 2005; Sallette et al. 2005; Srinivasan et al. 2011). There is also evidence that chronic exposure to competitive ligands preferentially enhances assembly of $(α4β2)_2β2$ nAChRs (Kuryatov et al. 2005; Sallette et al. 2005; Srinivasan et al. 2011). This selectivity is so strong that mammalian cell lines heterologously expressing mostly $(α4β2)_2α4$ nAChRs shift expression to $(α4β2)_2β2$ nAChR following chronic exposure to nicotine (Kuryatov et al. 2005; Moroni et al., 2006). Other factors that also influence the type of α4β2 nAChR expressed include an absolute or relative increase in β2 subunit levels (Nelson et al., 2003), lower incubation temperatures (Nelson et al., 2003), phospho-kinase A driven phosphorylation of α4 subunits (Exley et al., 2006) and ADNFLE epilepsy mutations (Son et al., 2009). The relevance of this plasticity for α4β2-driven behaviours or their potential use as therapeutic targets is not known, but it is noteworthy that a mouse α4 A529T polymorphism increases the $(α4β2)_2β2/(α4β2)_2α4$ strain-specific differences in measures of α4β2 nAChR function such as sensitivity to and, effects of nicotine on Y-maze activity, respiration rate and body temperature (Kim et al., 2003). Further work is needed to determine the neuroanatomical distribution of α4β2 nAChRs as well as the contribution of each stoichiometry to brain behaviours modulated by α4β2 nAChRs. The success of such studies largely rests on the availability of α4β2 stoichiometry-specific compounds. So far, a number of agonists have been developed that show preference for $(α4β2)_2β2$ nAChRs such as 4-(5-ethoxy-3-pyridinyl)-*N*-methyl-(3*E*)-3-buten-1-amine difumarate (TC-2559) (Moroni et al. 2006; Carbone et al. 2009) and TC-1734 (Gatto et al., 2004). Higher stoichiometry-selectivity has been achieved with allosteric modulators such as NS9283. This compound has been shown to increase agonist-evoked current responses at α4- and α2-containing nAChRs of stoichiometry $(αβ)_2α$ (Timmermann et al., 2012). It has no effects on receptors

with high sensitivity $(\alpha\beta)_2\beta$ stoichiometry or $\alpha3$-containing nAChR, and it cannot distinguish $\beta2$ from $\beta4$-containing receptors (Timmermann et al., 2012). Nonetheless, since NS9283 appears to be highly selective for the $(\alpha\beta)_2\alpha$, the compound shows promise both as a prototypic research tool and potential therapeutic drug.

1.6 α4β2* nAChRs in Brain Pathologies

α4β2* nAChRs are considered as valid targets for therapeutic intervention in diverse diseases such as Nic addiction, depression, ADNFLE, central or peripheral pain management and cognitive diseases. The evidence supporting the involvement of α4β2 nAChR in these diseases is discussed next.

1.6.1 α4β2* nAChR and Nic Addiction

Nic is one of the most widely used addictive drugs. Over three million smoking-related deaths occur per year in the world. In Western countries, it is believed that 20% of all deaths are caused by illnesses related to smoking (Peto et al., 1996; Laviolette & van der Kooy, 2004). Thus, an understanding of the mechanisms that cause addiction to Nic remains an important focus of medical research and drug discovery.

Addiction to Nic involves activation of the reward pathway in the brain. Here, several lines of evidence suggest that Nic mediates its addictive property via the regulation on the action of dopamine (DA) and non-DA neuronal substrates in the ventral tegmental area (VTA) (De Biasi & Dani, 2011). DA neurons from the VTA send projections to the nucleus accumbens (NAc) and the prefrontal cortex (PFC). The rewarding and aversive psychological properties of Nic are believed to involve the activation of these DA pathways in the VTA. Non-DA neuronal substrates comprise GABAergic neurones in the VTA and the tegmental pedunculopontine nucleus (TPP). In this system, VTA GABAergic neurones send descending projections to the TPP, which through ascending cholinergic and glutamatergic projections to the VTA also regulate the activity of DA neurons in the VTA.

α4β2 nAChRs were thought to be involved in Nic addiction since it was shown that these receptors form the high-affinity binding site for Nic in the brain (Picciotto et al., 2001). Later studies have shown that Nic does not modulate DA release in the VTA or in the NAc in β2 knock out (Picciotto et al., 1999) and this is accompanied by lack of Nic self-administration (Picciotto et al., 1999). Further support for the involvement of a receptor containing β2 subunits comes from studies in which the β2 subunit was reintroduced in β2 knock-out mice. Whilst

β2 knock in mice do not self-administrate Nic, reintroducing β2 using the lentivirus expression system, restores not only Nic self-administration behaviour but also Nic-induced DA release in the NAc (Maskos et al., 2005). Other studies have provided evidence in support of α4 subunit involvement in Nic addiction. Knock-in mice for the α4L9'A subunit shows Nic reinforcement behaviour at a concentration 50-fold lower than the concentration needed to induce the same response in wild type mice. α4L9'A is a α4 subunit that carries a mutation in position 9' of TM2 that markedly increases sensitivity to activation by Nic. The increased sensitivity is used to distinguish responses of α4-containing receptors from other nAChRs as the latter are not activated at concentrations of Nic eliciting full responses at receptors carrying α4L9'A mutant subunit (Tapper et al., 2004). Together, the studies with α4L9' and β2 knock in mice strongly support the involvement of α4β2 nAChRs in Nic addiction. As mentioned before, recent studies have shown an association between vulnerability to smoking addiction and a single-nucleotide polymorphism in the gene coding for the α5 subunit (CHRNA5)(rs16969968) (Berrettini & Doyle, 2012), although it is not known how this polymorphism may affect the pathways leading to smoking addiction.

A long standing question in the nAChR field is whether Nic exerts its addictive effect via activation or desensitisation of α4β2 nAChRs. α4β2 nAChRs are prone to long-term desensitisation when exposed chronically to agonists, which is the case during smoking. Thus, it is thought that the most likely scenario is that initially nicotine activates α4β2 nAChR on DA presynaptic terminals in NAc and the VTA, which leads to increased reward signals. However, continued exposure to nicotine desensitises α4β2 nAChR. Because α4β2 nAChRs control release of GABA from VTA GABAergic neurones that inhibit release of DA from dopaminergic neurones in the NAc, desensitisation of α4β2 nAChRs also increases DA release in NAc (Mansvelder et al., 2002). The current view is that the acute activation of DA neurons in VTA represents the basis for Nic reinforcing and rewarding, whilst the long lasting desensitisation of α4β2 nAChR in the VTA might represent nicotine tolerance (Mansvelder & McGehee, 2002).

Other nAChRs present in the VTA and NAc are likely to contribute to Nic addiction but as yet it is not clear how. Thus, α7 nAChRs are present in glutamatergic neurones in the VTA and, importantly, α7 nAChRs are not prone to desensitisation by low or non-activating concentrations of agonist as α4β2 nAChR, which suggest they may be activatable when α4β2 nAChR are desensitised. α6-containing nAChRs are also present in the VTA and NAc, particularly in the posterior VTA subnuclei, which project to the NAc (Ikemoto, 2007) as compared to the anterior subnuclei (Zhao-Shea et al., 2011). Interestingly, at Nic concentrations close to the plasma concentration found in smokers, α6-containing nAChRs are activated (Liu et al., 2012; Grady et al., 2012) and contribute to Nic-dependent activation of mesolimbic DA neurons (Zhao-Shea et al., 2011).

1.6.2 α4β2* nAChRs in depression

Both clinical and preclinical data support a potential therapeutic benefit of modulating the activity of CNS α4β2* nAChRs to treat mood and anxiety disorders. For instance, smoking is more prevalent in depressed subjects than in non-depressed patients (Covey et al., 1998). Panic disorder patients have higher rates of smoking than the general population (Ziedonis et al., 2008). Additionally, smokers report anxiety relief as a key reason for continued smoking and relapse from abstinence (McKee et al., 2011), and chronic exposure to Nic results in increased response to antidepressants (Andreasen et al., 2009). α4β2* nAChRs are expressed in neuroanatomic regions known to be involved in reward, mood and stress such as the VTA, NAc, locus coerelus, dorsal raphe nucleus, PFC, amygdala and hippocampus (Mineur & Picciotto, 2010; Maskos, 2010; Wonnacott et al., 2006). In these regions, α4β2* nAChRs are predominantly located presynaptically or preterminally, from where they modulate the release of ACh and other important neurotransmitters involved in mood, for example GABA and DA (Wonnacott et al., 2006). Furthermore, a number of established antidepressants, such as fluoxetine, sertraline and ibupropion, inhibit neuronal α4β2 nAChRs at relevant therapeutic drug concentrations (Mineur & Picciotto, 2010). nAChRs are also found in the hypothalamicpituitary–adrenal (HPA) axis, which is dysregulated in mood

disorders. Here, nAChRs under certain conditions play a part in modulating the release of corticotropin from the hypothalamus (Raber et al., 1995) and corticosterone from the adrenal gland (Wonnacott et al., 2006). Nic increases levels of circulating corticosteroids in both animal models and human smokers (Caggiula et al., 1991) while mecamylamine (Mec), a blocker of nAChRs, decreases circulating corticosteroids (Wilkins et al., 1982; Newman et al., 2001). Interestingly, aging knockout mice lacking the $\beta2$ subunit have elevated circulating levels of corticosteroids (Mineur & Picciotto, 2010).

The nAChRs receiving most attention for their potential therapeutic use in mood disorders are the $\alpha4\beta2^*$ nAChR. Studies with $\alpha4\beta2^*$ nAChR-preferring competitive antagonists, such as dihydro-β-erythroidine (DhβE), have demonstrated antidepressant-like effects in mice (Mineur & Picciotto, 2010; Rabenstein et al., 2006). Point mutant mice with hypersensitive $\alpha4$ subunit display altered basal levels of anxiety (Labarca et al., 2001). Targeted genetic deletion of the $\alpha4$ subunit from dopaminergic neurones has shown that the presence of $\alpha4$-containing nAChRs are necessary for the anxiolytic effects of nicotine (Mineur & Picciotto, 2010). Also, a polymorphism in the $\alpha4$ subunit gene (CHRNA4, rs1044396) is associated with negative emotionality (Markett et al., 2011). Interestingly, $\alpha4\beta2^*$ nAChRs are highly expressed in midbrain dopamine pathways known to be involved in reward and mood disorders while pharmacological studies of knock-out $\beta2$-/- mice suggest that $\alpha4\beta2$ receptors are essential for dopamine release (Mineur & Picciotto, 2010). $\alpha4\beta2$ nAChRs directly enhance the release of the neurotransmitter dopamine. However, they may also modulate it indirectly through their effects on the release of GABA. Such modulatory effects would be of relevance for the targeting of $\alpha4\beta2$ nAChRs for depression therapies. nAChRs receptors on GABAergic neurones have been implicated in the anxiolytic effects of nicotine, which are reversed by blocking GABA transmission (Paterson & Nordberg, 2000). Furthermore, there is increasing evidence that a central GABAergic dysfunction may be primarily related to the physiopathology of affective disorders.

1.6.3 α4β2 nAChR and ADNFLE

ADNFLE is a rare familial focal epilepsy characterized by brief nocturnal seizures that originate in the frontal lobe (Scheffer et al., 1995) and occur mainly during stage II of non-rapid-eye-movement sleep. ADNFLE is monogenic epilepsy linked, with high penetrance, to mutations in the α4β2 nAChR. So far, four α4 and five β2 mutations have been linked to ADNFLE (see Steinlein et al., 2012 for a comprehensive review). Among these, six mutations are located within or at the C-terminal end of the TM2 domain of the α4 (α4S248F; α4776insL; α4S252L; α4T265I) or the β2 (β2V287L; β2V287M) nAChR subunits. Studies on TM2 ADNFLE mutant α4β2 nAChRs expressed heterologously in surrogate cells have shown that these mutations affect sensitivity to activation by agonists, desensitisation and Ca^{2+} permeability (Steinlein et al., 2012).

Little is known about the mechanisms that may induce seizures in ADFNLE patients. One hypothesis suggests that the increased ACh sensitivity displayed by ADNFLE mutant α4β2 receptors could lead to seizures (Bertrand et al., 2002). An alternative hypothesis postulates that the reduced Ca^{2+} permeability of ADNFLE mutant α4β2 receptors decreases the influx of Ca^{2+} into GABAergic presynaptic terminals. This would decrease the release of the inhibitory neurotransmitter GABA, which would shift the brain excitation-inhibition equilibrium towards excitation (Rodrigues-Pinguet et al., 2005).

1.6.4 α4β2* nAChRs and analgesia

One of the most promising therapeutic applications of nicotinic agonists is in the control of pain. The analgesic effect of Nic was described 70 years ago but, because of its short-lived effect, it has been overlooked, and the development of nicotinic agonists as analgesics started only after the description of the antinociceptive effects of Epi, which exceed those of morphine (Daly et al., 2000). Reduced nociception in mice lacking α4 or β2 nAChR subunits suggests a key role for α4β2 nAChRs in analgesia, but (α4β2)2α5 may also be involved. The role of (α4β2)2α5 in analgesia is supported by studies showing an increase in spinal α5 expression in response to the spinal nerve ligation (Vincler & Eisenach,

2004) and lack of effect of nicotinic analgesics in mice lacking α5 subunit (Jackson et al., 2010). In addition to the α4β2* nAChRs, α9α10 located in sensory dorsal root ganglion neurones may also contribute to cholinergic-analgesic effects (Gotti et al., 2009).

As with Nic addiction, there is controversy as to whether activation or desensitisation of α4β2* nAChRs produces analgesia. Studies by Gao et al., (2010) on various *in vivo* and *in vitro* models have found that activation of α4β2 nAChRs was necessary but not sufficient to produce analgesia. More recent studies have shown that compounds that are more potent at desensitisation of α4β2* nAChRs are more effective at producing analgesia, which suggests that desensitisation contributes to the efficacy of nicotinic analgesics (Zhang et al., 2012). Thus, it seems that both activation and desensitisation may play a part in analgesia.

1.6.5 α4β2* nAChRs and cognition

Both muscarinic and nicotinergic signalling play a well-established role in cognitive processes including attention and working memory (Sarter et al., 2005). Analysis of the ability of nAChR stimulation to improve cognitive function has identified attention performance as the most likely component to be positively influenced by α4β2* nAChR activation. These effects are more readily seen in individuals with pathological disease states, rather than normal individuals (Levin & Simon, 1998). In animal models, nicotinic agonists improve learning, memory (Levin & Simon, 1998) and attention (Hahn et al., 2003).

1.7   The Pharmacological profile of α4β2 nAChRs

The section that follows will describe well-established competitive and non-competitive compounds of α4β2* nAChRs. Where possible from available information, the effects of the compounds described below on (α4β2)₂α4, (α4β2)₂β2 and (α4β2)₂α5 will be noted. A summary of the pharmacological profile of these receptors built over the years by Bermudez and her team is shown in **Table 1.1**. Some of the data shown for α4β2 nAChRs have been published (i.e., Moroni et al., 2006; Moroni et al., 2008; Carbone et al., 2009;

Mantione et al,. 2012) but the profile of $(\alpha4\beta2)_2\alpha5$ nAChRs is unpublished (I Bermudez, personal communication).

Table 1.1.   Pharmacological profile of α4β2* nAChRs.

All values are means ± S.E.M. from 5-10 cells. Key: dFBr, desformylflustrabromine; 5-Br-Cys, 5-Br-cytisine; NE, no effects; ND, not determined. Note that for dFBr only parameters estimated for positive allosterism are shown. Maximal response (I_{max}), and apparent potency of stimulation (EC_{50}) or inhibition (IC_{50}), were estimated from CRCs fit to the Hill equation as previously published (Moroni et al. 2006; Carbone et al. 2009). Data for ACh, A85380, 5I-A5380, Cyt, 5-Br-Cys, Epi, TC-2559 and Saz-A are adapted from Moroni et al. 2006; Zwart et al. 2006 and Carbone et al., 2009. Data for dFBr, estradiol, progesterone are from Mantione et al. 2012 and Zn^{2+} from Moroni et al. 2008. Data for $(\alpha4\beta2)2\alpha5$ nAChR are unpublished and are from a personal communication from I Bermudez.

	$(\alpha4\beta2)_2\beta2$		$(\alpha4\beta2)_2\alpha4$		$(\alpha4\beta2)_2\alpha5$	
	I_{max}/I_{ACh_max}	EC_{50} (μM)	I_{max}/I_{ACh_max}	EC_{50} (μM)	I_{max}/I_{ACh_max}	EC_{50} (μM)
ACh	1	2.4±0.5	1	111±15	1	2±0.4
A85380	1.86±0.1	0.3±0.07	1.32±0.06	2.7±0.05	1.1±0.3	0.08±0.007
5I-A85380	2.4±0.1	0.14±0.01	0.99±0.06	28.20± 5		
Cyt	NE		0.27±0.04	55±8	0.07±0.0001	0.008±0.0001
5-Br-Cyt	NE		0.28±0.05	11±3		
Epi	0.6±0.014	0.16±0.02	2.7±0.01	0.30±0.03	0.46±0.05	0.005±0.0001
Nic					0.52±0.04	0.4±0.06
TC-2559	4.18±0.1	2±0.05	0.13±0.1	0.91±0.05	0.83±0.03	1.5±0.02
Saz-A	1.01±0.01	0.007 ± 0.0009	0.008±0.0004	ND	1±0.005	0.006±0.0005
Progesterone		7±0.04 (IC_{50})		11±4 (IC_{50})		1.8±0.1
Estradiol	3±0.9	18±8	1.8 ±0.6	18±6	1.29±0.04	2.8±0.7
dFBr	2.6±0.8	16±5	3.9±0.4	0.5±0.03		
Zn^{2+}		17±2 (IC_{50})	1.5±0.2	49±5 (EC_{50}) 881±43 (IC_{50})		4±0.1 (IC_{50})

1.7.1 Agonists

Agonists bind the orthosteric sites of the nAChRs, leading to receptor activation. Typically, nicotinic agonists are endowed with at least one quaternary ammonium group or a protonated tertiary ammonium group. As mentioned previously, the ammonium group seems to interact via π-cation interactions with the side chains of the aromatic residues of the binding site. Established $\alpha 4 \beta 2$ nAChR-preferring agonists include Nic, TC-2559, cytisine (Cyt), varenicline (Var), Epi, 3-[(2S)-2-Azetidinylmethoxy pyridine dihydrochloride (A-85380), 5-iodo-A-85380 and sazetidine-A (Saz-A).

Nic is an alkaloid found in the *Solanaceae* family, particularly in tobacco plants. Nic acts on all nAChRs as an agonist but has higher-affinity for $\alpha 4 \beta 2^*$ nAChRs; reported binding affinity (K_i) and functional potency (EC_{50}) are at the nanomolar level **(Table 1.1)** (Jensen et al., 2005). In contrast, Nic displays moderate nanomolar binding and functional affinity for $\alpha 7$ nAChRs (K_i 400-15000 nM and EC_{50} 49-113 μM). Intermediate binding affinity and functional potency have been reported for $\alpha 3 \beta 4$ nAChRs (K_i 290-476 nM; EC_{50} 8.1-110 μM) (Jensen et al., 2005). In the case of $\alpha 9$ or $\alpha 9 \alpha 10$ nAChRs, Nic behaves as an antagonist (Verbitsky et al., 2000).

TC-2559 is a selective agonist of the $\alpha 4 \beta 2^*$ nAChRs (Chen et al., 2003), interestingly, TC-2559 showing different efficacy at $\alpha 4 \beta 2^*$ nAChRs **(Table 1.1)**. TC-2559 is a super agonist at $(\alpha 4 \beta 2)_2 \beta 2$, full agonist at $(\alpha 4 \beta 2)_2 \alpha 5$ nAChRs and a partial agonist at $(\alpha 4 \beta 2)_2 \alpha 4$ nAChR **(Table 1.1)** (Zwart et al., 2006; Carbone et al., 2009).

Cyt is an alkaloid with a strongly restricted conformation and well-established nicotinic agonist pharmacology, exhibiting low nano-molar affinity at $\alpha 4 \beta 2^*$ nAChRs and low micro-molar affinity at the $\alpha 7$ subtype (Slater et al., 2003). Cyt has almost no efficacy at $(\alpha 4 \beta 2)_2 \beta 2$ or $(\alpha 4 \beta 2)_2 \alpha 5$ nAChRs but at $(\alpha 4 \beta 2)_2 \alpha 4$ displays higher efficacy **(Table 1.1)** (Moroni et al., 2006; Carbone et al., 2009). The potency and the efficacy of Cyt increases following halogenation at the 3-position of the pyridine ring (Houlihan et al., 2001; Slater et al., 2003). Cyt is

used in Eastern European countries as an aid for smoking cessation and also has anti-depressant effects in animal models of depression (Mineur & Picciotto, 2010).

Varenicline (Var) marketed as Chantix™ or Chanpix™ is used as an aid for smoking cessation (Coe et al., 2005). It also produces antidepressant-like effects in animal models of depression but only at reduced doses (Rollema et al., 2010). Var is a partial agonist at α4β2* nAChRs displaying lower efficacy at $(α4β2)_2β2$ and $(α4β2)_2α5$ nAChRs than at $(α4β2)_2α4$ nAChRs (Table 1.1).

Epi was isolated from the skin of the Amazonian frog *Epidobates Tricoloris* (Badio & Daly, 1994). Epi is a potent agonist at all nAChRs, although its binding affinity and potency are highest at α4β2* nAChRs. The high potency of Epi at all nChRs leads to side effects, particularly of the autonomic type, making it impossible to use Epi as a therapeutic compound. However, the structure of Epi has been widely used as a template in drug discovery efforts (Americ et al., 2007).

A-85380 displays high affinity for αβ heteromeric nAChRs (Sullivan et al., 1996). Introducing an iodine atom into the pyridine ring of A-85380, results in the more potent α4β2-preferring compound 5-iodo-A-85380. This compound however also activates α6-containing nAChRs (Mogg et al., 2004; Mukhin et al., 2000) at concentrations slightly higher than those activating α4β2 nAChRs.

Saz-A has low nanomolar binding affinity for α4β2 nAChRs. Studies that showed no functional efficacy at α4β2 nAChRs led to the view that Saz-A is a highly desensitising α4β2 nAChR agonist, driving α4β2 nAChRs into a desensitised state without first activating them, a mechanism termed silent desensitisation (Xiao et al., 2006). However, other studies established that Saz-A is a stoichiometry-specific α4β2 nAChR agonist; thus, Saz-A is a full agonist at $(α4β2)_2β2$ and $(α4β2)_2α5$, but has very low efficacy (5%) at $(α4β2)_2α4$ stoichiometry (Table 1.1) (Zwart et al., 2008). As shown in Chapter 3 and 5 (Mazzaferro et al., 2011), the efficacy of Saz-A seems to be determined by its

inability to recognise an ACh binding site located at the $\alpha4(+)/\alpha4(-)$ interface of $(\alpha4\beta2)_2\alpha4$ nAChRs (Mazzaferro et al., 2011).

1.7.2 Antagonist of α4β2 nAChRs

Antagonists recognise specific sites in receptors and upon occupancy of those sites they reduce in a concentration dependent manner the responses elicited by agonists. Antagonists that recognise the agonist binding site are competitive ligands, whereas those that occupy other sites are non-competitive antagonists. The latter can be allosteric modulators or ion channel blockers.

DhβE, isolated from *Erythrina americana* seeds, is a reversible competitive antagonist of neuronal nAChRs. DhβE preferentially blocks β2-containing nAChRs; thus DhβE displays high potency at human and rat α4β2 and α3β2 nAChRs, whereas the potency at α7 and at α3β4 nAChRs is considerably decreased (10-50 fold less) (Jensen et al., 2005; Chavez-Noriega et al., 1997; Harvey et al., 1996). In hippocampal neurones sub-micromolar concentrations of DhβE blocks specifically α4β2*-mediated currents whereas α7 currents are insensitive at micromolar concentrations (Alkondon & Albuquerque, 1993). In animal models, DhβE has antidepressant-like effects in mice (Andreasen et al. 2009; Mineur and Picciotto, 2010) and has been used to dissect non-α7 nAChRs mechanisms in Nic addiction studies (Kenny & Markou, 2006). DhβE is more potent at $(\alpha4\beta2)_2\beta2$ and $(\alpha4\beta2)_2\alpha5$ nAChRs than at $(\alpha4\beta2)_2\alpha4$ nAChRs **(Table 1.1)** (Moroni et al., 2006; Carbone et al., 2009) but the difference in sensitivity is not sufficient to discriminate α4β2* nAChR subtypes (Moroni et al., 2006). Recent studies have shown that DhβE interacts with a β2D169 in loop E, an interaction that homology models of the α4β2 nAChRs suggests acts to keep loop C in an uncapped position (Iturriaga-Vásquez et al., 2010).

Mec is a non-competitive antagonist of nAChRs. Mec inhibits α/β heteromeric nAChRs at low micromolar concentrations (IC_{50} values between 0.1-10 μM), whereas it is less potent at homomeric α7 nAChRs (Jensen et al., 2005; Chavez-Noriega et al., 1997). At low concentrations Mec shows antidepressant like

effects in mice (Rabenstein et al., 2006) and these effects appear to be exerted through α4β2 nAChRs. Mec is a racemate of S-(+)- and S-(-)-enantiomers.

MK-801 (dizocilpine), developed as a channel blocker of N-methyl-D-aspartate receptors (NMDA), also blocks, as an open channel blocker, α7 and α4β2 nAChRs (Briggs & McKenna, 1996; Buisson & Bertrand, 1998b) .

Buproprion (Zyban™), a compound used as antidepressant and to aid smoking cessation, behaves as an inhibitor of noradrenaline and dopamine transporters. However, it also non-competitively inhibits α4β2, α3β2 and α7 nAChRs (Jensen et al., 2005). This cholinergic effect of bupropion adds to the body of evidence suggesting involvement of α4β2 nAChRs in depression.

1.7.3 Allosteric modulators

Binding of ligands to allosteric sites located elsewhere from the orthosteric sites can modulate nAChR signalling via an effect on the equilibrium between the resting, active or inactive states (Mantione et al., 2012). Positive allosteric modulators (PAMs) have been shown to increase agonist potency (e.g., benzodiazepine effects in GABA$_A$ receptors) and/or increase efficacy (e.g., barbiturate effects on GABA$_A$ receptors) (Mantione et al., 2012). PAMs can increase agonist potency by enhancing agonist binding to the receptor resting state. They can also increase agonist efficacy by reducing the energy of the transition between the closed and open states and/or increasing the energy tariff of the transition from the active to the desensitised states. In contrast, negative allosteric modulators (NAMs) can increase the energy barrier for activation and thus decrease or inhibit the effect of agonists. Alternatively, allosteric modulators can decrease the energy barrier to enter desensitisation, which leads to physiological inactivation.

A diverse group of allosteric modulators have been identified to interact with α4β2* nAChRs, However, with the exception of Zn^{2+} (Moroni et al., 2008) or Biphenyl-2-carboxylic acid 1-(3-phenyl-propyl)-piperidin-3-ylmethyl ester (KAB-18) (Henderson et al., 2010; Pavlovicz et al., 2011), there is limited

knowledge of the binding sites or transduction mechanisms associated with this family of $\alpha4\beta2^*$ nAChR ligands.

Zn^{2+} effects on $\alpha4\beta2$ nAChRs are stoichiometry selective. Zn^{2+} is a NAM of $(\alpha4\beta2)_2\beta2$ receptors, whereas it potentiates or inhibits, depending on its concentration, the function of $(\alpha4\beta2)_2\alpha4$ nAChRs **(Table 1.1)** (Moroni et al., 2008). Zn^{2+}potentiation of $(\alpha4\beta2)_2\alpha4$ nAChRs is determined by a site located at this receptor type stoichiometry-specific $\alpha4(+)/\alpha4(-)$ subunit interface, whereas Zn^{2+} inhibits both receptor types by binding a site located at the $\beta2(+)/\alpha4(-)$ interfaces, which are present in both receptor stoichiometries. The effects of Zn^{2+} on nAChRs are likely to be not physiologically relevant since the concentrations at which Zn^{2+} exerts its effect on $\alpha4\beta2$ nAChRs are above the levels found in the external medium or at synapses. Nevertheless, the identification of Zn^{2+} binding sites represents an important advance for $\alpha4\beta2$ nAChR research because it demonstrated for the first time the potential of stoichiometry-specific subunit interfaces as targets for drug discovery.

Steroid hormones estradiol (Paradiso et al., 2001) and progesterone (Buisson & Bertrand 1998a) have been found to modulate $\alpha4\beta2$ nAChRs. Progesterone exerts allosteric inhibition on $\alpha4\beta2$ nAChRs, whereas estradiol behaves as a PAM. Estradiol displays higher efficacy at $(\alpha4\beta2)_2\beta2$ nAChRs than at $(\alpha4\beta2)_2\alpha4$ nAChRs. It is likely that this is due to the presence of three estradiol binding sites on the $(\alpha4\beta2)_2\beta2$ nAChRs. The binding sites for estradiol are located in the C-terminus of the $\beta2$ subunit (Paradiso et al., 2001), hence, there are three of these sites on $(\alpha4\beta2)_2\beta2$ nAChRs. Interestingly, unlike the effects of progesterone and other modulators, the allosteric effects of estradiol are species specific. Human $\alpha4\beta2$ nAChRs are positively modulated by estradiol, whereas rat $\alpha4\beta2$ nAChRs are inhibited (Paradiso et al., 2001). Rat $\alpha4\beta2$ nAChRs lack the sequence segment in the C-terminus of the $\beta2$ subunit that contributes the binding site for estradiol in human $\alpha4\beta2$ nAChRs (Paradiso et al., 2001).

Desformylflustrabromine (dFBr), a tryptamine derivative, which is a metabolite of the marine bryozoan Flustrafoliacea, potentiates, in the micromolar range, $\alpha4\beta2$ nAChRs by increasing both the potency and efficacy of ACh (Weltzin &

Schulte, 2010). At concentrations higher than those exerting potentiation, dFBr inhibits α4β2 nAChRs, possibly by ion channel blockade (Weltzin & Schulte, 2010). dFBr shows higher affinity and efficacy at $(α4β2)_2α4$ nAChRs. Similar to $(α4β2)_2β2$, dFBr also enhances the function of other heteromeric nAChRs such as α2β2 and α3β2 nAChRs (Pandya & Yakel, 2011).

Galantamine and physostigmine are acetylcholine-esterase inhibitors that are believed to act as PAMs of nAChRs, including α4β2 nAChRs (Samochocki et al., 2003). However, there is a degree of controversy as to whether they are PAMs of α4β2* nAChRs. Galantamine has been reported to increase the potency of ACh responses of α4β2* nAChRs expressed heterologously in HEK cells (Samochocki et al., 2003). However, this effect is not reproduced on α4β2 nAChRs expressed in *Xenopus* oocytes (Kuryatov et al., 2008). In oocytes, galantamine inhibits at moderate micromolar concentrations the agonist-induced responses of heterologously expressed α4β2 nAChRs. Further work needs to be carried out to resolve this discrepancy. However, the lack of nAChR specificity and its moderate potency makes galantamine less promising as a template for the development of α4β2-specific compounds.

NS9283 developed by NeuroSearch is a novel compound that enhances the agonist- evoked responses of $(α4β2)_2α4$, $(α2β2)α2$ and $(α4β4)2α4$ receptors (Timmermann et al., 2012) but not those of nAChRs with the stoichiometry $(αβ)_2β2$ or containing α3 subunits. The use of NS9283 in diverse *in vivo* and *in vitro* tests has shown that this compound is precognitive and enhances the effects of α4β2 nAChRs in nociception (Rode et al., 2012). Furthermore, when co-administered with agonists, NS9283 enhances the analgesic efficacy of the agonists at well-tolerated clinical doses (Lee et al., 2011). The latter finding is of great interest for therapeutic strategies because it supports the view that allosteric modulators could be used as add-on therapies to either orthosteric agonists of α4β2 nAChRs or other established drugs to decrease side effects and/or increase clinical efficacy. The identification of the binding site for NS9283 on $(α4β2)_2α4$ nAChRs has not been reported; however, as mentioned above, given the selectivity profile of the compound, it is possible that NS9283 binds the signature α4(+)/α4(-) interface of $(α4β2)_2α4$ receptors.

[N-(1,2,3,4-tetrahydro-1-naphthyl)-4-nitroaniline] (UCI-30002) is a compound that is α4β2* nAChR preferring. UCI-30002 is reported to reduce nicotine self-administration in rats (Yoshimura et al., 2007).

KAB-18 is another compound reported to be a selective α4β2* nAChR NAM (Henderson et al., 2010; Pavlovicz et al., 2011). KAB-18 inhibits α4β2 nAChRs in the low micromolar range and its binding site is located in the α/β interface approximately 10 Å away from the agonist-binding pocket; with the key contributing amino residues on the β2 subunit (Pavlovicz et al., 2011).

The anthelmintic compound oxantel also behaves as a selective α4β2 nAChR NAM and may binds a site in the β/α subunit interfaces (Cesa et al., 2012). To the author's knowledge, α4β2 nAChR stoichiometry-specific effects of NAMs have not been reported. There is evidence that α4β2 nAChR-preferring NAMs interact with either the α/β (Pavlovicz et al., 2011) or the β/α (Cesa et al., 2012) subunit interfaces present in both α4β2 nAChR forms, suggesting that these compounds are unable to discriminate α4β2 nAChR stoichiometries.

1.8 Functional differences between α4β2* nAChRs

$(\alpha4\beta2)_2\alpha4$ and $(\alpha4\beta2)_2\beta2$ nAChRs differ approximately 100-fold in sensitivity to activation by ACh (Covernton & Connolly, 2000; Buisson & Bertrand, 2001; Houlihan et al., 2001; Nelson et al., 2003). As summarised in **Table 1.1**, these receptors also differ in sensitivity to activation by other agonists, including Epi, Cyt, halo- and nitro-Cyt, A-853801, 5-I-A853801, (Houlihan et al., 2001; Slater et al., 2003; Moroni et al., 2006; Zwart et al., 2006) Saz-A (Zwart et al., 2008), while competitive antagonists such as *d*-tubocurarine (d-TC) and DhβE inhibit them with different potencies (Moroni et al., 2006). Interestingly, agonists activate currents at $(\alpha4\beta2)_2\beta2$ and $(\alpha4\beta2)_2\alpha4$ nAChRs with strikingly different efficacies (Moroni et al., 2006; Zwart et al., 2008) **(Table 1.1)**. Also, $(\alpha4\beta2)_2\beta2$ and $(\alpha4\beta2)_2\alpha4$ nAChRs display different desensitisation kinetics (Nelson et al., 2003), unitary conductance (Nelson et al., 2003) and, Ca^{2+} permeability (Tapia et al., 2007). They also differ in sensitivity to modulation by Zn^{2+} (Moroni et al.,

2008), steroid hormones, dFBr and up-regulation by chronic exposure to nicotine (Nelson et al., 2003; Kuryatov et al., 2005; Moroni et al., 2006).

The sensitivity of $(\alpha 4\beta 2)_2\alpha 5$ nAChRs to activation by agonists is higher than that of $(\alpha 4\beta 2)_2\alpha 4$ nAChR but lower than that of $(\alpha 4\beta 2)_2\beta 2$ receptors (Kuryatov et al., 2008) **(Table 1.1)**. $(\alpha 4\beta 2)_2\alpha 5$ receptors desensitise more rapidly than $\alpha 4\beta 2$ nAChRs, and display the highest Ca^{2+} permeability of the $\alpha 4\beta 2^*$ nAChRs (Tapia et al., 2007). In addition, the $\alpha 5$ subunit confers sensitivity to positive allosteric modulation by galanthamine, which $(\alpha 4\beta 2)_2\beta 2$ and $(\alpha 4\beta 2)_2\alpha 4$ receptors lack (Kuryatov et al., 2008).

1.9   Subunit interfaces and stoichiometry-specific properties of α4β2 nAChRs

Work on the effects of Zn^{2+} on $\alpha 4\beta 2$ nAChRs (Moroni et al., 2008) has given insight into how the auxiliary subunit may confer functional signatures to $\alpha 4\beta 2$ nAChRs and it is described here. In one set of studies the effects of Zn^{2+} on the function of both $(\alpha 4\beta 2)_2\beta 2$ and $(\alpha 4\beta 2)_2\alpha 4$ nAChRs were studied because work on the related $GABA_A$ receptor and GlyR had shown that the effects of Zn^{2+} varies according to subunit composition (Miller et al., 2005; Bloomenthal et al., 1994; Smart et al., 1994). As mentioned previously, work on $\alpha 4\beta 2$ nAChR showed that Zn^{2+} exerts an inhibitory modulatory effect on $(\alpha 4\beta 2)_2\beta 2$ receptors, whilst it potentiates or inhibits, depending upon its concentration, the function of $(\alpha 4\beta 2)_2\alpha 4$ receptors. On the basis of homology modelling with the AChBP from several snail species (Brejc et al., 2001; Celie et al., 2004; Hansen et al., 2005) and the 4 Å resolution structural model of the *Torpedo* nAChR (Unwin, 2005), residues in the $\alpha 4$ and $\beta 2$ subunits that could contribute to Zn^{2+} coordination were systematically selected and mutated and then tested for effects on sensitivity to Zn^{2+}. This strategy led to the identification of two distinct sets of residues that may coordinate Zn^{2+}. One of these sites is inhibitory and is located at the interface between the (+) side of the $\beta 2$ subunit and the (-) side of an ACh-binding $\alpha 4$ subunit. The site is present on both stoichiometries and key contributors are $\alpha 4H195$ (loop F), and $\beta 2D218$ (loop C). The other site is potentiating and is present only on the $(\alpha 4\beta 2)_2\alpha 4$ nAChR. This site resides on

the α4(-)/α4(+) interface of the (α4β2)$_2$α4 nAChR, within a region that is homologous to the Zn^{2+} inhibiting site located on the β2(+)/α4(-) interface. α4H195 on the (-) face of an ACh-binding α4 subunit and α4E224 on the (+) side of non-ACh binding α4 subunit critically contribute to this site. Thus, the Zn^{2+} inhibiting and Zn^{2+} potentiating sites are located at equivalent positions, arising from subunit homology. Similar phenomena have been observed in other pseudo-symmetric proteins such as the $GABA_A$ receptor where the residues contributing to the benzodiazepine site are homologous to residues implicated in agonist binding (Sigel, 2005).

From the above discussion, it is clear that the non-agonist binding subunit in α4β2 nAChRs confers functional and pharmacological signatures to these receptors. How could these subunit interfaces impact α4β2 nAChRs properties? By analogy to the muscle α1γα1δβ1 nAChR (Unwin, 2005), it is presumed that in the α4β2 nAChR the subunit order around the channel is α4β2α4β2(α4/β2). Since the agonist binding sites are formed by conserved aromatic residues in the + face of the α4 subunit and the − face of the β2 subunit (Brejc et al., 2001; Unwin, 2005), the binding sites at the α4(+)/β2(-) interfaces are structurally identical, and thus unlikely to confer receptor subtype-specific functional signatures. However, the fact that the auxiliary subunit can be α4 or β2, leads to a different composition of non-agonist binding interfaces. In the (α4β2)$_2$β2 receptor there will be two β2(+)/α4(-) interfaces and a β2(+)/β2(-) interface, whereas in the (α4β2)$_2$α4 receptor there will be two β2(+)/α4(-) interfaces and an α4(+)/α4(-) interface. As the β2(+)/β2(-) and α4(+)/α4(-), interfaces are receptor subtype-specific, they are likely candidates for conferring functional signatures to α4β2 nAChRs. Similarly, the receptor-specific α4(-)/α5(+) and β2(+)/α5(-) in α4β2α4β2(α5) receptors are likely to play a key role in shaping the functional properties of this α4β2* nAChR subtype.

The hypothesis driving this thesis is that the auxiliary subunit confers receptor subtype functional signatures to the α4β2* nAChRs. These signatures could be (i) allosteric modulatory sites that form because of subunit homology, and/or (ii) receptor activation or inactivation characteristics that could arise from

interactions between closely apposed residues of the auxiliary and ligand-binding subunits, as suggested by the most recent structural data from Unwin (2005). The focus of this thesis is to examine the role of the α4(+)/α4(-) interface in the signature agonist profile of (α4β2)₂α4 nAChRs. **Chapter 3, 4** and **5** will present data that shows that this interface is largely responsible for the signature ligand sensitivity of (α4β2)₂α4 receptors.

1.10 Concatenated α4β2 nAChRs as tools to dissect the contribution of subunit interfaces to receptor function

Functional data from studies of α4β2 nAChRs assembled from loose α4 and β2 subunits are particularly difficult to interpret because of the concurrent expression of multiple stoichiometric arrangements, even after transfection/injection of drastic ratios of α4 and β2 subunits (Zwart et al., 2006; Carbone et al., 2009). This problem is particularly exacerbated by the fact that the α4 and β2 subunits are homologous and fairly conserved, which in practice makes the identification of ligand binding sites or down-stream pathways difficult (e.g., Moroni et al., 2008). This problem has been circumvented by concatenating the subunits covalently at the DNA level to create receptors with a defined subunit composition and subunit order. Carbone et al., (2009) have shown that covalently linking α4 and β2 subunits into pentameric concatamers with a subunit order of β2_α4_β2_α4_β2 or β2_α4_β2_α4_α4 produce receptors that express well in *Xenopus* oocytes **(Fig. 1.10)**. These concatenated receptors recapitulate the functional properties of non-linked (α4β2)₂β2 or (α4β2)₂α4 receptors. In addition, the functional expression of both β2_α4_β2_α4_β2 or β2_α4_β2_α4_α4 receptors is up-regulated by co-expression with chaperone protein 14-3-3 and in this thesis it is shown that their pattern of desensitisation by chronic exposure to agonist is also maintained **(see Chapter 4)**. Thus, subunit concatenation does not impair the functional properties of α4β2 nAChRs, making concatameric α4β2 nAChRs excellent tools to analyse the role of individual subunit interfaces on receptor function.

In addition to their ability to recapitulate the functional properties of α4β2 nAChRs, fully concatenated α4β2 nAChRs permit the introduction of mutations

in defined subunits. This in turn offers the unique possibility of studying the contribution of individual subunit interfaces to receptor function. Full subunit concatenation has contributed to the localization of a novel binding site for benzodiazepines in the $GABA_A$ receptor and has shown differences in the functional properties of the two agonist sites of the $GABA_A$ receptor (for a review see Sigel et al., 2009). The studies that are next described have been carried out on fully concatenated $\alpha4\beta2$ nAChRs.
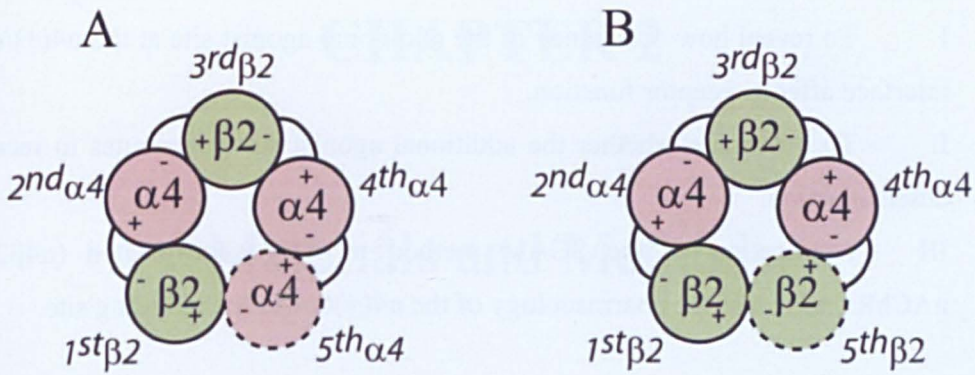
Figure 1.10. α4β2 concatenated receptors. (A) (α4β2)₂α4; (B) (α4β2)₂β2 receptors. The auxiliary subunit is outlined by dashed black lines.

Aims of the thesis

The overall goal of this study was to unveil the role of the $\alpha4(+)/\alpha4(-)$ subunit interface on the functional signatures of the $\alpha4\beta2$ nAChR. The use of concatameric $\alpha4\beta2$ nAChRs led during the early stages of this study to the identification of an additional fully operational ACh binding site at the $\alpha4(+)/\alpha(-)$ interface of the $(\alpha4\beta2)_2\alpha4$ nAChR. This finding led to the following specific aims.

I   To reveal how occupancy of the additional agonist site at the $\alpha4(+)/\alpha4(-)$ interface affects receptor function.

II   To determine whether the additional agonist site contributes to receptor desensitisation.

III   Application of the SCAM method to fully concatenated $(\alpha4\beta2)_2\alpha4$ nAChRs, to reveal the pharmacology of the $\alpha4(+)/\alpha4(-)$ ACh binding site.

CHAPTER 2

Materials and Methods

2.1 Reagents

Standard laboratory chemicals were of Analar grade. Collagenase Type IA, ACh, Epi and DhβE were purchased from Sigma-Aldrich (UK). Cyt, Nic and Saz- were purchased from Tocris Chemicals (UK). TC-2559 was a gift from Targacept Inc. (Winston-Salem, NC, USA) and Var was a gift from Pfizer (USA). Methenosulphate reagents (MTS) aminoethyl methanethiosulfonate (MTSEA) and [2-(Trimethylammonium)ethyl]methanethiosulfonate (MTSET) were purchased from Toronto Chemicals (Canada).

2.2 Animals

Xenopus laevis (*X. laevis*) were purchased from Portsmouth University. *Xenopus* care and experimental procedures were in accordance with the Home Office regulations and were approved by the Animal Use Committee of Oxford Brookes University. Briefly, *X. laevis* were housed in black tanks filled with dechlorinated water (> 15 L per toad) that was kept in a temperature-controlled room (18 C°). The animals were kept under a fixed 12 h light/dark cycle. Frogs were fed twice a week with worms purchased from Willy Worms (Yorkshire. UK). The water was refreshed twice a week.

2.3 Molecular Biology

DNA ligations, maintenance and growth of *Escherichia coli* bacterial strains and the use of restriction enzymes were carried out following the procedures described by Sambrook et al., (1989). Plasmid isolation and DNA gel purification were carried out using commercially available kits (Promega, UK). Capped cRNA coding for wild type and mutant concatameric receptors was synthesized by in vitro transcription from SwaI-linearized cDNA template using the mMessage mMachine T7 kit (Ambion, UK.). The integrity and size of the cRNA transcripts was confirmed using RNA gel electrophoresis.

2.3.1 Single Point Mutations

Point mutations were carried out using the QuikChange™ Site-Directed Mutagenesis Kit (Stratagene, The Netherlands). Oligonucleotides for PCR (Polymerase chain reaction) reactions were purchased from Eurofins (UK). The

full-length sequence of wild type and mutated subunit cDNAs were verified by DNA sequencing (BiosourceScience, Oxford). In order to increase the number of positive transformants, the protocol used was slightly modified from the manufacturer's instructions, as described below.

1)   Oligonucleotides primers (35 to 45 long, Melting T° > 80 C°) were synthesised carrying the desired mutations in the middle.

2)   The synthesised primers were diluted to a final concentration of 125 ng/µl and used in the subsequent PCR reaction.

3)   The PCR mix consisted of the following:

5 µl Pfu Buffer 10X

1 µl DNA template (stock 50 ng/µl)

1 µl of sense primer (125 ng)

1 µl of antisense primer (125 ng)

3 µl dimethyl sulphoxide

5 µl dNTPs (from 2 mM stocks)

1 µl High Fidelity Pfu enzyme

33 µl Nuclease free water

4)   The parameters for the PCR run were as follows:

Segment	Number of Cycles	Holding Temperature (C)	Time (minutes)
1	1	95	1
2	16	95	0.5
		55	1
		68	1 min per kbp
3	1	68	1 min per kbp

5)   1µl of the enzyme DpnI was added to the PCR mixture in order to degrade the parental methylated DNA, which corresponds to the template (non-

mutated DNA), and to leave intact only the newly formed DNA (non-methylated and likely containing the desired mutation).

6) X-Gold Competent cells were transformed with 30 μl of the digestion product. After overnight incubation at 37 C°, 3 colonies were picked and amplified by growing them in 10 ml of CircleGrow medium (Anachem, UK) at 37 C°. After overnight growth, the plasmid was isolated from the bacteria using commercially available DNA purification kits (Promega, UK), and fully sequenced to confirm the presence of the desired mutation and verified the sequence of the non-mutated regions.

The residue numbering used throughout this thesis includes the signal sequence. To obtain the position in the mature form, subtract 28 for α4 and 26 for β2.

2.3.2 Concatameric (α4β2)₂α4 and (α4β2)₂β2 receptors

The fully concatenated form of the (α4β2)₂α4 and (α4β2)₂β2 isoforms, constructs β2_α4_β2_α4_α4 and β2_α4_β2_α4_β2 were engineered as previously described by Carbone et al. (2009). Briefly, the signal peptide and start codon were removed from all the subunits but the first (a β2 subunit) and the subunits were bridged by AGS (alanine, glycine, serine) linkers. The number of AGS triplets was 6 between β2 and α4 subunits, and 9 between α4 and β2 subunits or between α4 subunits. Only the last subunit in the construct (an α4 subunit) contained a stop codon. The subunits were subcloned into a modified pCI plasmid vector (Promega, UK) using unique restriction enzyme sites flanking the N- and C-terminals of each subunit. Wild type or mutant concatenated receptors were assayed for integrity by determining the ACh sensitivity of concatenated receptors co-expressed with an excess of β2 or α4 monomers carrying the LT reporter mutation (L9'T in the second transmembrane domain). No changes were observed in comparison to constructs expressed alone. This indicates that the constructs used in this study did not degrade into lower-order concatamers or monomers as such degradation products would incorporate the β2LT or α4LT monomers into receptors of higher sensitivity to ACh than the intact concatenated (α4β2)₂α4 receptors (Groot-Kormelink et al., 2004). Henceforth,

concatenated receptors will be referred to as β2_α4_β2_α4_α4 whereas (α4β2)$_2$α4 or (α4β2)$_2$β2 will be used to denote receptors assembled from loose α4 and β2 subunits when α4 subunits are respectively, in excess or shortage over β2 subunits.

2.3.3 Engineering mutant β2_α4_β2_α4_α4 receptors

To introduce mutations into specific regions of β2_α4_β2_α4_α4 receptors, the mutation was first introduced into the appropriate individual subunit subcloned into a modified pCI plasmid as described in section 2.3. After confirming the presence of the desired mutation and verifying the sequence of the non-mutated regions, the subunit cDNA was digested with appropriate unique flanking restriction enzymes and then ligated into the desired position in the concatamer using standard cDNA ligation protocols with T4 ligase (New England Biolabs, UK). The presence of the mutated subunit was also confirmed by DNA sequencing. Following ligation and DNA amplification, the appropriate subunit was cut by enzyme restriction digestion from the concatamer and sequenced by standard DNA sequencing. For clarity, mutations in the concatameric receptors are shown as superscript positioned in the (+) or (-) face of the mutated subunit (e.g., in β2_^{W182A}α4_β2_α4_α4 the mutation W182A is located in the (+) face of the α4 subunit occupying the second position of the linear sequence of the concatamer, (see **Chapter 3** for experimental evidence showing the spatial orientation of the subunits in the concatamer).

2.3.4 Chimeric β2_α4_β2_α4_β2/α4 receptor

A subunit made of the N-terminal of the β2 subunit and the remaining part of the α4 subunit was ligated to β2_α4_β2_α4 to construct chimera β2_α4_β2_α4_β2/α4. β2_α4_β2_α4_β2/α4 was constructed by ligating a chimera β2/α4 subunit into the 5th position of the wild type β2_α4_β2_α4_α4 receptor. Chimeric β2/α4 subunit was constructed by first adding to both the α4 and β2 subunits a BspEI restriction enzyme site at the end of the ECD within a region, IRR, that is conserved in the nAChR family. The site was used to cut the subunits into two portions, the ECD-IR and the remaining subunit containing the four TMDs and the C-terminus (R-TMD-C-terminus). After digestion of the

subunits with BspEI and after gel purification, the restricted sites are ligated using standard DNA ligation procedures to form β2/α4 chimera. Thus, chimera β2/α4 comprises the N-terminal of β2 (1 to R231) and the remaining part of the α4 subunit (R241 to I628) to its stop codon.

2.4 *Xenopus laevis* oocytes preparation

Xenopus oocytes were collected from adult female *Xenopus laevis*, anaesthetised and sacrificed according to Home Office guidelines. A visceral incision was made through the skin and body wall. The ovaries were removed and stored in OR2 solution (82mM NaCl, 2mM KCl, 2mM MgCl 2.5mM HEPES (N-2-hydroxyethylpiperazine-N'-2-ethansulphonic acid) adjusted to pH 7.6 with NaOH). Only oocytes at the stage V and VI of maturation were isolated. The theca and epithelial layers were removed enzymatically by incubating the oocytes for about 2 h in Type IA collagenase (2 mg/ml) dissolved in OR2 and placed on a rotating platform at room temperature. Oocytes were maintained at 18 °C in an incubator in a modified Barth's medium (88 mM NaCl, 1 mM KCl, 2.4 mM NaHCO$_3$, 0.3 mM Ca(NO$_3$)$_2$, 0.41 mM CaCl$_2$, 0.82 mM MgSO$_4$, 15 mM HEPES supplemented with streptomycin 1 µg/ml, 1 U/ml penicillin, 50 µg/ml neomycin and 5% horse serum, pH 7.6 (adjusted with NaOH).

2.5 Microinjection of cRNA

Needles for microinjection were prepared from Drummond glass capillaries (Sartorius, UK), which were pulled in one stage using a horizontal microelectrode puller (Campden Instruments–Model 753). Prior to use, the tip of a selected needle was broken using fine forceps to give a narrow tip length of approximately 3 mm with an external ranging from 1.0 to 1.5 µm. The needle was back-filled with light mineral oil and loaded on to a Nanoject II microinjector (Drummond, USA). Wild type or mutant concatameric receptor cRNA were injected into the oocyte cytoplasm (50.6 nl at 0.1 ng/nl) as illustrated in **Fig.2.1**. Injected oocytes were transferred to 96 well sterile dish (one oocyte per well) containing modified Barth's solution and incubated at 18 C° for a maximum of 5 days.
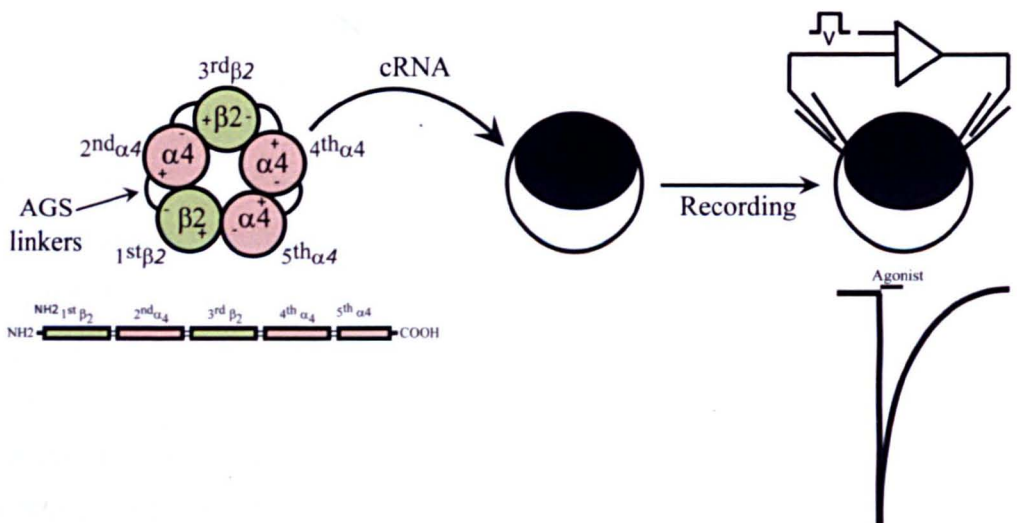
Figure. 2.1. **Diagram showing β2_α4_β2_α4_α4 cRNA injection into Xenopus oocytes.** After 2-3 days post-injection currents were recorded using two-electrode voltage clamp technique.

2.6   Electrophysiological Recordings

After 2-3 days post-injection oocytes were selected according to their appearance. Only oocytes with integral membrane and no signs of degradation were chosen for electrophysiological recordings. Oocytes were placed in a 30μl recording chamber (Digitimer Ltd, UK) and bathed with a modified Ringer solution (in mM: NaCl 150, KCl 2.8, HEPES 10, $BaCl_2$ 1.8; pH 7.2, adjusted with NaOH). A gravity driven perfusion system was used for all the experiments. All solutions were freshly made prior to recordings.

Oocytes were impaled by two electrodes connected to a Geneclamp 500B (Molecular Devices, USA) for standard voltage clamp recordings as illustrated in **Fig. 2.1**. Briefly, electrodes were made from borosilicate capillary glass (Harvard Apparatus, GC 150 TF) using a vertical two stage electrode puller (Narishige PP-83) to give a top diameter of 1-2μm. Prior to recordings electrodes were filled with 3 M KCl and only electrodes with a resistance between 0.5 and 2 MΩ were used for voltage clamping. Oocytes were continually perfused with fresh Ringer

solution at a rate of 10ml/min switching between different solutions occurred through manually activated valves.

2.7 CRC for agonists and antagonists

CRC for agonists were obtained by normalizing agonist-induced responses to the control responses induced by a near-maximum effective agonist concentration, as previously described (Moroni et al., 2006; Mazzaferro et al., 2011; Carbone et al., 2009). A minimum interval of 5 min was allowed between agonist applications to ensure reproducible recordings. Agonist CRC data were first fitted to the one-component Hill equation:

$$I = I_{max}/[1 + (EC_{50}/x)^{nH}]$$

Where EC_{50} represents the concentration of agonist inducing 50% of the maximal response (I_{max}), x is the agonist concentration and *nH* the Hill coefficient. When agonists induced biphasic receptor activation, agonist CRC were fitted with the sum of two Hill equations, (two-component Hill equation). Data were fit to the following equation from Prism v 5 (GraphPad 5 software):

$$Y=Top - Bottom + Span * Frac/(1 + 10^{\wedge}((logEC_{50\_1}-X)*nH1)) + Span$$
$$* (1-Frac)/(1 + 10^{\wedge}((LogEC_{50\_2}-X) * nH2))$$

where Top and Bottom are the plateaus at the right and left ends of the curve in the same units as Y; $logEC_{50\_1}$ and $logEC_{50\_2}$ are the concentrations that give half-maximal high sensitivity or low sensitivity stimulatory effects respectively; nH1 and nH2 are the unitless slope factors or Hill coefficients; Frac is the proportion of maximal response due to the higher sensitivity component; and Span is a fitted coefficient between 0 and 1 that gives the weight of the first component.

To determine the effects of the $\alpha4\beta2$-selective competitive antagonist DhβE on the ACh responses of wild type or mutant receptors, the antagonist was included in the ACh and perfusing (Ringer) solution. The responses to ACh obtained in

the presence of the antagonists were normalised to control ACh responses (responses to ACh evoked in the absence of the antagonist). The ACh responses used were elicited by concentrations close to the EC_{50} concentration.

2.8 Desensitisation protocol

Desensitisation of α4β2 nAChRs was assessed by determining the degree of functional inhibition caused by prolonged exposure to ACh as measured under equilibrium conditions. The protocol used was based on that designed by Corringer al., (1998) to measure desensitisation of α7-5-HT$_3$ chimeric receptors. Oocytes injected with nAChR cRNAs were challenged approximately every 90 s by short pulses (2 s) of ACh at a concentration near the ACh EC_{50} (test pulses), first in the absence and then during a prolonged perfusion with Ringer solution containing low concentrations of ACh (prepulse). Prepulses were applied until the amplitude of the test pulses were constant. Although the extent and rate of inhibition varied depending on the ACh concentration of the prepulse and the nature of the receptor under study, a 10 min prepulse period was sufficient to reach steady-state level of desensitisation for all ACh concentrations used. Desensitisation data were fitted using non-linear regression to the one component Hill equation: $I = I_{min} + (I_{max}-I_{min})/(1+10^{((LogIC_{50}-X)*nH)})$ where IC_{50} is the concentration of drug that inhibits 50% of maximum response. The amplitude of current at steady state conditions was used for data analysis.

2.9 Substituted cysteine accessibility method (SCAM)

The substituted cysteine accessibility method (SCAM) was used to both assess the impact of loop C of the auxiliary subunit (fifth subunit) of β2_α4_β2_α4_α4 receptors on receptor activation and the nicotinic ligand selectivity of ACh binding sites at α4(+)/β2(-) and α4(+)/α4(-) interfaces. SCAM was first applied to pLGIC to identify the amino acid residues lining the ion channel of the muscle nAChR (Karlin & Akabas, 1998). Since then, SCAM has become a powerful experimental strategy that has been successfully applied to gain invaluable insights into diverse aspects of pLGIC such as amino acid residues contributing to competitive or allosteric ligands bindings, structure of (e.g., Boileau et al., 1999; Holden & Czajkowski, 2002), conformational changes induced by agonist

or allosteric modulators, and secondary structure of functional domains. SCAM involves the introduction of cysteines, one at a time, into a protein region and the subsequent application of thiol-specific reagents to the engineered residues to determine whether they are modified by the thiol reagents (Karlin & Akabas, 1998). Modification of the introduced cysteine is monitored using electrophysiological or biochemical assays.

2.9.1 Modification of loop C by SCAM

MTSEA and MTSET were used to modify covalently a free cysteine residue in loop C. The free cysteine residue was created by dismantling the disulphide bond between vicinal C225 and C226 at the tip of loop C, through serine substitution of C226. The effect of the MTS reagents was assessed as illustrated in **Fig. 2.2.** Oocytes expressing receptors with cysteine substituted loop C or wild type receptors were first challenged with control ACh pulses (EC$_{50}$ x 5) every 5 minutes until a stable response was obtained. Oocytes were then perfused with Ringer solution containing MTSEA (2.5 mM) or MTSET (1 mM) for 180 seconds, after which time the impaled cells were washed with Ringer solution for 60 seconds. After washing, ACh was applied every 5 min until the amplitude of the responses was constant. The average of the current amplitudes prior to application of MTS reagents was the control response current ($I_{initial}$), and the average of current amplitudes after rinsing was the average response after MTS application ($I_{after\ MTS}$). The effect of the MTS reagents was estimated using the equation, % Change = $((I_{after\ MTS}/I_{initial}) - 1)$ x 100. The covalent effects of MTS were confirmed by exposing the oocytes to the reducing reagent dithiothreitol (DTT) (5mM) for 60 s (MTSET-treated oocytes) or 1 mM for 180 s (MTSEA-treated oocytes). In all cells tested the response after DTT treatment was comparable to the one prior to the MTSET or MTSEA application, confirming that the functional changes observed were due to the covalent modification of C225 by the MTS reagents.

2.9.2 Modification of ACh binding sites using SCAM

MTSET was used to modify covalently a cysteine residue introduced at the agonist site at α4(+)/β2(-) and α4(+)/α4(-) interfaces. The amino acids mutated,

one at a time, to cysteine were β2L146 and α4T152. Previous studies have shown that β2L146 in loop E at α4(+)/β2(-) is suited for cysteine substitution studies: β2L146C has little impact on receptor activation but in the presence of MTS reagents produces a profound decrease in the responses of α4β2 receptors to ACh (Papke et al., 2011). Structural modelling of the agonist site at the α4(+)/α4(-) interface showed that α4T152 occupies a position homologous to that to β2L146 in the agonist site at the α4(+)/β2(-) interfaces. Therefore, β2_α4_β2_α4^{T152C}_α4 and β2^{L146C}_α4_β2_α4_α4 receptors were engineered to characterise the pharmacology of agonist sites at, respectively the α4(+)/α4(-) and α4(+)/β2(-) interfaces. Mutant and wild type concatamers were expressed in *Xenopus* oocytes, and characterised using two electrode voltage clamping procedures, as described above.

2.9.3 Covalent modification of introduced cysteines by MTSET reagent

The effect of the MTSET reagent on agonist responses was assessed as shown in **Fig. 2.3**. Briefly, oocytes expressing receptors with a free cysteine or wild type receptors were first challenged with a control agonist (ACh, Cyt, Var, TC-2959) concentration every 5 min until a stable response was obtained. Oocytes were then perfused with Ringer's solution containing MTSET (1 mM) for 120 s after which time the impaled cells were washed with Ringer's solution for 90 s. After washing, the agonist was applied again every 5 min until the amplitude of the responses was constant to determine accessibility to the modified cysteine residue by the MTS reagent. The average of the current amplitudes prior to application of MTS was the control response current ($I_{initial}$), and the average of current amplitudes after rinsing was the average response after MTSET application ($I_{after\ MTS}$). The effect of the MTS reagents was estimated using the following equation: % Change = $((I_{after\ MTS}/I_{initial}) - 1) \times 100$. For both mutants, (β2_α4_β2_α4^{T152C}_α4 and β2^{L146C}_α4_β2_α4_α4 and wild type (β2_α4_β2_α4_α4) receptors, the concentration of MTSET used was 1mM (the optimal concentration for MTSET; Zhang & Karlin 1997). All mutants were also tested for the specificity of the MTSET reaction by treating the oocytes with

DTT (1 mM, 120 s), which reversed the inhibition caused by covalent modification.
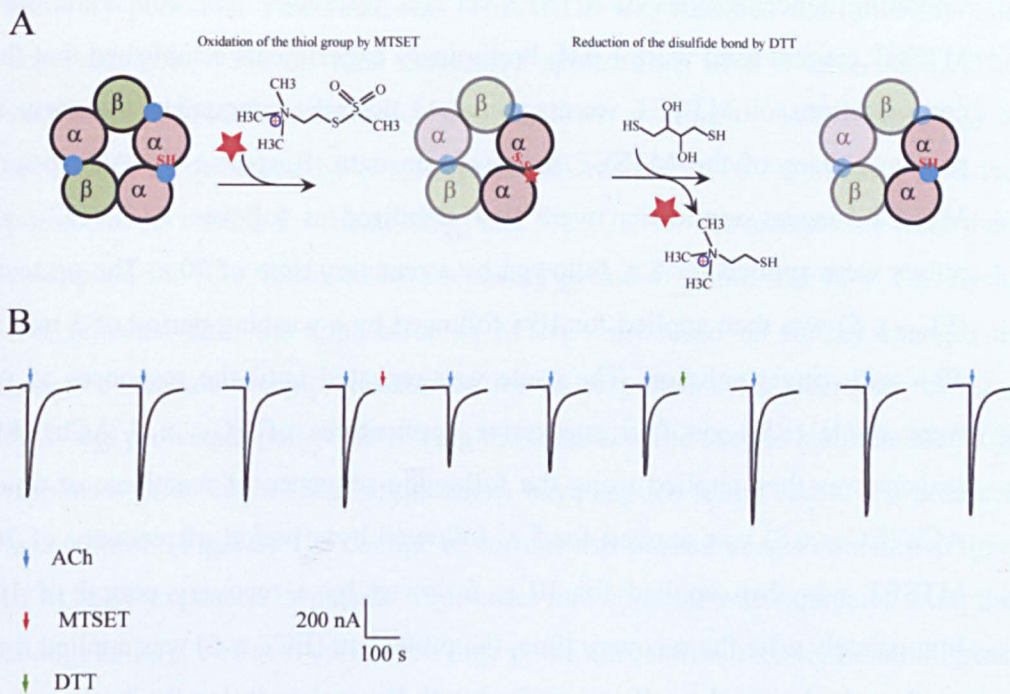
Figure 2.2. Covalent MTS modification of substituted cysteine in an identified subunit interface. The figure shows the effect of MTSET treatment on the ACh responses of the $\beta2\_\alpha4\_\beta2\_\alpha4^{T152C}\_\alpha4$ mutant. **(A)** Using concatenated $(\alpha4\beta2)_2\alpha4$ nAChRs it is possible to introduce single point mutations at an identified subunit interface. The diagram shows the reaction of MTSET with a cysteine introduced in the complementary face of the agonist site at the $\alpha4(+)/\alpha4(-)$ interface. The first reaction is between the thiolic group of the cysteine and MTSET whereas the second reaction shows the reversibility of the disulphide bond (cys-MTSET) by using DTT. **(B)** Representative traces that shows max inhibition of ACh current (blue arrows) after maximal MTSET concentration (1mM) treatment. MTSET is applied for 120 s (red arrow). The reaction is fully reversible after treatment with 1mM DTT (green arrow), as a consequence the level of ACh current, is completely re-established as prior the MTSET application.

2.9.4 MTSET reaction rates

To determine whether nicotinic ligands recognize the agonist site at the $\alpha4(+)/\alpha4(-)$ interface, we assayed the effect of nicotinic ligands on the rate of MTSET modification of C152. If reversible ligands reduce MTSET reaction rates, it was inferred that the reversible ligands bind the site, thus impeding,

likely by steric hindrance, the modification of the introduced cysteine residue by MTSET. The rate of MTSET covalent modification of introduced cysteines was first determined by measuring the effect of sequential applications of sub-saturating concentrations of MTSET on I_{ACh} responses. The concentrations of MTSET reagent used were 1 μM. Preliminary experiments established that these concentrations of MTSET were optimal to describe adequately the early and plateau phases of the MTSET reaction rate data. Responses to ACh prior to MTSET reagent application were first stabilised as follows: ACh (EC_{50} x 5) pulses were applied for 5 s, followed by a recovery time of 70 s. The protectant (EC_{50} x 5) was then applied for 10 s followed by a washing period of 3 min and 40 s with ringer solution. The cycle was repeated until the responses to ACh were stable (<5% on four successive applications of EC_{50} x 5 ACh). MTS reagent was then applied using the following sequence of reactions: at time 0, ACh (EC_{50} x 5) was applied for 5 s, followed by a period of recovery of 70 s; MTSET was then applied for 10 s, followed by a recovery period of 10 s. Immediately after the recovery time, the protectant (EC_{50} x 5) was applied for 10 s, after which time the cell was washed with Ringer's solution for 3 min and 40s. This cycle was repeated until MTSET applications produced no further changes in I_{ACh}. Because α4β2 nAChRs are highly prone to long-term desensitisation when exposed to agonists, the protectant was applied in the control experiments prior to the MTS reagent to correct for any process of desensitisation that could develop during the protection assays, when the protectant is added together with the MTSET reagent. To confirm that any observed decrease in I_{ACh} was due to the effects of MTSET and not to receptor desensitisation, ACh and protectant pulses (following the same scheme used to stabilize the ACh responses prior the MTSET application) were applied at the end of the protocol as illustrated in **Fig. 2.3.**

2.9.5 Protection assays with agonist/antagonists

The effects of agonists and antagonists on the rate of MTSET modification were tested by co-applying MTSET with agonist (5 x EC_{50}) or antagonist (5 x IC_{50}). The protocol used was identical to the one used to determine the rate of MTSET reaction, except that the reversible ligand (protectant) was co-applied with

MTSET reagent. The sequence of steps illustrated in **Fig. 2.3** was as follows: I_{ACh} was stabilised by applying 5 x EC_{50} pulses of ACh for 5 s, followed by a 70 s period of recovery, the protectant was then applied for 10s, followed by a recovery period of 3 min and 40s. This cycle was repeated until stability was achieved. (i.e., <5% on four successive applications of 5 x EC_{50} ACh). The sequence of MTSET reactions was as follows: at time 0, ACh (5 x EC_{50}) is applied (5 s), followed by a brief period of recovery (70 s); MTSET and the protectant (5 x EC_{50} for the agonists and 5 x IC_{50} for the antagonist) were then co-applied for 10 s, followed by a recovery period of 3 min and 40 s. This cycle was repeated until the application of MTSET produced no further changes in I_{ACh}. To exclude receptor desensitisation as responsible for decreases in I_{ACh}, ACh and protectant pulses (following the same scheme used to stabilize the ACh responses prior the MTSET application) were applied at the end of the protocol as a control. **(Fig.2.3)** The change in current was plotted versus cumulative time of MTSET exposure. A pseudo–first-order rate constant was calculated from the change in I_{ACh}. Peak values at each time point were normalized to the initial peak at time 0 s, and a pseudo–first-order rate constant ($k1$) was determined by fitting the data with a single exponential decay equation: $y = span \times e^{-kt} + plateau$ using Prism v.5.0 (GraphPad Software). Because the data are normalized to values at time 0, span = 1 - plateau. The second order rate constant ($k2$) for MTSET reaction was determined by dividing the calculated pseudo–first-order rate constant by the concentration of MTSET reagent used. The drug concentrations used to monitor changes in MTSET reactions were as follows: receptor $\beta2\_\alpha4\_\beta2\_\alpha4^{T152C}\_\alpha4$: MTSET 1 μM, ACh 1mM, Cyt 70 μM, Var 12 μM, TC2559 12 μM, Saz-A 1 μM; receptor $\beta2^{L146C}\_\alpha4\_\beta2\_\alpha4\_\alpha4$: MTSET 10 μM, ACh 1.6 mM.

2.10 Statistical analysis

Data analyses were performed using GraphPAD-Prism software (GraphPAD, CA, USA). Data were pooled from at least three different batches of oocytes. An F-test determined whether the one-site or biphasic model best fit the data; the simpler one-component model was preferred unless the extra sum-of-squares F test had a value of p less than 0.05. Log EC_{50} values for ACh or ACh plus DhβE,

changes in current amplitudes in response to mutations or MTS application were analysed using one-way ANOVA (analysis of variance) with a Dunnett or Bonferroni post hoc correction for the comparison of all mutated receptors, to determine significance between wild type and mutant receptors. Significance levels between mutant receptors were determined using unpaired t tests. Data are plotted as mean ± Standard error of the mean (SEM). Fit parameter values are the best fitting values with the SEM values estimated from the fit.
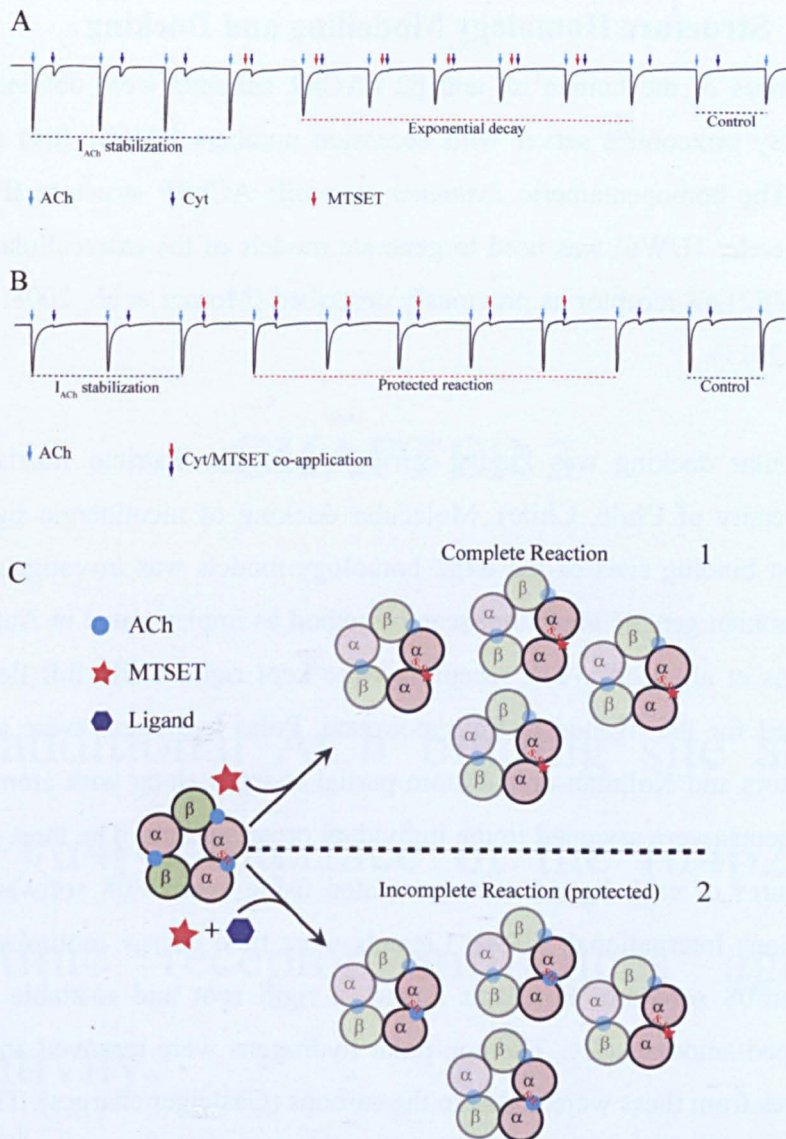
Figure 2.3. **Protection assay experiment for the partial agonist Cyt at the α4(+)/α4(-) interface of the β2_α4_β2_α4^{T152C}_α4 mutant.** **(A)** Representative traces of ACh responses prior, during and after cumulative MTSET application to determine the k_1 for the exponential decay of I_{ACh} (azure arrows) in presence of the partial agonist Cyt (blue arrows). MTSET (red arrows) was applied prior to Cyt. From the left to the right, the dashed lines, show respectively I_{ACh} stabilization prior the MTSET application (black dashed line), the exponential I_{ACh} decay due to MTSET reaction with the cysteine free (red dashed line) and the final control (black dashed line). **(B)** When Cyt and MTSET were co-applied (protected reaction), MTSET did not impair the I_{ACh} currents. **(C)** General scheme of the protection assay experiment. After cumulative MTSET application, the reaction is complete **(C, 1)** and the result is a decrease of the I_{ACh} current. However when MTSET is co-applied with a ligand that competes or impedes the MTSET reaction with the free cysteine introduced in the agonist site at the α4(+)/α4(-) interface, the reaction rate is slower **(C, 2)**.

2.11 Structure Homology Modelling and Docking

Sequences of the human α4 and β2 nAChR subunits were obtained from the ExPASy proteomics server with accession numbers P43681 (α4) and P17787 (β2). The homopentameric *Lymnaea stagnalis* AChBP structure (Protein Data Bank code: 1UW6) was used to generate models of the extracellular domain of the (α4β2)$_2$α4 receptor as previously described (Moroni et al., 2008; Mazzaferro et al., 2011).

Molecular docking was kindly carried out by Dr Patricio Iturriaga-Vasquez (University of Chile, Chile). Molecular docking of nicotinergic ligands at the agonist binding sites of the α4β2 homology models was investigated using the Lamarckian genetic algorithm search method as implemented in AutoDock v4.0 (Morris et al., 1998). The receptors were kept rigid, while full flexibility was allowed for the ligands to translate/rotate. Polar hydrogens were added to the receptors and Kollman-united atom partial charges along with atomic solvation parameters were assigned to the individual protein atoms. The three-dimensional structures of each ligand were generated using spartan'08 software (Software Solutions International, USA). Ligands were then energy minimized using the spartan'08 software. For each ligand, a rigid root and rotatable bonds were assigned automatically. The non-polar hydrogens were removed and the partial charges from these were added to the carbons (Gasteiger charges). The atom type for aromatic carbons was reassigned in order to use the AutoDock 4.0 aromatic carbon grid map. Docking was carried out using 60 × 60 × 60 grid points with a default spacing of 0.375 Å. The grid was positioned to include the full ligand binding pocket in the central part of the α4/β2 or α4/α4 subunit interfaces so as to allow extensive sampling around residue α4W182 (W143 in mature AChBP). Within this grid, the Lamarckian genetic search algorithm was used with a population size of 150 individuals, calculated using 200 different runs (*i.e.* 200 dockings). Each run had two stop criteria, a maximum of 1.5 × 10^6 energy evaluations or a maximum of 50,000 generations, starting from a random position and conformation; default parameters were used for the Lamarckian genetic algorithm search.

CHAPTER 3

An additional ACh binding site at the α4(+)/α4(-) interface of the (α4β2)2α4 nicotinic receptor influences agonist sensitivity

3.1   Introduction

The structural determinants that bestow isoform-specific agonist sensitivity to the alternate $\alpha4\beta2$ nAChRs have not been fully elucidated. Nonetheless, work on the effect of Zn^{2+} on $\alpha4\beta2$ nAChRs has highlighted the auxiliary subunit as a key determinant of stoichiometry-specific properties. Thus, it has been shown that the $\alpha4(-)/\alpha4(+)$ interface contains a Zn^{2+} potentiating site within a region that is homologous to a Zn^{2+} inhibiting site located on $\beta2(+)/\alpha4(-)$ interfaces in both receptor forms (Moroni et al., 2008). Furthermore, crystal structures of the AChBP lacking vicinal cysteines in loop C bound to allosteric ligands have suggested that interactions between modulators and heteromeric nAChRs may occur at non-$\alpha4$ interfaces through interactions with conserved aromatic residues (Hansen & Taylor, 2007). Therefore, because of subunit homology, it is plausible to speculate that additional agonist binding sites may be present at the $\beta2(+)/\beta2(-)$ and $\alpha4(+)/\alpha4(-)$ interfaces that are responsible for the isoform-specific agonist sensitivity of the alternate forms of the $\alpha4\beta2$ nAChR.

In this chapter, the possible impact of the $\alpha4(+)/\alpha4(-)$ interface on the agonist sensitivity of the $(\alpha4\beta2)_2\alpha4$ nAChR was investigated. Using fully concatenated $(\alpha4\beta2)_2\alpha4$ nAChRs containing a chimera $\beta2/\alpha4$ auxiliary subunit, it was found that the $\alpha4(+)/\alpha4(-)$ interface appears to define the agonist sensitivity of $(\alpha4\beta2)_2\alpha4$ receptors. Mutagenesis studies in conjunction with functional assays led to the identification of an additional ACh binding site at the $\alpha4(+)/\alpha4(-)$ interface. The site is capable of binding ACh, as suggested by functional assays of mutant receptors engineered by alanine substitution of conserved aromatic residues contributing to the consensus agonist sites located at $\alpha4(+)/\beta2(-)$ subunit interfaces. Subsequently, using mutated receptors with a free cysteine residue in loop C, together with covalent modifications with MTS reagents, it was demonstrated that the additional site contributes directly to channel gating. Overall, the studies described in this chapter strongly suggest that the additional site at the $\alpha4(+)/\alpha4(-)$ is operational and that its contribution to receptor activation defines the agonist sensitivity of the $(\alpha4\beta2)_2\alpha4$ nAChR isoform.

3.2   Results

3.2.1 Position of the auxiliary subunit and agonist sites in β2_α4_β2_α4_α4 nAChRs

The conservation of aromatic residues contributing to the agonist binding site in nAChR subunits, together with homology modelling of the extracellular domain of the (α4β2)$_2$α4 nAChR, suggested a putative ACh site at the α4(+)/α4(-) interface **(Figs. 3.1B, C)**. The primary (+) face of this putative agonist site would be contributed by the auxiliary α4 subunit, whilst the complementary (-) face would be contributed by an α4 subunit that simultaneously provides the primary face of the consensus agonist site at an α4(+)/β2(-) interface. The putative site is homologous to the agonist site at the α4(+)/β2(-) interfaces, having the conserved residues α4Y126 (loop A), α4W182 (loop B), α4Y223 and α4Y230 (loop C), on the primary face of the binding site. On its complementary side, α4W88 (loop D) is in homologous position to β2W82 in the agonist sites at α4(+)/β2(-) interfaces **(Fig. 3.1 C)**. The homologous residues in *Torpedo* and muscle nAChR are α1Y93, α1W149, α1Y190 and α1Y198, and residues W55 and W57 located in the complementary ε/γ or δ subunits of the binding site (Corringer et al., 2000).

To obviate uncertainties about subunit assembly, stoichiometry and positions, especially concerning placement of mutant or chimeric subunits in the additional as opposed to the consensus agonist binding positions when engaging heterologous expression from loose subunits, the studies described in this chapter were conducted using, as a template, a fully concatenated form of the (α4β2)$_2$α4 nAChR. Functional studies of β2_α4_β2_α4_α4 receptors expressed heterologously in *Xenopus* oocytes have shown that they replicate the functional properties of (α4β2)$_2$α4 nAChRs (Carbone et al. 2009). It has been shown previously that the α4 subunit is involved either in inhibitory effects of Zn^{2+} (due to ion binding at β2(+)/α4(-) interfaces) or in potentiating effects of Zn^{2+} (due to ion binding at the α4(+)/α4(-) interfaces) (Moroni et al., 2008). To determine which α4 subunit contributes to the Zn^{2+} potentiating site in β2_α4_β2_α4_α4 nAChRs, alanine substitution of α4H195 was carried out individually in the three α4 positions of the concatenated receptor **(Fig. 3.2)**. When the mutation was

incorporated into the α4 subunit in either the second or fifth position of the concatamer, the sensitivity to potentiation by Zn^{2+} was enhanced. However, when the mutation was introduced into the fourth position of the receptor, the potentiating effect of Zn^{2+} was almost abolished. The explanation for this result is that H195 in the α4 subunits at the second or fifth positions contributed to the inhibitory Zn^{2+} binding site that resides at the β2(+)/α4(-) interfaces of the receptor. Therefore, the potentiating site is located in the interface between the α4 subunit in the fourth and fifth positions of the β2_α4_β2_α4_α4 nAChR; α4 in the fourth position contributes H195, whereas the α4 subunit in the fifth position contributes the plus face of the Zn^{2+} binding site. From these findings, it was inferred that the consensus agonist sites at α/β interfaces are located at the interface between the first β2 and second α4 subunits and between the third β2 and fourth α4 subunits of the concatenated receptor **(Fig.3.2)**.

A

B

	W88	Y126	W182	Y223	Y230
h ACha4	NVWVK	VLYNN	GSWTY	RKYEC	EIMPD
h AChβ2	NVWLT	VLYNN	RSWTY	NPD--	STYVD
tc AChα1	NVRLR	VLYNN	GIWTY	VYMTC	TPYLD
tc AChδ	NVWMD	VLQNN	TALNY	YPDKF	TNYQD

C

D
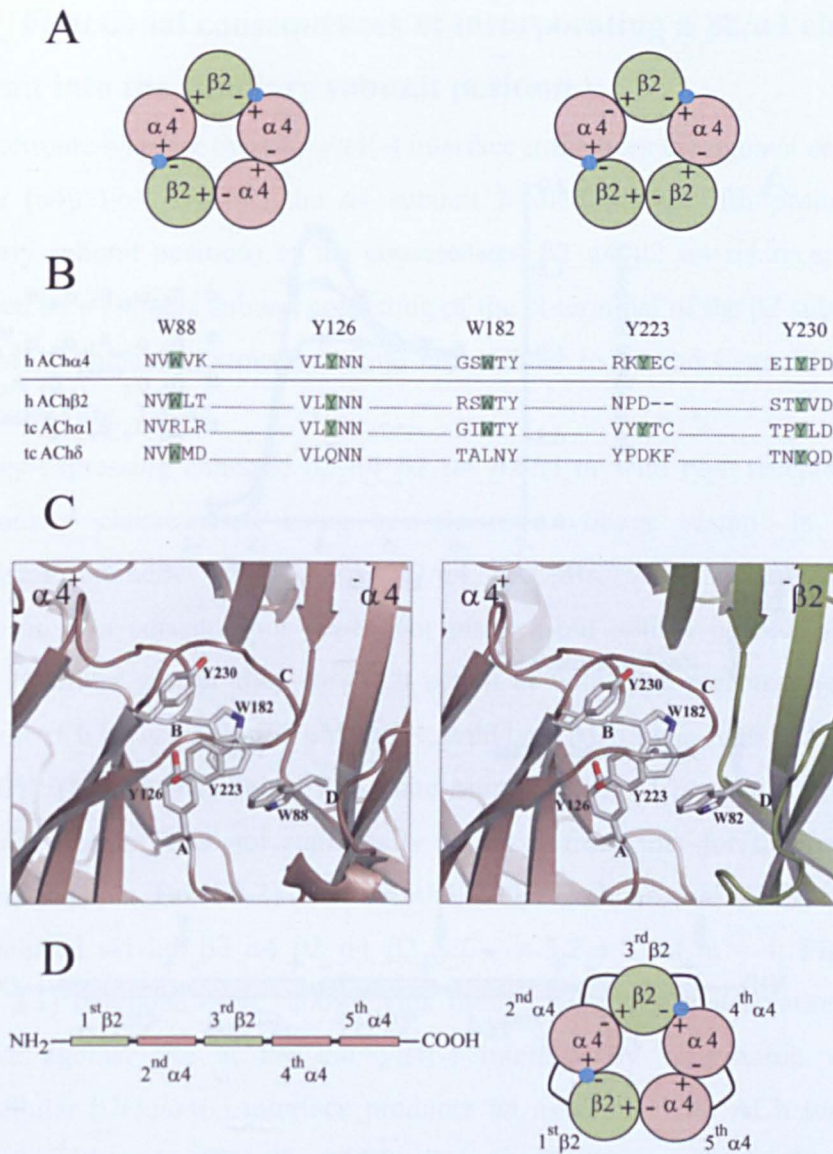
Figure 3.1. ACh binding sites at the (α4β2)2α4 nAChR. (A) Schematic representations showing the subunit arrangement and interfaces on the (α4β2)₂α4 nAChR (left panel) and (α4β2)₂β2 nAChRs. In both receptors, the α4(+)/β2(-) interfaces contain agonist sites. **(B)** Alignment of conserved aromatic residues contributing to agonist binding in human (h) α4β2 nAChRs and *Torpedo* (tc) α1 and δ nAChR subunits. **(C)** The left-hand panel is a side-on view of the α4(+)/α4(-) interface showing the location of conserved aromatic residues and loop C contributing to a putative agonist site. The right-hand panel is a side-on view showing the α4(+)/β2(-) agonist site. **(D)** Schematic representation of the linear sequence of the concatenated (α4β2)₂α4 nAChR is shown showing the orientation of the (+) and (–) faces of the subunits.
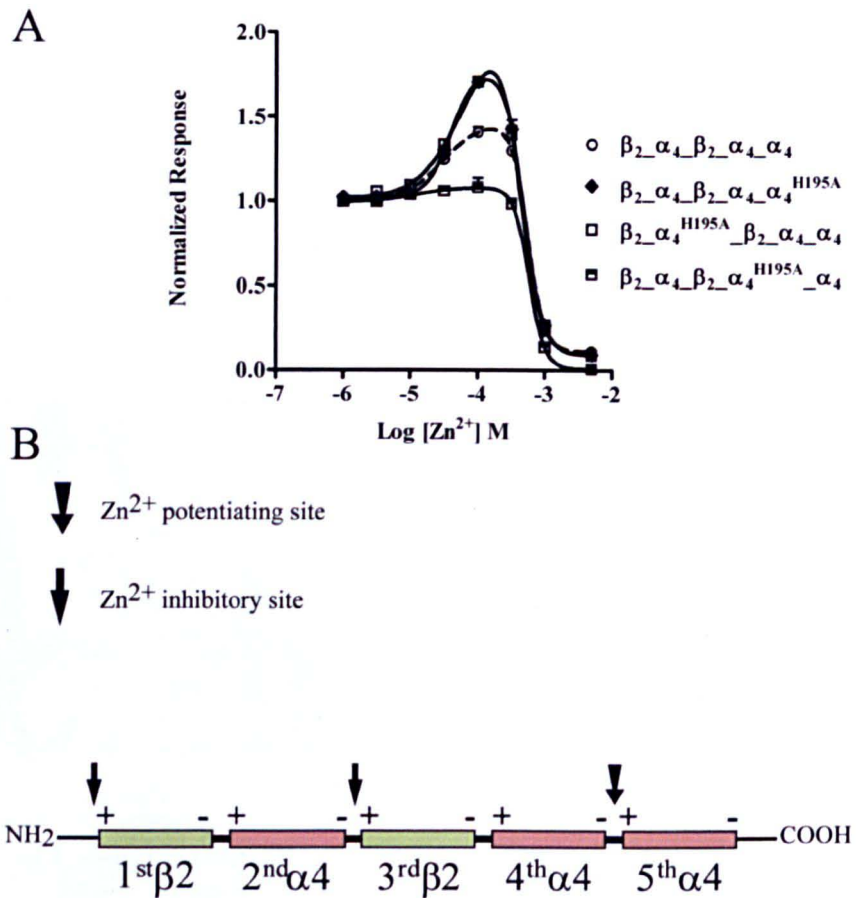
Figure 3.2. Position of the potentiating Zn^{2+} binding site in the concatenated $(\alpha4\beta2)2\alpha4$ nAChR. (A) CRC for the effect of Zn^{2+} in wild type and receptors carrying the $\alpha4H195A$ mutation on either of the $\alpha4$ subunits present in $\beta2\_\alpha4\_\beta2\_\alpha4\_\alpha4$ nAChRs. When the mutation was incorporated into the $\alpha4$ subunit in either the second or fifth position of the concatamer, the sensitivity to potentiation by Zn^{2+} was enhanced, whereas the same mutation on the fourth position of the receptor almost abolishes the potentiating effect of Zn^{2+}. **(B)** It is inferred therefore that the $\alpha4$ subunits at the second or fifth positions contributed with the H195 residue to the inhibitory Zn^{2+} binding site that resides at the $\beta2(+)/\alpha4(-)$ interfaces of the receptor. Therefore, the potentiating site resides in the interface between the $\alpha4$ subunit in the fourth and fifth positions of the $\beta2\_\alpha4\_\beta2\_\alpha4\_\alpha4$ nAChR; $\alpha4$ in the fourth position contributes H195, whereas the $\alpha4$ subunit in the fifth position contributes the plus face of the Zn^{2+} binding site.

3.2.2 Functional consequences of incorporating a β2/α4 chimeric subunit into the auxiliary subunit position

To determine whether the α4(+)/α4(-) interface influences the agonist sensitivity of the $(\alpha4\beta2)_2\alpha4$ nAChR, the α4 subunit located in the fifth position (the auxiliary subunit position) of the concatenated β2_α4_β2_α4_α4 receptor was replaced by a chimera subunit consisting of the N-terminal of the β2 subunit and the TM1-4 domains, extracellular and intracellular loops and C-terminal of the α4 subunit **(Fig. 3.3.A)**.

Oocytes expressing chimeric β2_α4_β2_α4_β2/α4 or wild type receptors were functionally characterised using two-electrode voltage clamp. In oocytes expressing chimeric β2_α4_β2_α4_β2/α4 nAChRs, ACh activated current responses in a concentration-dependent manner but with a potency that was about 10-folder greater than for ACh action at wild type receptors (chimeric receptor ACh EC_{50} = 8.2 ±0.5 μM, n = 4; wild type ACh EC_{50} 78±8 μM (n = 6; p < 0.001) **(Fig. 3.3B; Table 3.1)**. Interestingly, the ACh sensitivity of the chimeric receptor was not statistically different from that for the $(\alpha4\beta2)_2\beta2$ isoform (3.4 ± 1; **Table 3.2**) (Moroni et al. 2006; Carbone et al. 2009) or for its concatenated version β2_α4_β2_α4_β2 (EC_{50} = 3.2 ± 1μM, n = 4; **Fig. 3.3B; Table 3.1**) (Carbone et al., 2009). This finding suggested that ablation of the putative agonist site at the α4(+)/α4(-) interface by substitution with an extracellular β2(+)/α4(-) interface produces an assembly with ACh sensitivity approaching that of $(\alpha4\beta2)_2\beta2$ nAChRs. This possibility was examined by testing the functional effects of Cyt and Saz-A on β2_α4_β2_α4_β2/α4 nAChRs. As mentioned in **Chapter 1**, Cyt is a partial agonist at $(\alpha4\beta2)2\alpha4$ nAChRs or its concatenated template but it has negligible agonist efficacy at non-linked or concatenated $(\alpha4\beta2)_2\beta2$ nAChRs (Moroni et al., 2006; Carbone et al., 2006). In contrast, Saz-A displays poor efficacy at loose or concatenated $(\alpha4\beta2)_2\alpha4$ receptors (less than 0.05%) (Zwart et al., 2006; Carbone et al., 2009) but is a potent, full agonist at non-linked or concatenated $(\alpha4\beta2)_2\beta2$ nAChRs (Zwart et al., 2006; Carbone et al., 2009). Cyt failed to elicit currents at β2_α4_β2_α4_β2/α4 nAChRs, even at 100 μM, a concentration producing maximal effects at β2_α4_β2_α4_α4 nAChRs **(Figs. 3.3C)** (Carbone et al., 2009). Saz-A behaved as a full agonist at β2_α4_β2_α4_β2/α4 nAChRs and

displayed a potency (EC_{50} = 16 ± 9 nM; n = 3) that was comparable to that at loose or concatenated $(\alpha4\beta2)_2\beta2$ nAChR (EC_{50} = 7 ± 1 nM; (Carbone et al., 2009) **(Figs. 3.3C, D)**. These findings show that removal of the $\alpha4(+)/\alpha4(-)$ interface produces a $(\alpha4\beta2)_2\beta2$ nAChR-like agonist sensitivity and are thus consistent with the suggestion that the $\alpha4(+)/\alpha4(-)$ interface in $(\alpha4\beta2)2\alpha4$ nAChR may underlie the agonist sensitivity signature of the isoform $(\alpha4\beta2)_2\alpha4$ receptor.
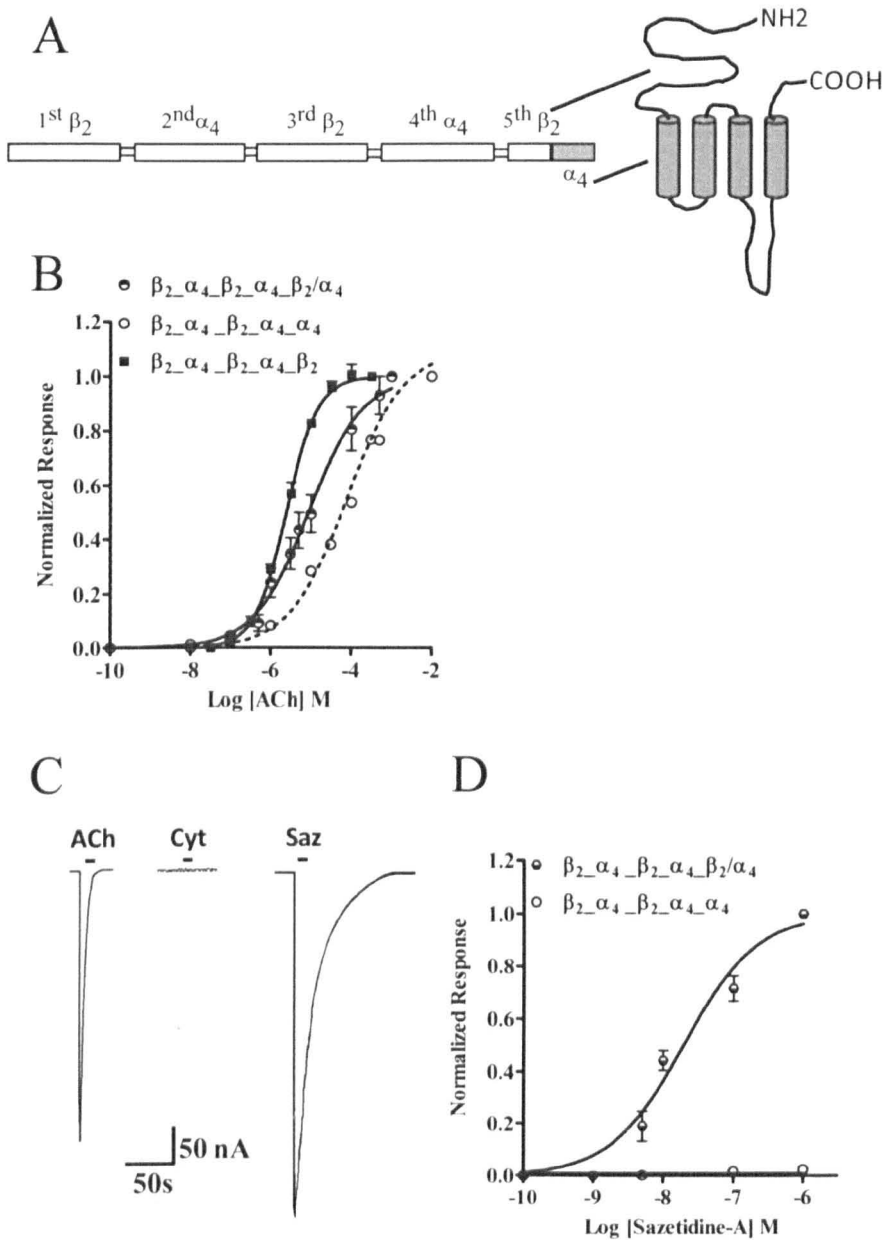
Figure 3.3. **Agonist sensitivity of a chimeric β2_α4_β2_α4_β2/α4 nAChR.**
(A) Cartoon of the chimeric β2_α4_β2_α4_β2/α4 nAChR. **(B)** ACh CRC at
β2_α4_β2_α4_β2/α4 nAChRs. The ACh CRC for wild type nAChRs are shown
for comparison. Data were fit by nonlinear regression analysis as described in
Materials and Methods. **(C)** Representative traces of the responses of chimeric
β2_α4_β2_α4_β2/α4 nAChRs to EC_{100} ACh (1 mM), Cyt (100 μM) and Saz-A
(1 μM). **(D)** The CRC for Saz-A. The mean of the I_{max} ± SEM for 4-10
experiments for each receptor were as follow: β2_α4_β2_α4_β2/α4 (ACh, 115 ±
28 nA), (Saz-A 142 ± 34 nA); β2_α4_β2_α4_α4 (ACh, 386 ± 77 nA);
β2_α4_β2_α4_β2 (ACh, 223 ± 70 nA) The data were analysed as described in
Chapter 2.

Table 3.1. **Summary of ACh effects on wild type and mutant β2_α4_β2_α4_α4 nAChRs.** Data are the mean ± SEM for 4-10 experiments. ACh EC_{50} values, Hill coefficients, and high sensitivity fractions (HF) are indicated. *Values are significantly different from wild type, $p < 0.05$ (one way ANOVA).

Receptor Type	ACh EC_{50} μM	nH	ACh $EC_{50\_}1$ μM	nH1	ACh $EC_{50\_}2$ μM	nH2	HF
β2_α4_β2_α4_β2	3.2±1	1.2±0.5					
β2_α4_β2_α4_α4	78±8	0.72±0.02					
β2_α4_β2_α4_β2/α4	8.2±0.5	1.1±0.1					
β2_^{WI82A}α4_β2_^{WI82A}α4_^{WI82A}α4	684±63*	1.37±0.1					
β2_^{WI82A}α4_β2_α4_α4			1.51±0.02*	0.55±0.1	566±62*	2.5±0.7	0.63±0.1
β2_α4_β2_^{WI82A}α4_α4			1.23±0.03*	0.70±0.2	668±63*	2±0.7	0.64±0.07
β2_α4_β2_α4_^{WI82A}α4			28±2*	1.4±0.2	3483±25*	3.8±1.2	0.66±0.06
β2_^{WI82A}α4_β2_^{WI82A}α4_α4			38±18*	0.32±0.1	679±78*	1.4±0.5	0.32±0.09
β2_^{WI82A}α4_β2_α4_^{WI82A}α4			10±4*	1.9±0.9	724±54*	3.8±0.8	0.34±0.02
β2_α4_β2_^{WI82A}α4_^{WI82A}α4			5.1±2*	1.3±0.2	441±65*	1.8±0.3	0.11±0.07
β2_^{Y230A}α4_β2_α4_α4			3.10±0.6*	0.76±0.2	540±43*	3.9±2	0.35±0.07
β2_α4_β2_^{Y230A}α4_α4			3.29±0.3*	0.63±0.05	538±51*	3.7±0.8	0.37±0.1
β2_α4_β2_α4_^{Y230A}α4			1.64±0.07*	1.1±0.6	251±61	2.0±0.8	0.15±0.06
β2_^{C226S}α4_β2_α4_α4			2.19±0.5*	1.6±0.3	352±43*	1.3±0.2	0.17±0.06
β2_α4_β2_^{C226S}α4_α4			1.61±0.1*	1.4±0.2	527±65*	1.1±0.3	0.16±0.06
β2_α4_β2_α4_^{C226S}α4			1.12±0.5*	1.1±0.4	385±79*	1.2±0.6	0.13±0.09

Table 3.2.   CRC data for ACh activation of wild type and mutant α4β2 nAChR isoforms. The maximal current of the mutant receptors was normalised to that of wild type receptors to estimate the relative maximal ACh responses of mutant receptors. Data represent the mean ± SEM for 7-9 experiments. ND, not determined. NR, no functional responses elicited by ACh.

	(α4β2)$_2$α4			(α4β2)$_2$β2		
	I/I_{max} μA	EC_{50} μM	nH	I/I_{max} μA	EC_{50}	nH
Wild type	1	81±14	0.72±0.07	1	3.4±1	0.68±0.07
α4Y126A	0.056±0.004	ND	ND	0.063±0.008	ND	ND
α4W182A	0.87±0.08	634±78	1.3±0.5	0.76±0.05	500±78	1.6±0.4
α4Y223A	NR	-	-	NR		
α4Y230A	0.23±0.04	478±99	1.3±	0.15±0.07	504±112	1.5±0.5
β2W82A	0.46±0.12	256±67	1±0.4	NR	-	-

3.2.3 Mutant agonist sites produce biphasic ACh effects

Given that the putative site at the α4(+)/α4(-) interface is homologous to the agonist binding sites at the α4(+)/β2(-) interfaces, it may be possible that the site at the α4(+)/α4(-) interface influences receptor function possibly by binding agonists. Therefore, conserved aromatic residue α4W182 in the α4(+)/α4(-) interface was substituted with alanine aiming to demonstrate that ACh binds this site. α4W182 is equivalent to muscle α4W149 and establishes cation-π interactions with the quaternary ammonium group of ACh (Xiu et al., 2009) and affects binding affinity as well as gating (Akk, 2001; Akk & Auerbach, 1999). As shown in **Table 3.2**, alanine substitution of α4W182 on loose subunit (α4β2)$_2$α4 nAChRs reduces sensitivity to activation by ACh without impacting functional expression.

Introducing α4W182A into the (+) face of the putative agonist site at the α4(+)/α4(-) interface produced mutant β2_α4_β2_α4_^{W182A}α4 nAChRs responding to ACh with a biphasic CRC ($p < 0.003$; n = 10), including a component that comprised about 65% of the curve, and had an ACh EC_{50} value that was about 3-fold lower than that for wild type **(Fig. 3.4A; Table 3.1)**.
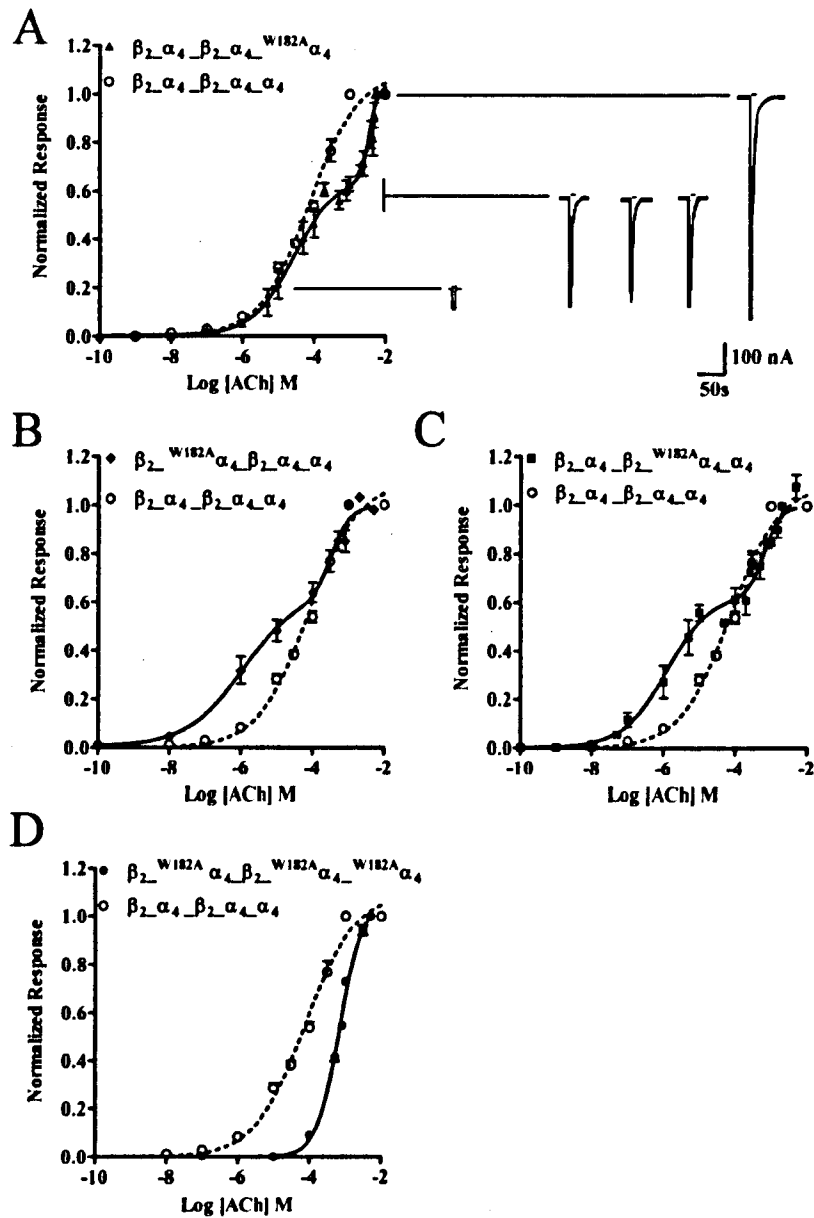
Figure. 3.4. Effect of α4W182A subunit on the ACh sensitivity of β2_α4_β2_α4_α4 nAChR. When the W182A mutation was introduced into α4 in the fifth (**A**), second (**B**) or fourth (**C**) positions of the concatenated receptor biphasic ACh CRCs were obtained; whereas introducing the W182A mutation in all the α4 subunits (**D**) the CRC were monophasic. The mean of the $I_{max} \pm$ SEM for 4-10 experiments for each receptor were as follow: β2_α4_β2_α4_α4 (386 ± 77 nA). β2_^{W182A}α4_β2_α4_α4 (404 ± 55 nA); β2_α4_β2_^{W182A}α4_α4 (425 ± 82 nA); β2_α4_β2_α4_^{W182A}α4 (347 ± 55 nA); β2_^{W182A}α4_β2_^{W182A}α4_^{W182A}α4 (250 ± 30 nA). Data were fit by nonlinear regression analysis as described in **Chapter 2**.

The second CRC component became evident at ACh concentrations higher than 500 μM and displayed an ACh sensitivity that was 45-fold lower than that for wild type $\beta2\_\alpha4\_\beta2\_\alpha4\_\alpha4$ receptors ($p < 0.0001$, n =10) **(Table 3.1)**. When the mutation was simultaneously introduced into the $\alpha4(+)/\alpha4(-)$ and the two $\alpha4(+)/\beta2(-)$ interfaces (triple mutant receptor) in the $\beta2\_\alpha4\_\beta2\_\alpha4\_\alpha4$ receptor the ACh CRC was monophasic ($p < 0.001$; n = 10) and with an ACh EC_{50} value that was no different from that obtained for non-linked $(\alpha4^{W182A}\beta2)_2\alpha4^{W182A}$ nAChRs **(Fig. 3.4B; Tables 3.1, 3.2)**. This finding suggested that the biphasic ACh CRC for $\beta2\_\alpha4\_\beta2\_\alpha4\_^{W182A}\alpha4$ receptors reflects the presence of unaltered agonist sites at the $\alpha4(+)/\beta2(-)$ interfaces and the mutated site at the $\alpha4(+)/\alpha4(-)$ interface. To test this possibility, $\alpha4W182A$ was introduced into the (+) face of either of the agonist binding sites at the $\alpha4(+)/\beta2(-)$ receptor interfaces to produce mutant $\beta2\_^{W182A}\alpha4\_\beta 2\_\alpha4\_\alpha4$ or $\beta2\_\alpha4\_\beta2\_^{W182A}\alpha4 \_\alpha4$ receptors. As shown in **Figs. 3.4C, D**, the effects of ACh on $\beta2\_^{W182A}\alpha4\_\beta2\_\alpha4\_\alpha4$ or $\beta2\_\alpha4\_\beta2\_^{W182A}\alpha4\_\alpha4$ receptors were biphasic ($p < 0.001$; n = 6). The relative abundance of the CRC component with the highest sensitivity for ACh was similar for all three mutant receptors. However, the ACh sensitivity of this component in the CRC for $\beta2\_^{W182A}\alpha4\_\beta2\_\alpha4\_\alpha4$ or $\beta2\_\alpha4\_\beta 2\_^{W182A}\alpha4\_\alpha4$ receptors was ~60-fold greater than wild type, making it comparable to the ACh sensitivity of $(\alpha4\beta2)_2\beta2$ or chimeric $\beta2\_\alpha4\_\beta2\_\alpha4\_\beta2/\alpha4$ receptors, both of which lack the $\alpha4(+)/\alpha4(-)$ interface **(Table 3.1)**. In contrast, in the case of $\beta2\_\alpha4\_\beta 2\_\alpha4\_^{W182A}\alpha4$ receptors, the ACh sensitivity for the equivalent CRC component was increased by only 3-fold, relative to wild type **(Table 3.1)**. The ACh CRC component with the lowest ACh sensitivity also differed in both types of mutant receptors. For receptors with mutant $\alpha4(+)/\beta2(-)$ interfaces, the ACh sensitivity of this component was 8-fold lower than wild type **(Table 3.1)**, whereas for $\beta2\_\alpha4\_\beta 2\_\alpha4\_^{W182A}\alpha4$ nAChRs it was 45-fold lower than wild type **(Table 3.1)**. For all three mutant receptors, the Hill coefficient of the component with lowest ACh sensitivity increased to 2-3 relative to wild type, whereas changes in the Hill coefficient of the CRC component with the highest ACh sensitivity were not significant, in comparison to wild type.

Next, $\alpha4W182A$ was introduced simultaneously into the (+) face of two subunit interfaces to create mutant $\beta2\_\alpha4\_\beta2\_^{W182A}\alpha4\_^{W182A}\alpha4$,

$\beta2\_{}^{W182A}\alpha4\_\beta2\_\alpha4\_{}^{W182A}\alpha4$, or $\beta2\_{}^{W182A}\alpha4\_\beta2\_{}^{W182A}\alpha4\_\alpha4$ receptors. As shown in **Fig. 3.5**, introducing W182A simultaneously into two $\alpha4$ subunits of $\beta2\_\alpha4\_\beta2\_\alpha4\_\alpha4$ receptors produced biphasic ACh CRC.
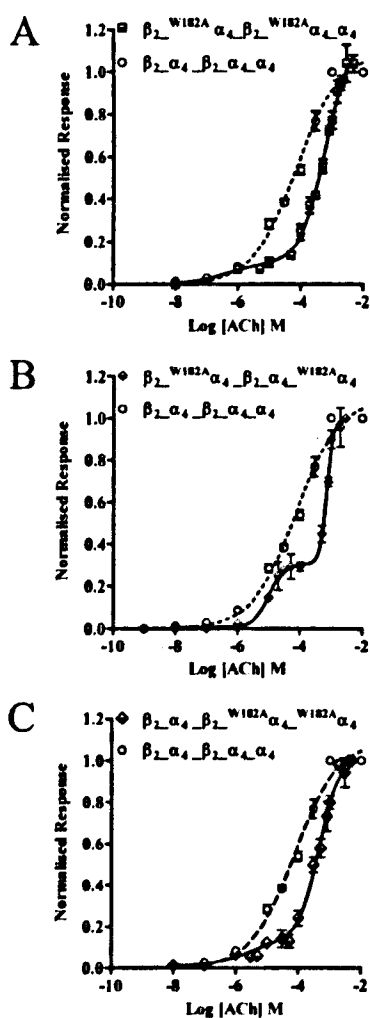
Figure 3.5. **Activation** of $\beta2\_\alpha4\_\beta2\_\alpha4\_\alpha4$ receptors containing two $\alpha4$W182A mutant subunits. Simultaneous introduction of $\alpha4$W182 into two sites to produce $\beta2\_{}^{W182A}\alpha4\_\beta2\_{}^{W182A}\alpha4\_\alpha4$ (**A**), $\beta2\_{}^{W182A}\alpha4\_\beta2\_\alpha4\_{}^{W182A}\alpha4$ (**B**) or $\beta2\_\alpha4\_\beta2\_{}^{W182A}\alpha4\_{}^{W182A}\alpha4$ (**C**) led to biphasic ACh CRC. The mean of the I_{max} $\pm$ SEM for 4-10 experiments for each receptor were as follow: $\beta2\_\alpha4\_\beta2\_\alpha4\_\alpha4$ (386 $\pm$ 77 nA). $\beta2\_{}^{W182A}\alpha4\_\beta2\_{}^{W182A}\alpha4\_\alpha4$ (473 $\pm$ 106 nA); $\beta2\_{}^{W182A}\alpha4\_\beta2\_\alpha4\_{}^{W182A}\alpha4$ (555 $\pm$ 112 nA); $\beta2\_\alpha4\_\beta2\_{}^{W182A}\alpha4\_{}^{W182A}\alpha4$ (296 $\pm$ 58 nA). Data were fit by nonlinear regression analysis as described in **Chapter 2**.

In comparison to single mutant receptors, the relative abundance of the CRC component with higher sensitivity to ACh was reduced in all three mutants ($p <$ 0.001; n = 6-12) **(Figs. 3.4 & 3.5, Table 3.1)**. For all three mutant receptors, the ACh sensitivity of this component was enhanced, as compared to wild type, but decreased as compared to the equivalent ACh EC_{50} for single mutant receptors (p < 0.01; n = 6-8) **(Table 1)**. The relative abundance of the CRC fraction with the highest ACh sensitivity was influenced by the position of the mutated $\alpha4$ subunit within the receptor **(Fig. 3.5, Table 3.1)**. The ACh EC_{50} estimated for the component with the lowest ACh sensitivity was similar for all three double mutant receptors and was not different from the ACh EC_{50} for $(\alpha4^{W182A}\beta2)_2\beta2$ receptors (EC_{50} = 500 ± 78 μM; **Table 3.2**). Overall, these findings, together with the effects of $\alpha4W182A$ on non-linked $\alpha4\beta2$ nAChR function **(Table 3.2)**, indicate that the ACh CRC component with the highest sensitivity for ACh is contributed predominantly by unaltered binding sites, whereas the mutated sites contribute predominantly to the CRC component with the lowest sensitivity for ACh. Because introducing W182 into the auxiliary subunit produced a CRC fraction with diminished sensitivity for ACh, the findings are consistent with the possibility that the $\alpha4(+)/\alpha4(-)$ interface is capable of binding agonist.

3.2.4 DhβE inhibits the α4(+)/α4(-) site

DhβE displays high affinity (low nM Ki values) competitive antagonism for $\alpha4\beta2$ nAChRs **(Table 1.1)** (Moroni et al., 2006; Carbone et al., 2009). Demonstrating that the site at the $\alpha4(+)/\alpha4(-)$ interface is inhibited by DhβE would further support the suggestion that the site is capable of binding agonist. This possibility was assessed by determining the ACh sensitivity of mutant $\beta2\_\alpha4\_\beta2\_\alpha4\_^{W182A}\alpha4$ in the presence and absence of 1 μM DhβE. Because $\alpha4W182$ contributes to inhibition of $\alpha4\beta2$ nAChR by DhβE (Iturriaga-Vasquez et al., 2009) and, as suggested by the present studies, binds agonist in the putative site at the $\alpha4(+)/\alpha4(-)$ interface, it was anticipated that DhβE would decrease the sensitivity of both mutant $\alpha4(+)/\alpha4(-)$ and unaltered $\alpha4(+)/\beta2(-)$ sites, albeit with different potency. As shown in **Figs. 3.6A, B**, inhibition of the ACh responses of $\beta2\_\alpha4\_\beta2\_\alpha4\_^{W182A}\alpha4$ nAChRs by DhβE reached a plateau at ACh concentrations higher than 800 μM, producing monophasic ACh CRC lacking

the component with the lowest ACh sensitivity detected in the absence of the antagonist. As shown in **Figs. 3.6C-E**, the ACh CRC for receptors with mutant $\alpha 4(+)/\beta 2(-)$ binding sites (i.e., $\beta 2\_^{W182A}\alpha 4\_\beta 2\_\alpha 4\_\alpha 4$ or $\beta 2\_\alpha 4\_\beta 2\_^{W182A}\alpha 4\_\alpha 4$ nAChRs) also became monophasic in the presence of DhβE. However, by comparison to $\beta 2\_\alpha 4\_\beta 2\_\alpha 4\_^{W182A}\alpha 4$ receptors, DhβE inhibited more potently the responses elicited by concentrations of ACh lower than 10 μM, a concentration range activating non-mutated agonist sites.
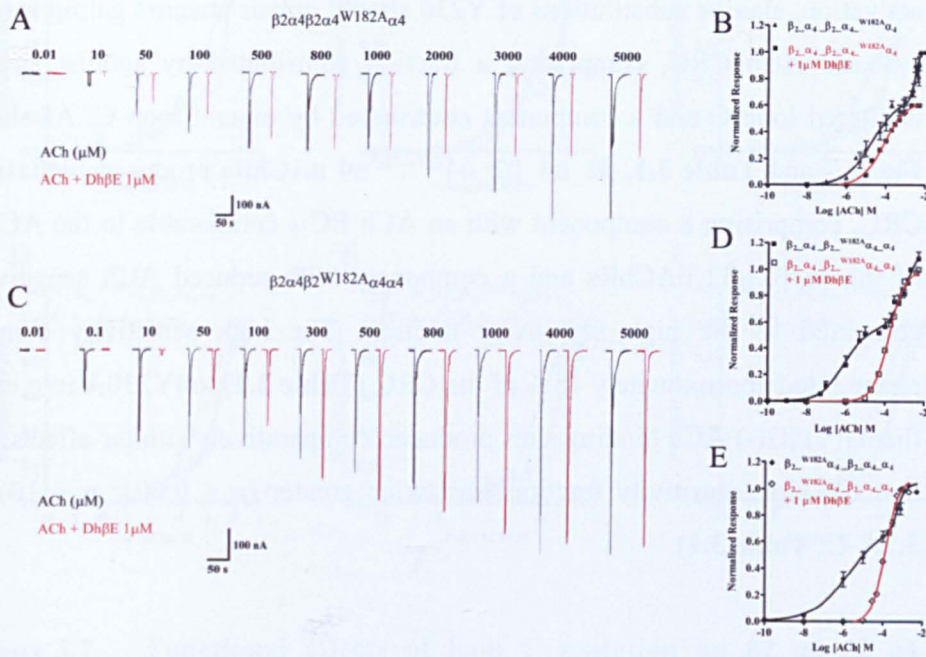
Figure 3.6.   Effects of the antagonist DhβE on mutant β2_α4_β2_α4_α4 nAChRs. (A) Typical traces showing the effects of ACh on β2_α4_β2_α4_ ^{W182A}α4 nAChRs in the absence (black) and presence of 1 μM DhβE (red). **(B)** CRC for the effects of DhβE on the ACh responses of β2_α4 _β2_α4_ ^{W182A}α4 nAChRs. Data were fit by nonlinear regression analysis as described in **Chapter 2**. **(C)** Representative traces showing the effects of 1 μM DhβE (in red) on the ACh responses (in black) of β2_α4_β2_ ^{W182A}α4_α4 nAChRs. **(D, E)** ACh CRC in absence or presence of 1 μM DhβE obtained at β2_α4 _β2_α4_ ^{W182A}α4 or β2_ ^{W182A}α4_β2_α4_α4 nAChRs, respectively. Data were fit by nonlinear regression analysis as described in **Chapter 2**.

3.2.5 Loop C in the auxiliary subunit affects receptor function

As discussed in **Chapter 1**, agonist binding in Cys-loop LGICs elicits loop C capping, and this is considered to lead to channel gating via molecular interactions in the coupling interface. To assess the significance of loop C on the function of the putative site at the α4(+)/α4(-) interface, α4Y230 was introduced into the (+) face of the site and then assayed its effects on the function of β2_α4_β2_α4_α4 receptors were assayed. α4Y230 is equivalent to muscle α1Y198 in the C-terminal of loop C. It has been shown to affect gating but not agonist binding affinity in muscle nAChR and in the (α4β2)$_2$α4 receptors

81

decreases the sensitivity to ACh and functional expression **(Table 3.2)**. If the site at the $\alpha4(+)/\alpha4(-)$ interface had the capability of contributing to receptor activation, alanine substitutions of Y230 should impair channel gating leading to biphasic ACh CRC, comprising a fraction contributed by agonist sites with unaltered loop C and a component contributed by mutant loop C. As shown in **Fig. 3.7** and **Table 3.1**, $\beta2\_\alpha4\_\beta2\_\alpha4\_^{Y230A}\alpha4$ nAChRs produced biphasic ACh CRC, comprising a component with an ACh EC_{50} comparable to the ACh EC_{50} of the $(\alpha4\beta2)_2\beta2$ nAChRs and a component with reduced ACh sensitivity, as compared to the high sensitivity fraction. The high sensitivity component represented approximately 15% of the CRC **(Table 3.1)**. $\alpha4$Y230A into either of the $\alpha4(+)/\beta2(-)$ ACh binding sites produced comparatively similar effects, except that the high sensitivity fraction was twice greater ($p < 0.001$; n = 10) **(Figs. 3.7A-C; Table 3.1)**.
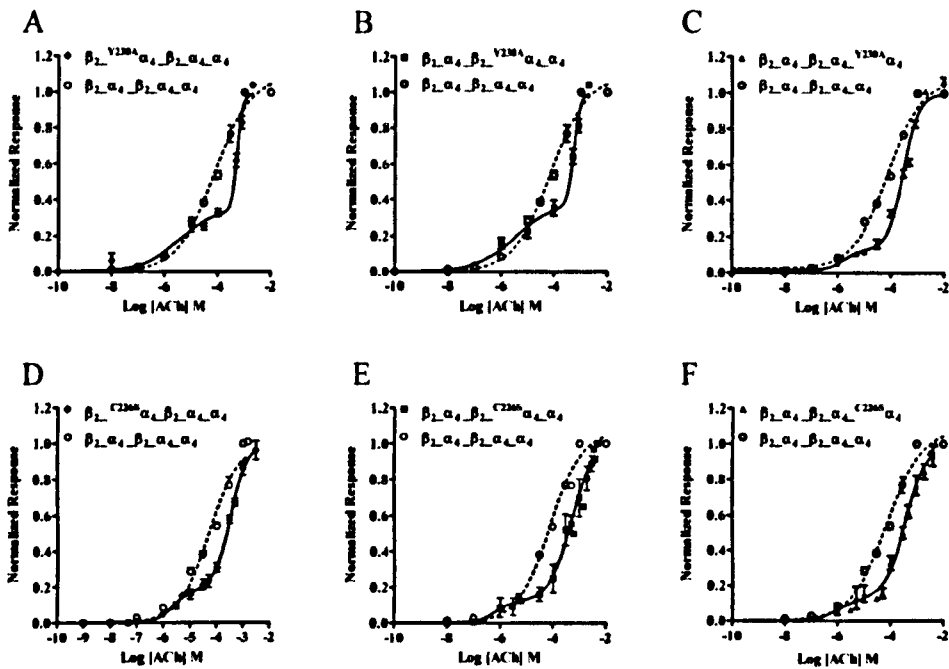
Figure 3.7. Functional effects of loop C mutation on β2_α4_β2_α4_α4 nAChR function. ACh produced biphasic CRC in oocytes expressing β2_^{Y230A}α4_β2_α4_α4 receptors **(A)**, β2_α4_β2_^{Y230A}α4_α4 **(B)** or β2_α4_β2_α4_^{Y230A}α4 receptors **(C)**. Data were fit to the monophasic or biphasic equations described in the Materials and Methods. Introducing C226S into the second **(D)**, fourth **(E)** or fifth **(F)** positions of the β2_α4_β2_α4_α4 nAChR produced biphasic ACh responses. The mean of the I_{max} ± SEM for 4-10 experiments for each receptor were as follow: β2_α4_β2_α4_α4 (386 ± 77 nA). β2_^{Y230A}α4_β2_α4_α4 (46 ± 14 nA); β2_α4_β2_^{Y230A}α4_α4 (28 ± 6 nA); β2_α4_β2_α4_^{Y230A}α4 (84 ± 20 nA); β2_^{C226S}α4_β2_α4_α4 (283 ± 81 nA); β2_α4_β2_^{C226S}α4_α4 (367 ± 149 nA); β2_α4_β2_α4_^{C226S}α4 (213 ± 48 nA). Averaged parameters of best fits to CRC are given in **Table 3.1**.

3.2.6 Modification of loop C with MTS Reagents

Demonstrating that conformational changes in loop C in the auxiliary α4 subunit alter the ACh responses of the β2_α4_β2_α4_α4 nAChR would strengthen the conclusion that the putative agonist binding site in the α4(+)/α4(-) interface contributes directly to channel gating. Loop C conformational transitions can be inferred from changes in the agonist responses of receptors brought about by covalent modification of substituted (Venkatachalan & Czajkowski, 2008) or free (Wang et al., 2009) cysteine residues in loop C by MTS reagents. Accordingly, serine was substituted for C226 at the tip of loop C to dismantle the disulphide bond between C225 and C226 in order to make C225 accessible to MTS reagents

(MTSET or MTSEA; **Fig. 3.8A**). Substitution of serine for C226 in any of the three α4 subunits of the β2_α4_β2_α4_α4 nAChR yielded biphasic ACh CRC that were comparable to those produced by the α4Y230A mutation **(Figs. 3.7D-F;3.8B; Table 3.1)**. These findings are in accord with recent studies of muscle nAChR showing that removal of the cysteine bridge in loop C decreases agonist sensitivity without abolishing loop C function (Mukhtasimova et al., 2009). To assess the effects of MTS reagents on the function of intact and mutated sites, we performed the experiments using 800 μM or 3 μM ACh. 800 μM ACh produces near maximal activation of the ACh CRC fraction with the lowest ACh sensitivity, whereas 3 μM ACh produces almost maximal activation of the ACh CRC fraction with the highest ACh sensitivity **(Figs. 3.7D-F; Table 3.1)**. We have shown above that ACh produces biphasic CRC at β2_α4_β2_α4_α4 receptors with one mutant agonist site and that the CRC component with the lowest ACh sensitivity is contributed predominantly by the mutated site, whereas the component with the highest sensitivity component reflects predominantly the activation of intact binding sites. As shown in **Fig. 3.8C**, when the current responses of β2_α4_β2_α4_^{C226S}α4 nAChRs were activated by 800 μM ACh, MTSET decreased the amplitude of the ACh responses by ~30%. In accord with a covalent interaction between α4C225 and MTSET, exposure to DTT reversed the effects of MTSET **(Fig. 3.8C)**. By comparison, MTSET had no effects on the amplitude of the responses evoked by 3 μM ACh **(Fig. 3.8C)**. These results were expected because 3 μM ACh activates predominantly intact agonist sites, MTSET produced similar effects on the ACh responses of β2_^{C226S}α4_β2_α4_α4 or β2_α4_β 2_^{C226S}α4 _α4 mutant nAChRs **(Fig. 3.8E)**. Exposure to MTSEA did not have any apparent effect on the current responses elicited by 800 μM ACh in β2_α4_β2_α4_^{C226S}α4 nAChRs **(Fig. 3.8 D)**. However, when the responses were elicited by lower concentrations of ACh (3 μM) after MTSEA treatment, the amplitude of the ACh responses was enhanced markedly and this effect was reversed by DTT **(Fig. 3.8D)**. This result demonstrated that MTSEA enhanced the ACh responses of the mutant receptor by covalently modifying C225. Comparable effects were observed when β2_^{C226S}α4 _β2_α4_α4 or β2_α4_β2_^{C226S}α4_α4 were exposed to MTSEA **(Fig. 3.8E)**. Although we observed differences in the effects of MTS at each agonist site, the differences were not significant.
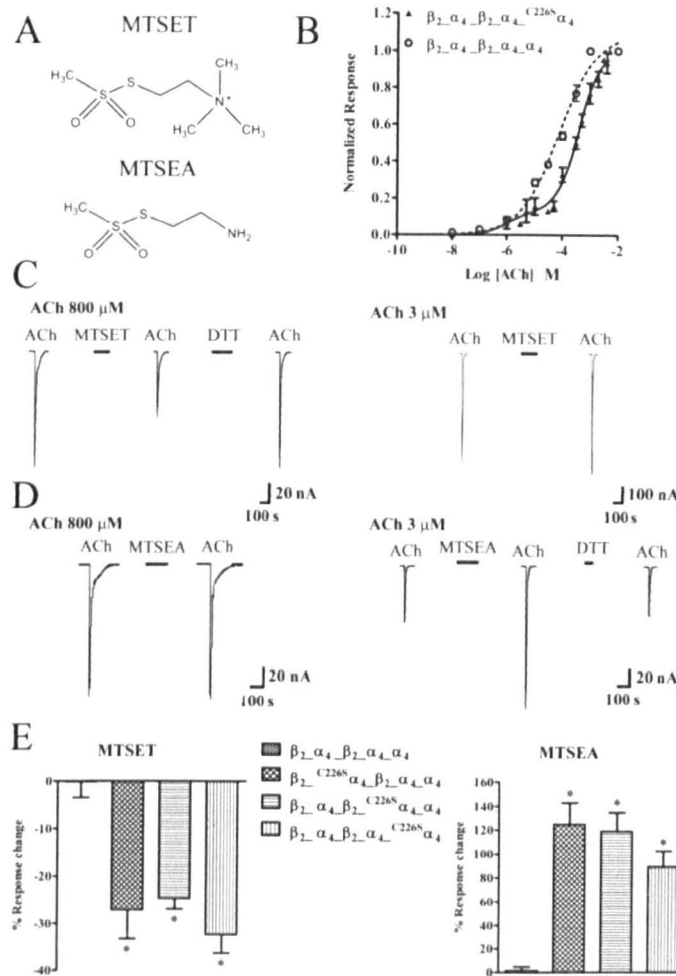
Figure 3.8. **Effects of MTS reagents on mutant β2_α4_β2_α4_α4 nAChRs.**
(A) Structure of MTS reagents used to covalently modify free C225 in loop C.
(B) β2_α4_β2_α4_^{C226S}α4 receptors displayed biphasic ACh responses. For
comparison, the ACh CRC at wild type is also shown. Data were analysed by
nonlinear regression as described in **Chapter 2**. (C) Representative current traces
of the responses to ACh (800 μM or 3 μM) from two different oocytes
expressing β2_α4_β2_α4_^{C226S}α4 receptors before and after modification by
MTSET. DTT was applied at the end of the experiments to confirm that the
effects observed were due to the covalent modification of C225. (D)
Representative current traces of the responses to ACh (800 μM or 3 μM) from
two different oocytes expressing β2_α4_β2_α4_^{C226S}α4 receptors before and
after modification by MTSEA. DTT reversed the effects of MTSEA. (E) Bar
graph summary of the percentage of change (mean ± SEM) in the amplitude of
the ACh currents after MTS treatment on wild type and mutant receptors. *,
values are significantly different from amplitudes of the ACh responses prior to
MTS treatment ($p < 0.001$ one-way ANOVA).

3.3 Discussion

The α4 and β2 subunits of the nAChR assemble into alternate forms that differ markedly in sensitivity to activation by agonists. Because α4β2 nAChRs contain two identical agonist binding sites at the α(+)/β(-) interfaces, a long-standing question has been what structural features confer agonist sensitivity to the alternate forms of the α4β2 nAChR. Here, we provide evidence that an additional site at the α4(+)/α4(-) interface in the (α4β2)$_2$α4 nAChR underlies the agonist sensitivity signature of the isoform (α4β2)$_2$α4. The additional site binds ACh and when engaged by ACh, contributes to channel gating through a coupling pathway that includes loop C. The findings have important structural and functional implications about the role of subunit composition on the structural-functional properties of the α4β2 nAChR and the manner by which agonists activate heteromeric pLGIC.

The agonist site at the α4(+)/α4(-) is a major determinant of the agonist sensitivity of the (α4β2)$_2$α4 nAChR. Its removal increases ACh sensitivity and Saz-A efficacy and obliterates Cyt efficacy, all of which are signatures of the isoform (α4β2)$_2$β2 nAChR. Moreover, the agonist binding at the α4(+)/α4(-) site was weakened by α4W182A where ACh produced biphasic agonist responses, in accord with the functional behaviour of a receptor containing unaltered and mutated agonist sites. The high sensitivity component of the curve represented the contribution of unaltered agonist sites at the α4(+)/β2(-) interfaces, whereas the low sensitivity component was contributed by the mutated agonist site, as demonstrated by the differential sensitivity of these components to ACh or the antagonist DhβE. The site clearly impacts the activation of the receptor by agonist in a manner comparable to the effect of the consensus agonist site located at the α4(+)/β2(-) interfaces. When loop C in the primary face of the α4(+)/α4(-) was impaired, through alanine substitution of Y230 or serine substitution of C226 or by covalent modification of a free C225 by MTS reagents, the amplitude of the ACh responses was reduced (alanine substitution, MTSET) or enhanced (MTSEA). Although this site resides in the same interface where the signature potentiating Zn^{2+} site of the (α4β2)$_2$α4 isoform is located (Moroni et al., 2008) or analogous to that of the benzodiazepine site in $GABA_A$ receptors (Galzi &

Changeux 1994), it is not a classic allosteric site. Neither Zn^{2+} nor benzodiazepines is capable of channel gating but appear to enhance receptor responses to agonist by increasing channel opening frequency [benzodiazepines; (Rogers et al., 1994)] or by increasing burst duration [Zn^{2+}; (Hsiao et al., 2008)]. Instead, the site is comparable to the agonist sites in homomeric LGICs (Beato et al., 2004; Rayes et al., 2009).

MTS-modification of a free cysteine engineered at the tip of loop C in the auxiliary α4 subunit provided strong support for the idea that the putative site at the α4(+)/α4(-) interface contributes to channel gating. Interestingly, MTSET and MTSEA affected loop C function differentially. It is possible that MTS reagents lock loop C into different conformations depending on how the Cys-MTS moiety orientates within the binding pocket. MTSET could attenuate ACh responses by stabilising the mutated loop C into an extended, antagonist-bound like conformation, thus reducing ACh efficacy. By comparison, MTSEA could enhance ACh responses by locking the mutated loop C into a capped, agonist-bound-like conformation, which would increase agonist efficacy leading to the activation of the mutated sites at submaximal ACh concentrations. High resolution X-ray crystal structures of a MTS-Y53C mutant of the AChBP support this view (Brams et al., 2011). Loop C in MTSET-Y53C AChBP is in an extended, antagonist-bound conformation, which is consistent with the finding that α7 W55C-MTSET nAChRs are unresponsive to ACh (Brams et al., 2011). Another reagent, Methyl methanesulfonothioate (MMTS), enhances the ACh responses of α7 Y53C nAChR and locks loop C in MMTS-Y53C AChBP into a close, agonist-bound-like conformation (Brams et al., 2011). Although MTSET and MTSEA may affect the contribution of loop C to receptor activation differentially, it is clear from their effects on the ACh responses of the mutant agonist sites that all three sites contribute to activation of (α4β2)$_2$α4 nAChRs. This additional contribution appears to increase the efficacy of ACh because the maximal current responses of single mutants were markedly greater than those obtained by maximal activation of the non-mutated agonist sites.

The sites at the α4(+)/β2(-) and α4(+)/α4(-) interfaces respond differentially to alanine substitutions in respect of sensitivity to ACh or DhβE and the relative

proportions of the components of the ACh CRC. This could arise from differences in the overall architecture of the agonist sites. Unlike the primary face of the agonist sites, the complementary face is not identical. In the case of the agonist site at the α4(+)/α4(-) interface, the complementary face is contributed by an α4 subunit, providing a likely structural determinant for differential agonist-binding site interactions. Moreover, the coupling pathway leading to gating is also different in both types of agonist sites and this could affect the type of interfacial interactions implicated in coupling and gating. In accord with this idea, it has been reported that some conserved residues in the agonist site of α4β2 nAChR differentially regulate receptor activation by agonists, whereas other equally well conserved residues do not (Williams et al., 2009).

Sensitivity to activation by ACh increased through either ablation of the α4(+)/α4(-) interface or through alanine substitution in the α4(+)/α4(-) or either of α4(+)/β2(-) sites. Moreover, the pattern of agonist sensitivity of the single or double agonist binding mutants, as observed in terms of relative abundance of the ACh CRC components, sensitivity to ACh and changes in the nH coefficient, suggest a complex, likely allosteric, interaction between the agonist sites. Because macroscopic EC_{50} values are composites of binding, gating desensitisation as well as ion channel blockade, interpretation of the data in terms of molecular mechanisms is limited. However, considering that in homomeric LGIC agonist sites contribute interdependently and asymmetrically to channel gating (Rayes et al., 2009), which implies as yet unknown interfacial interactions in the coupling pathway, it is possible to surmise that the agonist sites at $(α4β2)_2α4$ receptors may contribute similarly to receptor activation. Studies of the microscopic currents of the $(α4β2)_2α4$ nAChR should aid the understanding of the observed differences.

CHAPTER 4

The additional acetylcholine binding site at the α4(+)/α4(-) interface of the (α4β2)2α4 nicotinic acetylcholine receptor contributes to desensitisation

4.1 Introduction

α4β2 nAChRs undergo acute and high-affinity desensitisation. Acute desensitisation refers to the loss in receptor response during a single exposure to high (~EC_{60} - EC_{100}) concentrations of agonist, whereas high-affinity desensitisation is induced by chronic exposure to low or non-activating agonist concentrations (Steinbach, 1990; Giniatullin et al., 2005; Gopalakrishnan et al., 1996; Paradiso & Steinbach, 2003; Lester, 2004). The molecular mechanisms producing acute or high-affinity desensitisation have not been fully identified. It is also unclear whether the two types of desensitisation are the result of a single process. Mutations within the second transmembrane domain of the α4 subunit (S248F and 776ins3) that affect both the apparent affinity to ACh and acute and chronic desensitisation (Bertrand et al., 1998) suggest a single desensitisation pathway. In addition, studies with chimeric nAChRs have shown that the N-terminal domain of the α4 subunit, along with the first three transmembrane domains and the N-terminal domain of the β2 subunit are involved in high-affinity desensitisation (Corringer et al., 1998; Kuryatov et al., 2000). However, other single point mutations in the α4 subunit can cause changes in desensitisation without effect on agonist binding (Matsushima et al., 2002).

In this chapter, the individual contribution of the three agonist sites in (α4β2)$_2$α4 nAChRs to high-affinity desensitisation were studied. The sites were individually mutated, and consequences of these mutations on ACh-induced activation and high-affinity desensitisation were assessed. It was found that the additional agonist site decreases sensitivity to activation and high-affinity desensitisation. Interestingly, the desensitisation studies reported here provide further evidence of functional non-equivalency between the agonist sites at the α4(+)/β2(-) and α4(+)/α4(-) interfaces.

4.2 Results

4.2.1 Desensitisation of (α4β2)$_2$α4 receptors

The contribution of the ACh binding sites of (α4β2)$_2$α4 receptors to desensitisation was determined by measuring the fraction of activatable receptors

remaining after prolonged exposure to a range of ACh concentrations. As in the studies reported in the previous chapter, the studies were carried out using the concatenated version of $(\alpha4\beta2)_2\alpha4$ nAChRs.

Representative traces of the responses of $\beta2\_\alpha4\_\beta2\_\alpha4\_\alpha4$ receptors to short (2 s) ACh test pulses at a concentration near the EC_{50} ACh (100 µM) in the absence of and during the ACh prepulse application are shown in **Fig. 4.1A**. Exposure to ACh prepulses decreased the peak amplitude of the responses evoked by EC_{50} ACh pulses in a concentration-dependent manner. Concentrations lower than 0.01 µM did not produce measurable effects on the responses to ACh test pulses. .Inhibition reached equilibrium within a few minutes following initiation of the prepulse applications and some recovery was observed when going back to control conditions. Plots of peak ACh EC_{50} current responses measured at equilibrium conditions as a function of the concentration of the ACh prepulses produced monophasic sigmoidal inhibitory CRC **(Fig. 4.1B)**. The estimated IC_{50} was approximately 500-fold greater than the EC_{50} for ACh-induced activation ($p < 0.05$; n = 8) **(Table 4.1)** and the Hill coefficient was less than 1. For comparison, the values for the ACh-induced functional inactivation of $(\alpha4\beta2)_2\alpha4$ receptors assembled from loose subunits are included in **Table 4.1.** Desensitisation of $(\alpha4\beta2)_2\alpha4$ by ACh was measured using the same protocol described for $\beta2\_\alpha4\_\beta2\_\alpha4\_\alpha4$ receptors. Fits to the data yielded IC_{50} and Hill coefficient values that were comparable to those estimated for $\beta2\_\alpha4\_\beta2\_\alpha4\_\alpha4$ receptors **(Table 4.1)**.
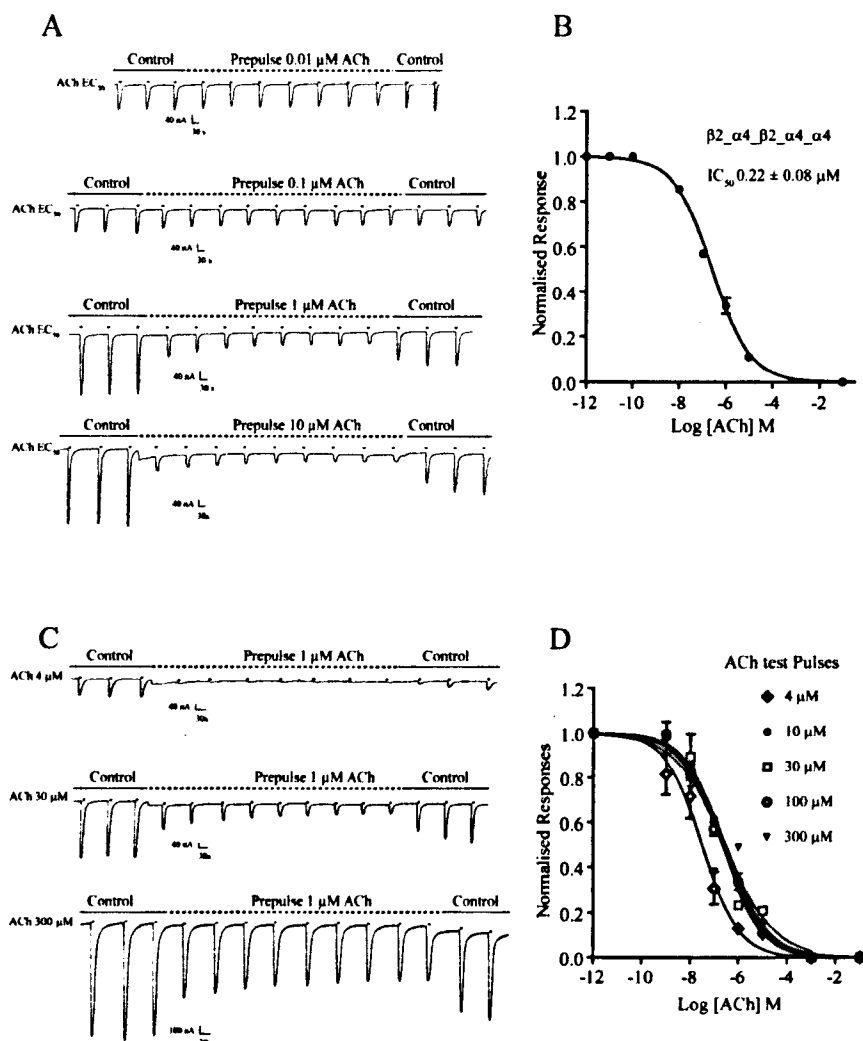
Figure 4.1. **Functional inhibition of β2_α4_β2_α4_α4 nAChRs. (A)** Typical traces of β2_α4_β2_α4_α4 nAChRs obtained by using the prolonged exposure to ACh protocol described in the Methods section. Impaled oocytes were challenged at regular intervals (90 s) by a 2 s pulse of 100 μM ACh, a concentration of ACh near the EC_{50}. Responses evoked prior to prepulses show no desensitisation but prepulses (ACh prepulse, dashed lines) produce a concentration-dependent decrease of the responses evoked by 100 μM ACh. On termination of the prepulse some recovery was observed. **(B)** CRC for the desensitisation of β2_α4_β2_α4_α4 nAChR produced by the protocol shown in A. The peak current of the EC_{50} ACh responses immediately before the end of the period of prolonged exposure to ACh was normalised to the control ACh responses. The data were best fitted to the monophasic Hill equation described in Methods. The estimated IC_{50} and Hill coefficient are summarized in **Table 4.1.** **(C)** Typical traces of β2_α4_β2_α4_α4 nAChRs stimulated by a 4 μM, 30 μM or 300 μM ACh test pulses exposed to Ringer's solution containing 1 μM ACh. **(D)** CRC for the desensitisation of β2_α4_β2_α4_α4 nAChR currents stimulated by a range of ACh test pulses. The exposure protocol used to induce desensitisation was identical to the one shown in A, except that the ACh test pulses were 4 μM, 10 μ, 30 μM or 300 μM. The peak current of the EC_{50} ACh responses immediately after the prepulses were normalised to the control ACh responses. The data were best fitted to the monophasic Hill equation described in Methods. The estimated IC_{50} and Hill coefficient are summarised in **Table 1.**

Table 4.1. **Summary of desensitisation and activation of α4β2 nAChRs by ACh.** EC_{50} or IC_{50} values were determined by fitting respectively the activation or inhibition data to the equations given in Methods. $(\alpha4\beta2)_2\alpha4$ and $(\alpha4\beta2)_2\beta2$ receptors were expressed from individual subunits injected into oocytes as previously described (Moroni et al., 2006). Desensitisation of concatenated β2_α4_β2_α4_α4 receptors was measured using ACh test pulses of 4 μM (^), 10 μM (^^), 30 μM (^^^), 100 μM (^^^^) or 300 μM (^^^^^). IC_{50} and EC_{50}/IC_{50} values for $(\alpha4\beta2)_2\beta2$ or β2_α4_ β2_α4_ β2 receptors were statistically different (noted by *) from those estimated for the desensitisation of β2_α4_β2_α4_α4 receptors measured using ACh pulses of 100 μM, 10 μM, 30 μM or 300 μM. IC_{50} and EC_{50}/IC_{50} values estimated for the desensitisation of the responses elicited by 4 μM ACh at β2_α4_β2_α4_α4 receptors were statistically different from the values estimated for the desensitisation of the responses evoked by higher concentrations of ACh at β2_α4_β2_α4_α4 receptors (noted by +). Statistical comparisons were carried out as described in Methods.

Receptor	EC_{50}(μM)	nH	IC_{50}(μM)	nH	EC_{50}/IC_{50}
β2_α4_β2_α4_α4	99±12	1.10±0.09	0.032±0.007[^+]	0.57±0.06	3093[+]
			0.29±0.08[^^]	0.54±0.03	341
			0.23±0.06[^^^]	0.56±0.04	430
			0.22±0.04[^^^^]	0.60±0.06	450
			0.27±0.04[^^^^^]	0.52±0.09	367
$(\alpha4\beta2)_2\alpha4$	101±21	0.95±0.08	0.18±0.01	0.61±0.07	561
β2_α4_β2_α4_β2	2.8±0.8*	1.05±0.09	0.058±0.001*	0.61±0.02	48.28*
$(\alpha4\beta2)_2\beta2$	2.2±0.3*	0.79±0.09	0.071±0.001*	0.54±0.01	31.03*

To test if the concentration of the ACh test pulse affected the degree of functional inhibition induced by prolonged exposure to ACh, we measured desensitisation of β2_α4_β2_α4_α4 receptors using ACh test pulses of 4 μM, 10 μM, 30 μM or 300 μM. ACh prepulses higher than 0.01 μM produced inhibition of all the ACh test pulses studied. **Fig. 4.1C** shows representative traces of the inactivation of current responses evoked by the various ACh test pulses studied by an ACh prepulse of 1μM. The inhibitory CRC produced by the inhibion data are shown in **Fig. 4.1D**. The estimated IC_{50} and Hill coefficient values for the desensitisation of currents evoked by ACh test pulses of 10 μM, 30 μM or 300 μM were not different from each other or from the IC_{50} and Hill coefficient values estimated from the inhibition of currents evoked by 100 μM ACh test

pulses **(Table 4.1)**. In contrast, when the ACh test pulse was 4 μM, a concentration of agonist that elicited less than 10% of the maximal ACh response, the estimated IC_{50} value was about 9-fold lower ($p < 0.05$; n = 4) **(Fig. 4.1D; Table 4.1)**. A contributor to the observed concentration-dependent effects could be procedural. Desensitisation may not have reached equilibrium at low concentrations of ACh, or processes such as ion channel blockade by ACh may have contributed to the observed functional inhibition at high concentrations of ACh test pulses (Bertrand et al., 1992; Chavez-Noriega et al., 1997). This is unlikely for the following reasons. Firstly, if at low concentrations of ACh test pulses desensitisation had not completely attained steady-state conditions, the extent of desensitisation elicited may not yet be complete. Under these conditions, the inhibition CRC would have shifted to the right yielding higher IC_{50} values for desensitisation. Secondly, if at higher concentrations of ACh test pulses other inhibitory processes such as ion channel blockade by ACh added to the inhibitory process, sensitivity to desensitisation would have increased.

There is evidence that both $(\alpha4\beta2)_2\alpha4$ and $(\alpha4\beta2)_2\beta2$ receptors may be expressed in the brain (Marks et al., 1999; Gotti et al., 2008; Marks et al., 2010; Rode et al., 2012). Therefore, the desensitisation of β2_α4_β2_α4_β2 nAChRs, the concatenated form of the $(\alpha4\beta2)_2\beta2$ nAChR (Carbone et al., 2009), was also measured. The $(\alpha4\beta2)_2\beta2$ nAChR displays 100-fold higher sensitivity for activation by ACh than the $(\alpha4\beta2)_2\alpha4$ isoform (Nelson et al., 2003; Moroni et al., 2006; Carbone et al., 2009). Typical recordings obtained for the inhibition of EC_{50} (2 μM) ACh responses of β2_α4_β2_α4_β2 nAChRs using the prolonged exposure to low ACh concentrations protocol are shown in **Fig. 4.2A**. The data produced monophasic sigmoidal inhibition curves as shown for β2_α4_β2_α4_α4 receptors **(Fig. 4.2B)**. The EC_{50} and Hill coefficient values estimated from the fit are shown in **Table 4.1**. The IC_{50} value for β2_α4_β2_α4_β2 receptors (0.058 ± 0.001 μM) was comparable to that estimated for $(\alpha4\beta2)_2\beta2$ receptors (0.071 ± 0.001 μM) **(Table 4.1)**. The IC_{50} value obtained for β2_α4_β2_α4_β2 was about 3.8-fold lower, in comparison to the IC_{50} values estimated for the desensitisation of the responses of β2_α4_β2_α4_α4 receptors stimulated by concentrations of ACh higher than 4 μM. However, there was no statistical differences between the IC_{50} values

estimated for $\beta2\_\alpha4\_\beta2\_\alpha4\_\beta2$ receptors and for $\beta2\_\alpha4\_\beta2\_\alpha4\_\alpha4$ receptors activated by ACh test pulses of 4 μM.

The window current of ligand-gated ion channels is the range of agonist concentrations at which receptors can be activated by agonists before desensitisation is complete (Steinbach, 1990). To provide an estimate of the window current for each $\alpha4\beta2$ receptor form, we replotted the desensitisation CRC obtained for EC_{50} ACh test pulses and the activation concentration response curve of each receptor type on the same axes **(Fig. 4.2B)**. The concentration range at which the activation and desensitisation curves overlap indicates the window current of receptors (Steinbach, 1990; Lester, 2004). **Figs 4.2B** and **C** show that for $\beta2\_\alpha4\_\beta2\_\alpha4\_\beta2$ receptors the window current extended from about 0.1 nM to 300 μM ACh with the peak occurring at 0.1 μM ACh. In contrast, for $\beta2\_\alpha4\_\beta2\_\alpha4\_\alpha4$ receptors stimulated by EC_{50} ACh test pulses the window current was between 10 nM and 500 μM ACh with the peak occurring at about 10 μM ACh. At the peak of the window current only about 17% of the maximal response elicited by ACh at $\beta2\_\alpha4\_\beta2\_\alpha4\_\alpha4$ receptors was activated, whereas for $\beta2\_\alpha4\_\beta2\_\alpha4\_\beta2$ receptors the percentage of the maximal response stimulated was 24%. The EC_{50}/IC_{50} ratio for the two types of receptors differed by about 9-fold ($p < 0.05$; n = 4) **(Table 4.1)**. Interestingly, the value of the EC_{50}/IC_{50} ratio for $\beta2\_\alpha4\_\beta2\_\alpha4\_\alpha4$ receptors varied depending on the concentration of the ACh test pulse used in the desensitisation experiments. When the ACh test pulse was 4 μM the EC_{50}/IC_{50} ratio was 7-fold lower than the EC_{50}/IC_{50} values estimated for $\beta2\_\alpha4\_\beta2\_\alpha4\_\alpha4$ receptors activated by higher concentrations of ACh test pulses **(Figs., 4.2B and C;Table 4.1)**. Also, compared to test pulses of higher ACh concentrations, the peak of the window current obtained with 4 μM ACh test pulses was approximately 7-fold lower (1.5 μM), and at this point only 10% of the maximal response to ACh was stimulated **(Figs. 4.2B, C)**.
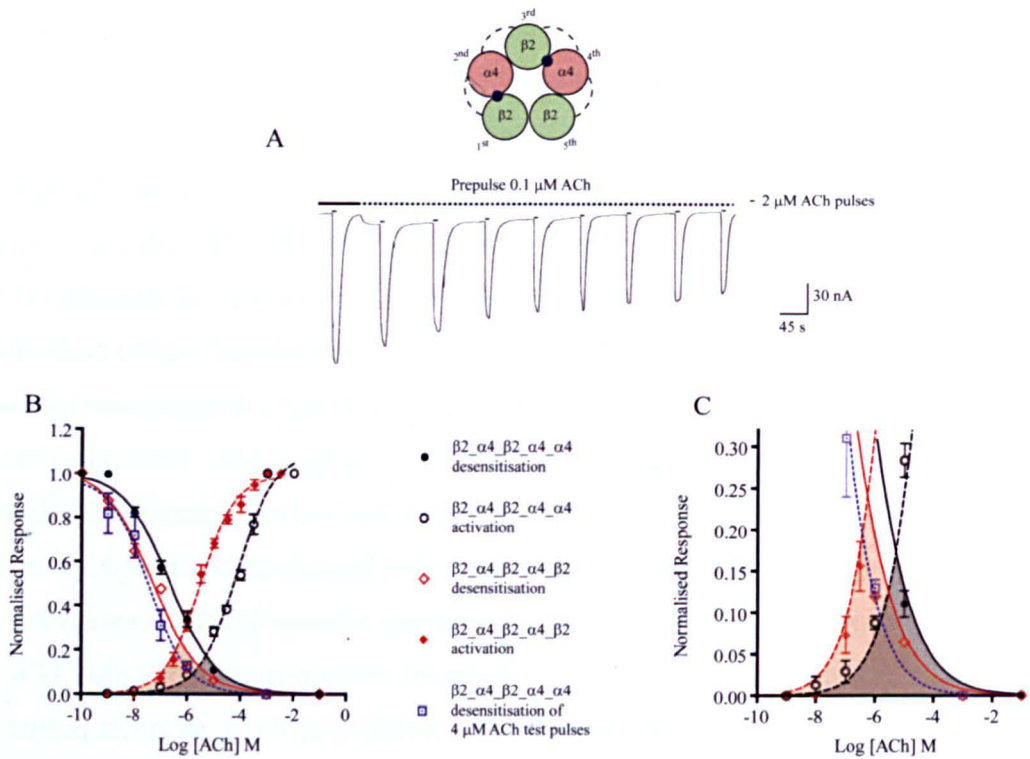
Figure 4.2. **High-affinity desensitisation in concatenated (α4β2)2β2 and (α4β2)2α4 nAChRs. (A)** Representative traces obtained from β2_α4_β2_α4_β2 receptors using the desensitisation protocol described in Methods. Oocytes expressing β2_α4_β2_α4_β2 receptors were challenged at regular intervals (90 s) by a 2 s ACh test pulse of 2 μM, a concentration of ACh near the ACh EC_{50} at this receptor type. The control responses decreased in amplitude upon chronic exposure to low concentrations of ACh. **(B)** Activation and desensitisation CRC of β2_α4_β2_α4_α4 or β2_α4_β2_α4_β2 receptors. Activation and desensitisation curves obtained with EC_{50} ACh test pulses are plotted on the same axis to reveal the window current for the α4β2 nAChR isoforms. The region where the activation and desensitisation concentration response curve overlap represents the window current of the receptors. We also include the data for the stimulation of β2_α4_β2_α4_α4 nAChRs with 4 μM ACh (blue dots). Each activation and desensitisation data point represents the mean ± S.E.M of 4 - 6 independent experiments. Data were best fit to the monophasic Hill equation described in Methods ($p < 0.001$; n = 4-8). The estimated EC_{50}, IC_{50} and Hill coefficients values are summarised in **Table 1**. **(C)** Detail of plot in **B**, showing the overlapping regions of the activation and desensitisation ACh CRC.

4.2.2 The ACh binding site at the α4(+)/α4(-) interface contributes to desensitisation

Since agonist-induced desensitisation occurs following occupation of agonist sites (Steinbach 2000; Giniatullin et al., 2005), impairment of the ACh binding site at the α4(+)/α4(-) interface by alanine substitution of α4W182 should affect desensitisation of β2_α4_β2_α4_α4 receptors, if the additional ACh site contributed to it. To test the validity of this view, the ACh-induced desensitisation of β2_^{W182A}α4_β2_^{W182A}α4_^{W182A}α4 was first determined. As reported in the previous chapter, introducing α4W182A simultaneously into the three α4 subunits of β2_α4_β2_α4_α4 receptors produces monophasic ACh sensitivity to activation by ACh and a seven-fold decrease in sensitivity to activation (**Chapter 3**; Mazzaferro et al., 2011). Chronic exposure to low concentrations of ACh desensitised the current responses evoked by 700 μM ACh (a concentration near the ACh EC_{50} of β2_^{W182A}α4_β2_^{W182A}α4_^{W182A}α4; see **Chapter 3** or Mazzaferro et al., 2011). Compared to wild type, sensitivity to desensitisation was reduced significantly from 0.22 ± 0.04 μM to 60 ± 2.1 μM ($p < 0.001$; n = 6) (**Fig. 4.3A**) thus, impairment of agonist binding reduces sensitivity to desensitisation. As expected from this finding, the window current of β2_^{W182A}α4_β2_^{W182A}α4_^{W182A}α4 was shifted to the right ($p < 0.001$; n = 4) (**Fig. 4.3B**). These results indicated that α4W182A could be used to measure the contribution of individual agonist binding sites to desensitisation.

It was shown in **Chapter 3** that binding of ACh to the unaltered binding sites at the α4(+)/β2(-) subunit interfaces of β2_α4_β2_α4_^{W182A}α4 receptors gives rise to the higher sensitivity component of the activation concentration response curve, whilst the mutated site at the α4(+)/α4(-) interface contributes mostly to the low sensitivity component of the curve. Therefore, in order to provide estimates of desensitisation for intact and impaired agonist sites, the effects of prolonged exposure to ACh prepulses on the responses elicited by ACh test pulses of either EC_{50-1} (mostly intact agonist sites) ACh or EC_{50-2} (intact agonist sites plus mutated agonist sites) ACh were measured. Representative current responses obtained for the β2_α4_β2_α4_^{W182A}α4 receptors using this protocol are shown in **Fig. 4.3.A**. The peak currents obtained with either of the ACh EC_{50}

pulses were desensitised by ACh prepulses. For both ACh test pulses, desensitisation produced monophasic inhibition curves ($p < 0.001$; n = 5) **(Fig. 4.3B)**. However, the IC_{50} values estimated from these curves were about 280-fold different ($p < 0.05$; n = 5) **(Table 4.2)**. The mutated agonist site at the α4(+)/α4(-) interface was less sensitive to desensitisation than the non-mutated agonist sites, which is consistent with the previous observation that impairment of ACh binding sites decreases sensitivity of α4β2 nAChRs to desensitisation **(Fig. 4.2A)**. Also, the IC_{50} value estimated for the component with lower sensitivity to activation was about 41-fold greater compared to the IC_{50} estimated for currents evoked by EC_{50} ACh on wild type β2_α4_β2_α4_α4 receptors. Interestingly, the estimated IC_{50} at intact agonist sites (IC_{50-1}) was not statistically different from that estimated for ACh-induced desensitisation in β2_α4_β2_α4_β2 receptors **(see Tables 4.1 and 4.2)**, or for desensitisation of the responses of β2_α4_β2_α4_α4 receptors to 4 μM ACh pulses.
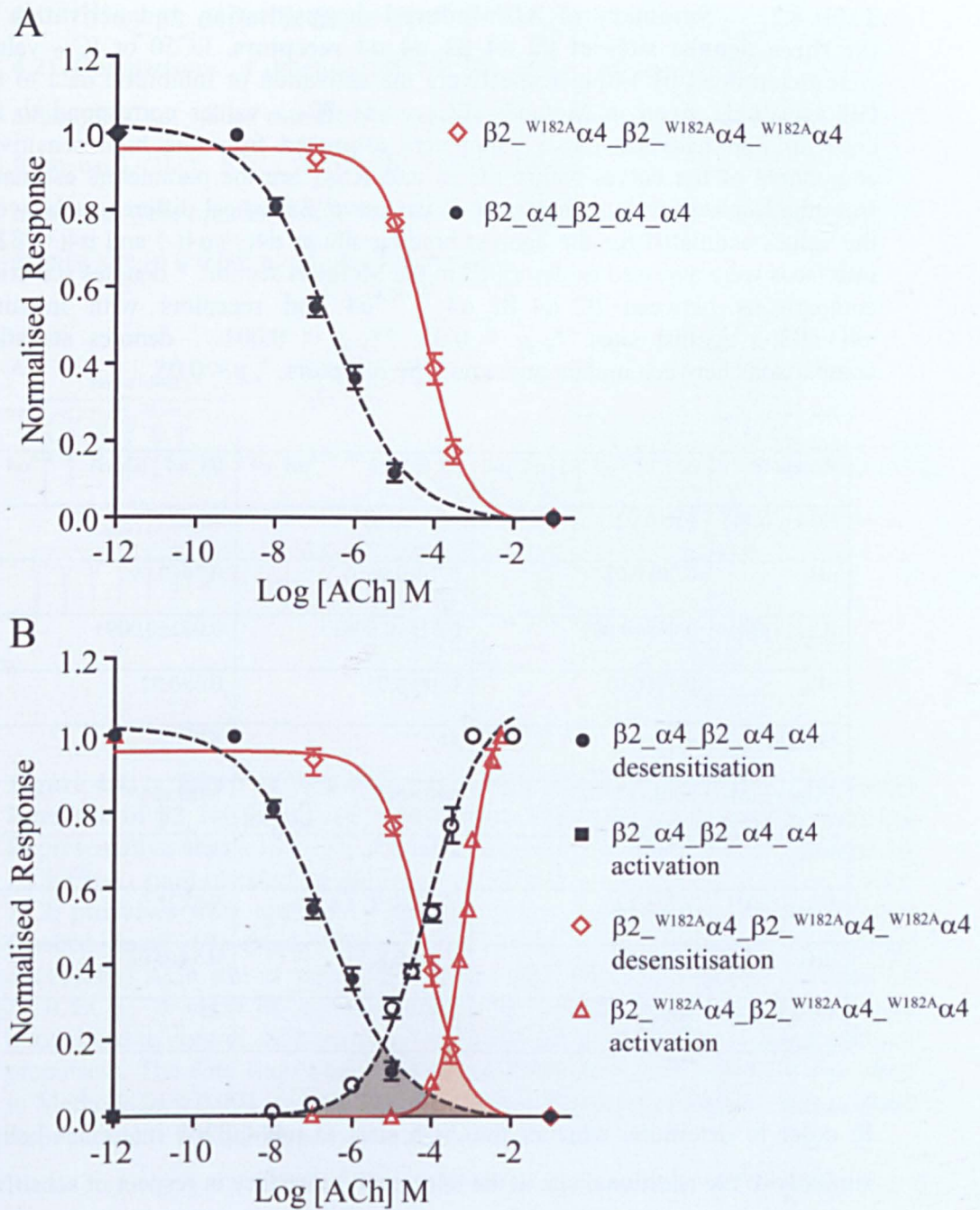
Figure 4.3. **Effect of W182A on the high-affinity desensitisation of β2_α4_β2_α4_α4 receptors.** **(A)** Wild type and mutant (β2_^{W182A}α4_β2_^{W182A}α4_^{W182A}α4 receptors) inhibition CRC. Desensitisation was induced using a prolonged application of ACh test pulse protocol. The data were best fit to the monophasic Hill model described in Methods. IC$_{50}$ and Hill coefficient values are shown in **Table 1** (wild type receptors) or **Table 2** (mutant receptor). **(B)** Plots of activation and inhibition CRC data plotted on the same axes. The area under the curves where the activation and desensitisation CRC overlap represents the window current of the receptor.

Table 4.2. **Summary of ACh-induced desensitisation and activation of the three agonist sites of β2_α4_β2_α4_α4 receptors.** EC50 or IC_{50} values were determined by fitting respectively the activation or inhibition data to the Hill equations given in Methods. EC_{50-1} and IC_{50-1} values correspond to the concentration response curve parameters estimated from the high sensitivity component of the curve, whilst EC_{50-2} and IC_{50-2} are the parameters estimated from the low sensitivity component of the curve. Statistical differences between the values estimated for the agonist binding site at α4(+)/α4(-) and α4(+)/β2(-) interfaces were assessed as described in the Methods section. * denotes statistical comparisons between β2_α4_β2_α4_^{W182A}α4 and receptors with impaired α4(+)/β2(-) agonist sites. *, $p < 0.05$; **, $p < 0.001$. $^+$ denotes statistical comparisons between mutant and wild type receptors. $^+, p < 0.05$.

Receptor	β2_^{W182A}α4_β2_α4_α4	β2_α4_β2_^{W182A}α4_α4	β2_α4_β2_α4_^{W182A}α4
EC50_1 (µM)	1.8±0.02$^+$	1.20 ±0.03$^+$	28 ±2*,$^+$
nH1	0.78±0.08	0.71±0.06	0.74±0.09
IC50_1 (µM)	0.038±0.009$^+$	0.025±0.008+	0.032±0.009+
nHin	0.54±0.01	0.48±0.08	0.5±0.02
EC50/IC50	47$^+$	48$^+$	875+
EC50_2 (µM)	630±71$^+$	640 ±65$^+$	3483±25*,$^{++}$
nH2	1.3±0.5	1.4±0.7	1.8±1
IC50_2 (µM)	1.72±0.2$^+$	1.68 ±0.2$^+$	9±0.2*,$^+$
nHin	0.6±0.02	0.54±0.8	0.54±0.02
EC50/IC50	366	376	387

In order to determine whether the ACh sites at α4(+)/β2(-) interfaces behave similarly to the additional site at the α4(+)/α4(-) interface in respect of sensitivity to desensitisation, we engineered mutant receptors β2_^{W148A}α4_β2_α4_α4 or β2_α4_β2_^{W148A}α4_α 4 and determined their sensitivity to desensitisation induced by ACh prepulses. As for mutant β2_α4_β2_α4_^{W182A}α4 receptors, desensitisation associated with intact or mutant ACh sites was monitored by assaying the effects of ACh prepulses on currents evoked by either ACh EC_{50-1} or ACh EC_{50-2} (**Fig. 4.4A, B**). Introduction of α4W182A into any of the two agonist sites located at α4(+)/β2(-) interfaces altered wild type sensitivity to desensitisation induced by ACh. Patterns of desensitisation for intact or mutant agonist sites at

$\beta2\_^{W148A}\alpha4\_\beta2\_\alpha4\_\alpha4$ or $\beta2\_\alpha4\_\beta2\_^{W148A}\alpha4\_\alpha4$ receptors were similar **(Table 4.2)**. Comparisons of desensitisation in the three mutant receptors showed that although IC_{50-1} values estimated for all three mutant receptors were not different from each other, IC_{50-2} values for mutant agonist sites located at $\alpha4(+)/\beta2(-)$ interfaces were approx. 7-fold lower than the IC_{50-2} value for mutant $\alpha4(+)/(-)\alpha4$ agonist site ($p < 0.05$; n = 5 -7) **(Table 4.2)**.
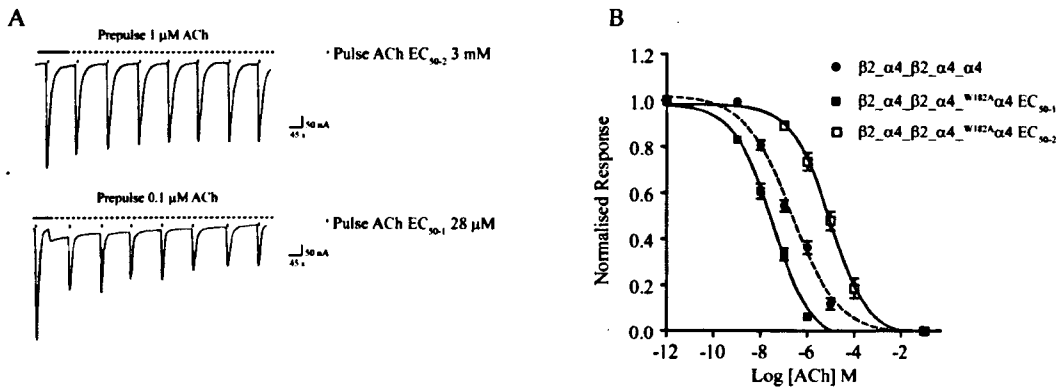
Figure 4.4. **Effect of impairing the ACh binding site at the $\alpha4(+)/\alpha4(-)$ interface of $\beta2\_\alpha4\_\beta2\_\alpha4\_\alpha4$ receptors on high-affinity desensitisation. (A)** Representative traces showing the desensitisation of ACh currents evoked by ACh EC_{50-1} (non-mutated agonist sites) or ACh EC_{50-2} (mutated $\alpha4(+)/\alpha4(-)$ site). ACh prepulses were applied by adding ACh to the perfusing Ringer solution (dashed lines). **(B)** Desensitisation CRC of ACh EC_{50} responses of mutated $\alpha4(+)/\alpha4(-)$ ACh site or intact $\alpha4(+)/\beta2(-)$ sites. The peak currents evoked by ACh EC_{50-1} or ACh EC_{50-2} measured at the end of the ACh prepulses, were normalised to control ACh currents (ACh currents evoked prior to application of prepulses). The data were best fitted to the monophasic Hill equation described in Methods ($p < 0.001$; n = 6). For comparison, the desensitisation concentration response curve for wild type is included (dashed lines).

A

B
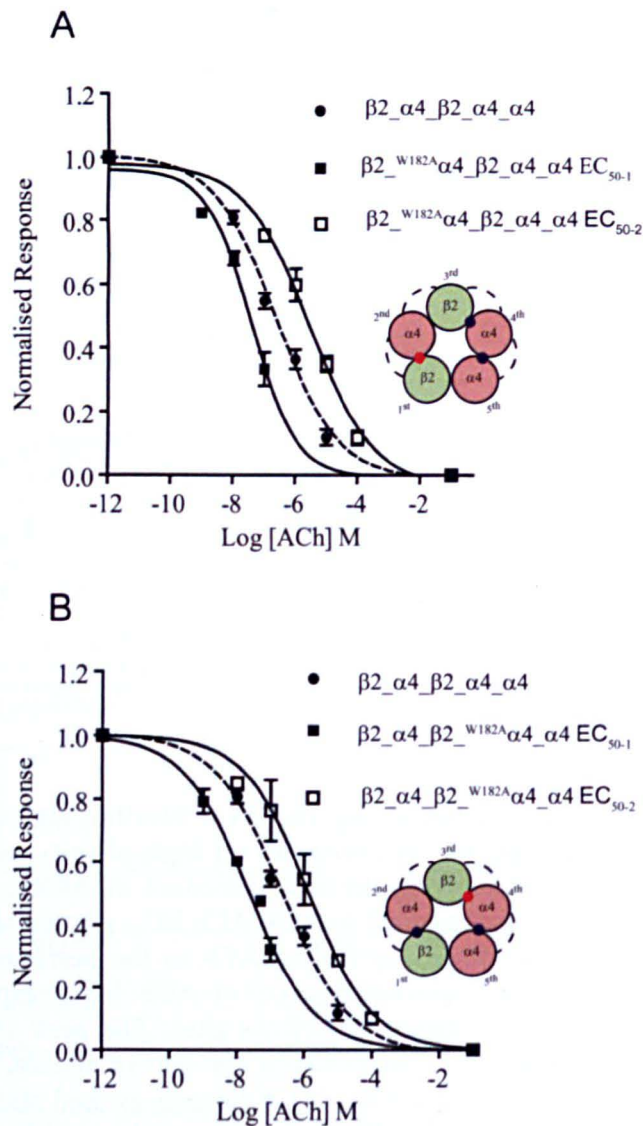
Figure 4.5. **Mutant ACh agonist sites at α4(+)/β2(-) interfaces affect activation and high-affinity desensitisation of β2_α4_β2_α4_α4 nAChRs. (A, B)** Desensitisation CRC of ACh responses of mutated α4(+)/β2(-) and intact agonist sites in $β2\_^{W182A}α4\_β2\_α4\_α4$ or $β2\_α4\_β2\_^{W182A}α4\_α4$ receptors ($^{W182}α4$ is indicated by a closed red circle). The peak currents evoked by ACh EC_{50-1} or ACh EC_{50-2} measured at the end of ACh prepulses were normalised to control ACh currents (ACh currents evoked prior to application of prepulses). The data were best fit to the monophasic Hill equation described in Methods ($p < 0.002$; n = 5). For comparison, the wild type desensitisation concentration response curve was included (dashed lines). There is no significant difference in the activation or high-affinity desensitisation of $β2\_^{W182A}α4\_β2\_α4\_α4$ and $β2\_α4\_β2\_^{W182A}α4\_α4$ receptors.

4.3 Discussion

All agonist sites in $(\alpha4\beta2)_2\alpha4$ receptors contribute to agonist-induced desensitisation.

The desensitisation of $\alpha4\beta2$ nAChRs is a complex process. Previous studies on $\alpha4\beta2$ nAChRs of unknown stoichiometry have shown the existence of two desensitised states (Fenster et al., 1997; Buisson et al. 2000; Paradiso & Steinbach, 2011). Recovery from desensitisation is also biphasic, although a third desensitised state may also exist (Paradiso & Steinbach, 2003). High-affinity desensitisation and recovery from desensitisation of $\alpha4\beta2$ nAChRs are both agonist-dependent, which is likely to reflect differential affinity of agonists for the desensitised states (Marks et al., 2010; Paradiso & Steinbach, 2003). The findings of this study add further complexity to the activation/desensitisation of $\alpha4\beta2$ nAChRs by showing that the effects of $\alpha4$W182A on desensitisation (and activation) are agonist site-specific. This strongly suggests that the agonist sites of $(\alpha4\beta2)_2\alpha4$ receptors have different sensitivity to both stimulation by ACh and high-affinity desensitisation. Moreover, the observation that impairment of any of the agonist sites by $\alpha4$W182A produced biphasic sensitivity to activation and that a small fraction (less than 10%) of the maximal ACh response desensitised with higher sensitivity than greater response fractions suggests that two agonist sites, or perhaps one, when engaged by agonist, can lead to activation and then desensitisation with a sensitivity that is different from that observed with full occupancy. Thus, it appears that the agonist sites in $(\alpha4\beta2)_2\alpha4$ receptors are not functionally equivalent.

Functional differences between the agonist sites in $(\alpha4\beta2)_2\alpha4$ nAChRs may arise from structural differences between the agonist sites and downstream pathways producing the coordinated motions triggered by agonist binding that lead to gating (Auerbach, 2010). The primary face in the agonist site at $\alpha4(+)/\alpha4(-)$ and $\alpha4(+)/\beta2(-)$ interfaces are identical but the complementary face is not. In the case of the agonist site at the $\alpha4(+)/\alpha4(-)$ interface, the complementary face is contributed by the (-) face of the adjacent $\alpha4$ subunit. Studies of $GABA_A$ receptors, which are endowed with two structurally identical agonist sites, have shown that even structurally identical agonist sites may function non-

equivalently (Baumann et al., 2003). In the case of $GABA_A$ receptors, non-equivalency may arise from differences in the subunits flanking each agonist site, which could produce agonist-site specific conformational transitions and hence agonist-site specific activation and/or desensitisation states (Baumann et al., 2003). However, previous studies of the muscle nAChR, which is the prototype protein for the pentameric ligand-gated ion channel family, have shown that even though the two agonist sites have different complementary subunits (δ or γ/ε) and, thus, different structural properties, they are functionally comparable, with each having approximately the same affinity for ACh regardless of the conformational state (i.e., open or close) of the receptor (Jha & Auerbach, 2010).

Incorporation of $\alpha 4W182A$ into any of the agonist binding sites decreased sensitivity of the site to both activation and desensitisation, but the effects were more striking on activation, consistent with the key role of $\alpha 4W182$ in ACh binding (Corringer et al., 1998; Mazzaferro et al., 2011). The effect of $\alpha 4W182$ on desensitisation confirms earlier findings that high-affinity desensitisation is partly influenced by amino acid residues in the N-terminal domain of the $\alpha 4$ subunit. Other regions that have also been implicated in high-affinity desensitisation are transmembrane domains M2 (Bertrand et al. 1998;) M1 and M3 (Kuryatov et al., 2000). The mechanism connecting the open receptor states to the desensitised states are not fully understood (Auerbach, 2010). Recent studies on the $\alpha 7$ nAChR have suggested that desensitisation of nAChRs may be governed by the balance between agonist binding, coupling and gating (Zhang et al., 2011). According to this proposal agonist binding induces conformational changes in the coupling region (N terminal loops 2 and 7 with M2-M3 linker from the transmembrane domain) that generate sufficient energy to overcome the gating energy barrier to open the channel. However, the coupling region tends to uncouple due to instability of the open state conformation, as compared to the closed state, triggering desensitisation (Zhang et al., 2011). This possibility is consistent with our finding that weakening agonist binding by incorporation of W182A in $\beta 2\_\alpha 4\_\beta 2\_\alpha 4\_\alpha 4$ receptors decreases sensitivity to desensitisation. Presumably, W182A decreases coupling strength, which would in turn affect the critical balance between coupling and gating towards a decrease in sensitivity to desensitisation.

Considering the activation and desensitisation of $(\alpha4\beta2)_2\alpha4$ nAChRs in comparison to $(\alpha4\beta2)_2\beta2$ nAChRs, it seems that full agonist occupation in $(\alpha4\beta2)_2\alpha4$ nAChRs decreases sensitivity to both activation and desensitisation. Recent studies on $\alpha7$ nAChRs assembled from ((5-Chloro-2,4-dimethoxyphenyl)-*N*-(5-methyl-3-isoxazolyl)-urea)-sensitive (PNU-120596) and PNU-120596-resistant $\alpha7$ subunits have suggested that heteromeric receptor desensitisation is determined by the fastest desensitising subunit (Dacosta & Sine, 2013). Since our data suggest that engagement of two binding sites by agonist activates and desensitises $(\alpha4\beta2)_2\alpha4$ nAChRs with sensitivities typical of $(\alpha4\beta2)_2\beta2$ nAChRs, it seems that for $(\alpha4\beta2)_2\alpha4$ nAChRs occupation of the third agonist site modulates the function of the two other agonist sites by decreasing their sensitivity to high affinity desensitisation.This modulatory effect could be exerted at the gate or could be transmitted to the adjacent binding sites to affect agonist binding, and hence, the energy transitions leading to gating. Modulation of the function of two agonist sites by a third agonist site has been previously observed in homomeric 5-HT$_3$-$\alpha7$ chimeric receptors, although in this receptor construct full occupancy increases sensitivity to activation and possibly to desensitisation (Rayes et al., 2009).

It is difficult to propose a kinetic scheme that could represent adequatedly the activation and desensitisation of the $(\alpha4\beta2)_2\alpha4$ receptors because the data shown here cannot provide estimates of the affinity of each type of agonist site for the various states of the receptors, including closed, open and desensitised, or give insights on how these various states are connected. Single channel analysis of the activation and desensitisation of this receptor type should help to address this issue. Notwithstanding this lack of detail, the data strongly suggests that occupancy of two agonist sites is sufficient to activate and desensitise the $(\alpha4\beta2)_2\alpha4$ nAChR and that full occupation adds an additional active and desensited state. From the findings, these additional states are likely to be reached at concentrations of ACh that produce more than 10% stimulation of the maximal response, from which point receptor function appears to be predominantly shaped by the modulatory activity exerted by the third agonist site over the two other agonist sites.

Finally, studies of mouse native thalamic $\alpha4\beta2$ nAChR receptors which show biphasic agonist CRC for stimulation of putative $(\alpha4\beta2)_2\alpha4$ and $(\alpha4\beta2)_2\beta2$ nAChR function, have suggested that $(\alpha4\beta2)_2\alpha4$ and $(\alpha4\beta2)_2\beta2$ receptors have similar sensitivity to high-affinity desensitisation, although the receptors differ in their window current due to differences in agonist sensitivity (Marks et al., 2010). We found that the receptors desensitise with different sensitivities. Although possible artifacts introduced by concatenation cannot be discarded, our findings may differ from those reported by Marks et al., (2010) because native $\alpha4\beta2$ nAChR function reflects stimulation of $(\alpha4\beta2)_2\alpha4$, $(\alpha4\beta2)_2\beta2$ and $(\alpha4\beta2)_2\alpha5$ nAChRs (Marks et al., 2010; Gotti et al., 2008; Grady et al., 2012).

In summary the ACh site at the $\alpha4(+)/\alpha4(-)$ interface confers distinct sensitivity to activation and slow desensitisation by ACh to $(\alpha4\beta2)_2\alpha4$ receptors which further supports our view that this site is responsible for the functional signatures of the $(\alpha4\beta2)_2\alpha4$ nAChR. The additional agonist site is not functionally equivalent to the sites located at the $\alpha4(+)/\beta2(-)$ interfaces and this may be what determines the properties of this receptor type compared to the isoform $(\alpha4\beta2)_2\beta2$. The additional site not only contributes to global receptor activation and slow desensitisation but also appears to modulate the function of the agonist sites located at the $\alpha4(+)/\beta2(-)$ interfaces. Finally, slow desensitisation is likely to play an important role in modulating the duration and conducting states of the alternate $\alpha4\beta2$ nAChRs and hence their effects in integrated neuronal behaviours. Indeed, the slow desensitisation profiles of the $\alpha4\beta2$ nAChRs have important consequences for the window current of the alternate $\alpha4\beta2$ receptors. The EC_{50}/IC_{50} ratio for $(\alpha4\beta2)_2\alpha4$ receptors is much higher than that for $(\alpha4\beta2)_2\beta2$ receptors, which suggests that $\alpha4\beta2$ nAChR activity through the $(\alpha4\beta2)_2\beta2$ isoform would be more prominent under conditions of prolonged exposure to low concentrations of ACh, as it occurs through volume transmission.

CHAPTER 5

The ligand selectivity of the agonist site at the α4(+)/α4(-) interface of the (α4β2)2α4 nAChR revealed by cysteine substitution accessibility method

5.1 Introduction

(α4β2)₂α4 and (α4β2)₂β2 receptor isoforms respond with different sensitivity to nicotinic competitive compounds (Moroni et al., 2006; Zwart et al., 2008; Carbone et al., 2009; Mazzaferro et al., 2011) (for a summary of available data, **see Table 1.1**). In **Chapter 3**, it was shown that the additional agonist site that operates from the α4(+)/α4(-) interface determines the signature ACh sensitivity of (α4β2)₂α4 receptors (see also, Mazzaferro et al., 2011; Harpsoe et al., 2011). The site is located at a position homologous to the ACh binding sites housed by α4(+)/β2(-) interfaces, and homologous amino acid residues of α4 and β2 subunits form the agonist binding site pocket, which suggests that all agonist sites in (α4β2)₂α4 receptors share similar functional properties. However, pharmacological studies that showed the potency and efficacy of agonists ACh, Cyt and Saz-A at (α4β2)₂α4 nAChRs lacking the α4(+)/α4(-) interface is (α4β2)₂β2 nAChR-like (**Chapter 3**; Mazzaferro et al., 2011), suggest different functional properties for the two types of agonist sites, which most likely accounts for the pharmacology of (α4β2)₂α4 nAChRs (Moroni et al., 2006; Carbone et al., 2009). Therefore, if we are to fully understand the structural determinants and molecular mechanisms underlying the agonist sensitivity of (α4β2)₂α4 receptors, it is necessary to determine the functional sensitivity of the additional site to nicotinic compounds. In work reported in this chapter, a free cysteine residue was introduced in the complementary face of the agonist site at the α4(+)/α4(-) face in order to apply the SCAM method to characterise for the first time the competitive ligand selectivity of the agonist site at the α4(+)/α4(-) interface. The rate of reaction, between the cysteine and MTSET, in the absence or presence of nicotinic ligands was measured to determine the ability of the ligands to recognise the site. It is demonstrated that the agonist site at α4(+)/α4(-) and α4(+)/β2(-) interfaces display different properties for agonists and that this difference defines the overall agonist selectivity profile of the receptor, as compared to (α4β2)₂β2 nAChRs. The findings suggest that the relative efficacy of agonists at (α4β2)₂α4 receptors is defined by both their ability to recognise the agonist site at the α4(+)/α4(-) interface and by agonist-specific interactions with residues on the agonist binding pocket. The findings add another level of

complexity to the molecular mechanisms that define ligand efficacy in the pentameric ligand-gated ion channel family.

5.2 Results

5.2.1 Pharmacological characterization of $\beta2\_\alpha4\_\beta2\_\alpha4^{T152C}\_\alpha4$ receptors

The nicotinic pharmacology of the agonist site at the α4(+)/α4(-) interface was examined by determining if α4β2-preferring ligands could impede the reaction between MTSET and a free cysteine residue (α4T152C) introduced by single point mutation into loop E of the agonist site at the α4(+)/α4(-) interface. α4T152 occupies a position homologous to β2L146 in the agonist sites at α4(+)/β2(-) interfaces. Previous studies by Papke et al., (2011) showed that neither β2L146C nor α4T152C have significant impact on the function and expression of α4β2 nAChRs, and that both are accessible to modification by MTS reactions. Oocytes were injected with the mutant or wild type receptor cRNAs and were assayed for ACh and other nicotinic ligands responsiveness using two-electrode voltage clamp.

ACh, Cyt, Var, TC-2559 and Saz-A elicited currents from oocytes expressing $\beta2\_\alpha4\_\beta2\_\alpha4^{T152C}\_\alpha4$ receptors, indicating that the T152C substitution was tolerated and yielded functional receptors **(Fig. 5.1)**. The maximal macroscopic currents elicited by ACh, Cyt, Var, TC-2559 and Saz-A at $\beta2\_\alpha4\_\beta2\_\alpha4^{T152C}\_\alpha4$ receptors were similar to wild type. Compared to wild type, α4T152C did not change the monophasic responses to ACh, Cyt, Var or TC2559 **(Fig. 5.1, Table 5.1)**. Compared to wild type, α4T152C had no effects on the potency or efficacy of agonist Cyt or competitive antagonist DhβE, but the potency of ACh decreased by 2.4-fold and the potency of Var and TC-2559 increased by 4-fold and 2-fold, respectively **(Table 5.1)**. These effects are modest, which together with the lack of effect on functional expression and maximal macroscopic currents warranted the use of α4T152C for the ligand protection assays described below.

To test if the pattern of agonist responses found for $\beta2\_\alpha4\_\beta2\_\alpha4^{T152C}\_\alpha4$ receptors was agonist-site specific, $\beta2^{L146C}$ was introduced on the homologous position on the agonist site on the $\alpha4(+)\beta2(-)$ interface farthest from the $\alpha4(+)/\alpha4(-)$ interface **(Fig. 5.3)**, and consequences of this substitution on the effects of ACh, Cyt Var or TC-2559 were studied. As shown in **Fig. 5.1** and **Table 5.1**, ACh produced biphasic activation in $\beta2^{L146C}\_\alpha4\_\beta2\_\alpha4\_\alpha4$ receptors ($p < 0.0001$; F 9.826), even though the confidence interval for estimated high-sensitivity EC_{50} value was broad. The estimated EC_{50} value for the high sensitivity component (EC_{50-1}) of the curve was 69 (2-2296) µM, whilst for the low sensitivity component (EC_{50-2}) the value was 1600 (1180-2203) µM. It has been shown previously that impairment of any of the agonist sites in $\beta2\_\alpha4\_\beta2\_\alpha4\_\alpha4$ receptors by alanine or cysteine substitution of conserved aromatic residues in loop B or C leads to biphasic ACh concentration responses comprising a high sensitivity component contributed mostly by intact agonist sites and a low-sensitivity component contributed by intact and impaired sites (Mazzaferro et al., 2011). Unlike $\beta2\_\alpha4\_\beta2\_\alpha4^{T152C}\_\alpha4$ receptors, $\beta2^{L146C}\_\alpha4\_\beta2\_\alpha4\_\alpha4$ receptors displayed wild type sensitivity for Var but reduced sensitivity for Cyt and TC2559. Agonist relative efficacy was comparable at wild type and $\beta2\_\alpha4\_\beta2\_\alpha4^{T152C}\_\alpha4$ receptor, **(Table 5.2)**. These findings indicate that the agonist sites at $\alpha4(+)/\alpha4(-)$ and $\alpha4(+)/\beta2(-)$ sites have different sensitivity for agonists.
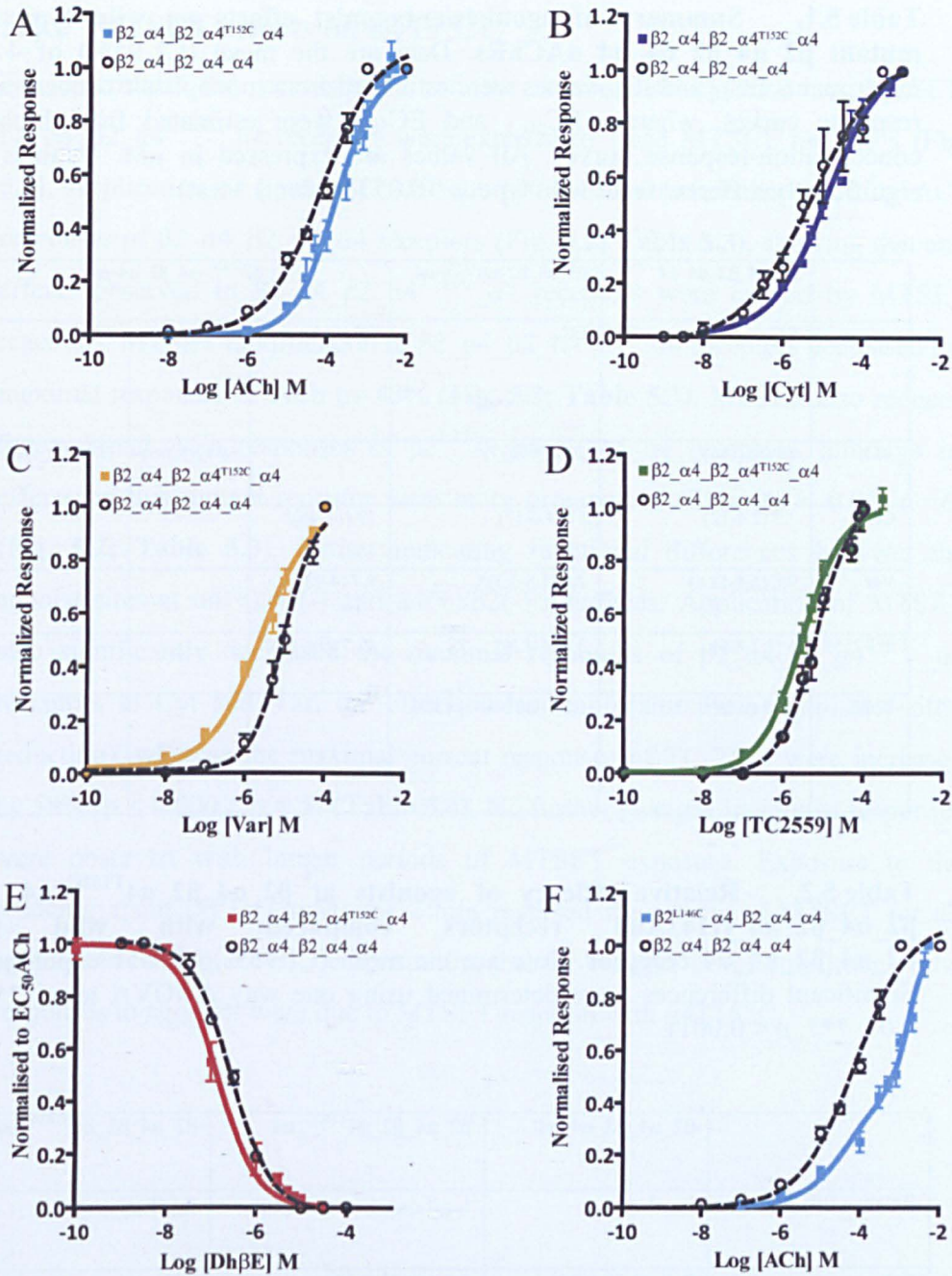
Figure. 5.1. **Functional sensitivity of β2_α4_β2_α4T152C_α4 receptors to nicotinic ligands.** All compounds tested produced monophasic concentration responses curves **(A-I)**. For comparison, the ACh concentration-response curve at β2^{L146C}_α4_β2_α4_α4 receptors is shown **(F)**. β2^{L146C}_α4_β2_α4_α4 receptors ACh produced a biphasic concentration response curve. Data points represent the mean of at least four independent experiments. The mean of the I$_{max}$ ± SEM for 4-10 experiments for each receptor were as follow: β2_α4_β2_α4_α4, (ACh, 386 ± 77 nA), (Cyt, 241 ± 71 nA), (Var, 464 ± 123 nA), (TC-2559, 203 ± 32 nA); β2_α4_β2_α4^{T152C}_α4, (ACh, 532 ± 103 nA), (Cyt, 292 ± 70 nA), (Var, 373 ±112 nA), (TC-2559, 304 ± 87 nA); β2^{L146C}_α4_β2_α4_α4, (ACh, 265 ± 42 nA). Data were fitted by nonlinear regression as described in **Chapter 2**.

Table 5.1.   Summary of agonists/antagonist effects on wild type and mutant β2_α4_β2_α4_α4 nAChRs. Data are the mean (CI 95%) of 4 -10 experiments EC_{50} and IC_{50} values were estimated from monophasic concentration response curves, whereas EC_{50_1} and EC_{50_2} were estimated from biphasic concentration-response curves. All values are expressed in μM. *Values are significantly different from wild type, $p < 0.05$ (Students t-test).

	β2_α4_β2_α4_α4	β2_α4_β2_α4^{T152C}_α4	β2^{L146C}_α4_β2_α4_α4		
	EC_{50}	EC_{50}	EC_{50}	EC_{50_1}	EC_{50_2}
ACh	86 (57-116)	206 (75-337)*		69 (2-2296)	1600 (1180-2203)
Cyt	7.3 (2.4-12)	11 (4.6-17)	19 (11-26)*		
Var	9.5 (5.4-13.6)	2.4 (1.5-3.3)*	8.7 (4-13)		
TC-2559	6 (3.7-8.5)	3 (1.6-4.5)*	12.7 (9.4-16)*		
DhβE	0.28 (0.24-0.33) (IC_{50})	0.25 (0.07-0.43) (IC_{50})			

Table 5.2.   Relative efficacy of agonists at β2_α4_β2_α4^{T152C}_α4, and β2_α4_β2_α4_H142Aα4 receptors compared with wild type β2_α4_β2_α4_α4 receptor. Data are the mean (CI 95%) of 4-11 experiments. Significant differences were determined using one way ANOVA tests (**$p < 0.01$, ***, $p < 0.001$).

	β2_α4_β2_α4_α4	β2_α4_β2_α4^{T152C}_α4	β2_α4_β2_α4^{H142A}_α4
Relative Efficacy	I_{max}/I_{ACh_max}	I_{max}/I_{ACh_max}	I_{max}/I_{ACh_max}
Cyt	0.19 (0.18-0.20)	0.21 (0.09-0.34)	ND
Var	0.29 (0.14-0.44)	0.22 (0.16-0.28)	ND
TC-2559	0.22 (0.16-0.27)	0.12 (0.07-0.17)	0.83 (0.76-0.90)***
Saz A	0.11 (0.08-0.14)	0.10 (0.05-0.14)	0.55 (0.42-0.68)***

5.2.2 MTSET effects on α4T152C

To determine the accessibility of the introduced cysteine to MTSET, $\beta2\_\alpha4\_\beta2\_\alpha4^{T152C}\_\alpha4$ receptors were exposed to 1mM MTSET for 120 s **(Fig. 5.2)**. Application of 1 mM MTSET for 120 s had no effect on the EC_{50} ACh responses of $\beta2\_\alpha4\_\beta2\_\alpha4\_\alpha4$ receptors **(Fig. 5.2; Table 5.3)**, showing that any effects observed in $\beta2\_\alpha4\_\beta2\_\alpha4^{T152C}\_\alpha4$ receptors were caused by MTSET reactions. MTSET modification of $\beta2\_\alpha4\_\beta2\_\alpha4^{T152C}\_\alpha4$ receptors decreased the maximal responses of ACh by 43% **(Fig. 5.2; Table 5.3)**. MTSET also reduced the maximal ACh responses of $\beta2^{L146C}\_\alpha4\_\beta2\_\alpha4\_\alpha4$ receptors, although its effects on this mutant receptor were more pronounced (71%) (*p* < 0.03; n =6) **(Fig. 5.2; Table 5.3)**, further indicating functional differences between the agonist sites at α4(+)/α4(-) and α4(+)/β2(-) interfaces. Application of MTSET also significantly decreased the maximal responses of $\beta2\_\alpha4\_\beta2\_\alpha4^{T152C}\_\alpha4$ receptors to Cyt and Var; the effects were similar for these agonists (~50% reduction), whereas the maximal current responses of TC-2559 were increased by 58% (p < 0.0001; n = 5) **(Table 5.4)**. No further changes in agonist responses were observed with longer periods of MTSET exposure. Exposure to the reducing agent DTT (1 mM) for 2 min reversed the effects of MTSET for all agonist tested **(Fig. 5.3B)**, demonstrating that the changes in the amplitude of the responses to agonists were due to MTSET reaction with α4T152C.
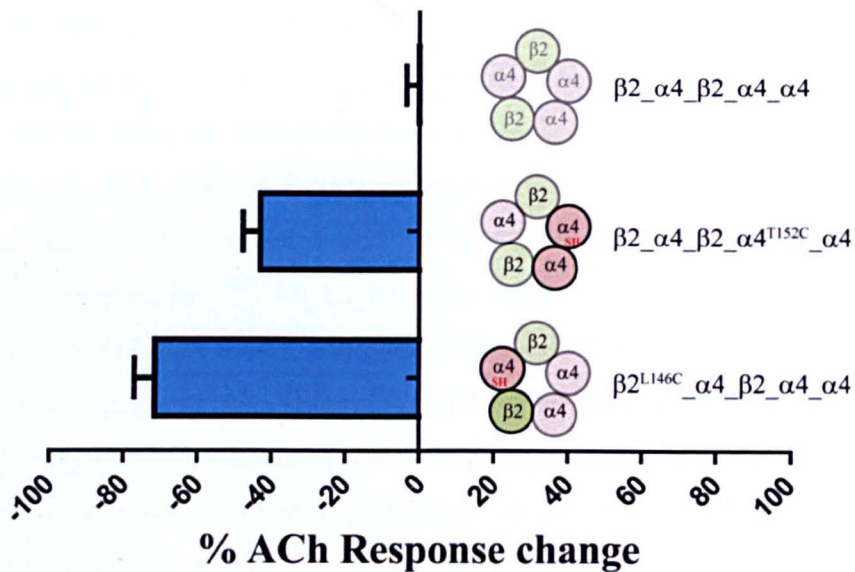
Figure 5.2.   Effect of MTSET on the ACh responses of wild type and mutant β2_α4_β2_α4_α4 receptors. The percentage change in the responses elicited by ACh EC_{50} concentrations on wild type and 5 x EC50 on the mutant β2_α4_β2_α4^{T152C}_α4 and β2^{L146C}_α4_β2_α4_α4 receptors after 2 min applications of 1 mM MTSET is defined as [(Iafter MTS/ Iinitial)-1) x 100], where I indicates the current responses to agonists. The negative values represent an inhibition of the ACh responses after MTSET application. Data represent the mean from at least four independent experiments.

Table 5.3.   Effects of MTSET on ACh responses of wild type and mutant β2_α4_β2_α4_α4 receptors. The percentage change in the responses elicited by 5 x EC_{50} agonist concentrations on wild type and mutant β2_α4_β2_α4_α4 receptors after a 2 min applications of 1 mM MTSET is defined as [(I_{after} MTS/ $I_{initial}$)-1) x 100], where I are the current responses to agonist. Negative values represent an inhibition of agonist responses after MTSET reaction. Data are the mean (95% CI) for 4 -10 experiments. Significant differences were determined using one way ANOVA tests (**$p < 0.01$, ***, $p < 0.001$).

% Change of ACh responses MTSET reaction		
β2_α4_β2_α4_α4	β2_α4_β2_α4^{T152C}_α4	β2^{L146C}_α4_β2_α4_α4
-0.13 (-8, +8)	-43 (-56, -30)**	-71(-87, -56)***

Figure 5.3. **Effects of MTSET on maximal nicotinic agonist currents. (A)**
Representative traces of the maximal responses elicited by ACh, Cyt, Var and
TC-2559 at $\beta2\_\alpha4\_\beta2\_\alpha4^{T152C}\_\alpha4$ before and after MTSET reaction. MTSET
reduce the maximal response of all agonist tested except that of TC-2559, which
was increased. The effects of MTSET on the responses of all agonists were
reversed after 2 min exposure to 1 mM DTT. The diagram immediately above
the traces shows the steps of the MTSET application protocol used. **(B)**
Histogram showing the percentage change in the amplitude of the agonist
responses after MTSET application. The percentage change in the responses to
agonists is defined as $[(I_{after\ MTS}/ I_{initial})-1) \times 100]$. Negative values represent
an inhibition of the responses to agonists after MTSET reaction, whereas positive
values represent an increase in the agonist responses after MTSET reaction. Data
represent the mean of at least four independent experiments.

Table 5.4.   Effects of MTSET on agonist responses of wild type and mutant β2_α4_β2_α4_α4 receptors. The percentage change in the responses elicited by 5 X EC_{50} agonist concentrations on wild type and mutant β2_α4_β2_α4^{T152C}_α4 receptors after a 2 min applications of 1 mM MTSET is defined as [(Iafter MTS/ Iinitial)-1) x 100]. Negative values represent an inhibition of agonist responses after MTSET reaction, whereas positive values represent an increase of the agonist responses after MTSET reaction. Data are the mean (95% CI) for 4 -10 experiments. Significant differences were determined using one way ANOVA tests (* < 0.05, **p < 0.01, ***, p < 0.001).

	% Change of $I_{Agonist}$ after application of 1 mM MTSET for 120s
β2_α4_β2_α4_α4	
ACh	-0.13 (-8, +8)
β2_α4_β2_α4^{T152C}_α4	
ACh	-43.00 (-56, -30)**
Cyt	-51 (-69, -32)***
Var	-43 (-64, -22)***
TC-2559	+58 (+29, +87)***
Saz A	ND.

5.2.3 MTSET reaction rates

The rates at which MTSET modified the engineered $\alpha 4T152C$ were determined by measuring the effect of sequential applications of 1 μM MTSET on the responses elicited by the application of 5 s pulses of 5 x EC_{50} ACh. As these reactions were used as controls to assess the effects of $\alpha 4\beta 2$ receptor agonists or the competitive antagonist $Dh\beta H$ on rates of MTSET reaction, the responses of ACh used to measure the rates of MTSET reaction were stabilised in the presence of nicotinic ligand to ensure that any changes in the responses to ACh pulses observed during the protection assays were attributed to MTSET reaction rather than to processes such as agonist-induced desensitisation or open channel block. Under these conditions, the estimated control rates of MTSET reactions were not significantly different from each other **(Table 5.5)**, indicating that the effects of MTSET were due to its reaction with $\alpha 4T152C$. The maximum effect of 1 μM MTSET (the plateau of the decay curves) for each of the control curves shown in **Fig. 5.4** was comparable to that obtained following application of 1 mM MTSET **(Fig. 5.4, Table 5.4)**. Evidence for MTSET modification of $\beta 2^{L146C}\_\alpha 4\_\beta 2\_\alpha 4\_\alpha 4$ receptors was observed by using a 10-fold higher concentration of MTSET and the EC_{50_2} ACh for the low sensitivity component of the ACh concentration response curve. Under these conditions, the control rate of MTSET reaction estimated for $\beta 2^{L146C}\_\alpha 4\_\beta 2\_\alpha 4\_\alpha 4$ receptors was 3-fold slower than the corresponding rate estimated for $\beta 2\_\alpha 4\_\beta 2\_\alpha 4^{T152C}\_\alpha 4$ receptors **(Fig. 5.4G; Table 5.4)**.

5.2.4 Effect of nicotinic ligands on MTSET reaction rates

To determine the nicotinic ligand selectivity of the agonist site at the $\alpha 4(+)/\alpha 4(-)$ interface, the rate of modification of $\alpha 4T152C$ by low concentrations of MTSET (1 μM) was measured in the absence and presence of 5 X EC_{50} concentrations of either ACh, Cyt, Var, TC-2559, Saz-A or $Dh\beta E$. The MTSET reaction rates were markedly slower in the presence of ACh, Cyt or Var such that not even after 90 s of co-application the MTSET reaction reached completion **(Fig. 5.4; Table 5.5)**. The rate of MTSET modification was also markedly slower in the presence of the antagonist $Dh\beta E$, indicating that the effects of the agonist used in the protection assay slowed down MTSET reactions by impeding MTSET

modification of α4T152C rather than by indirect effects through agonist-induced conformational changes in the agonist binding site. In contrast, co-application of TC-2559 or Saz-A had no effects on the rate of MTSET modification **(Fig. 5.4; Table 5.5)**, indicating that neither of these agonists can impede MTSET modifying α4T152C.
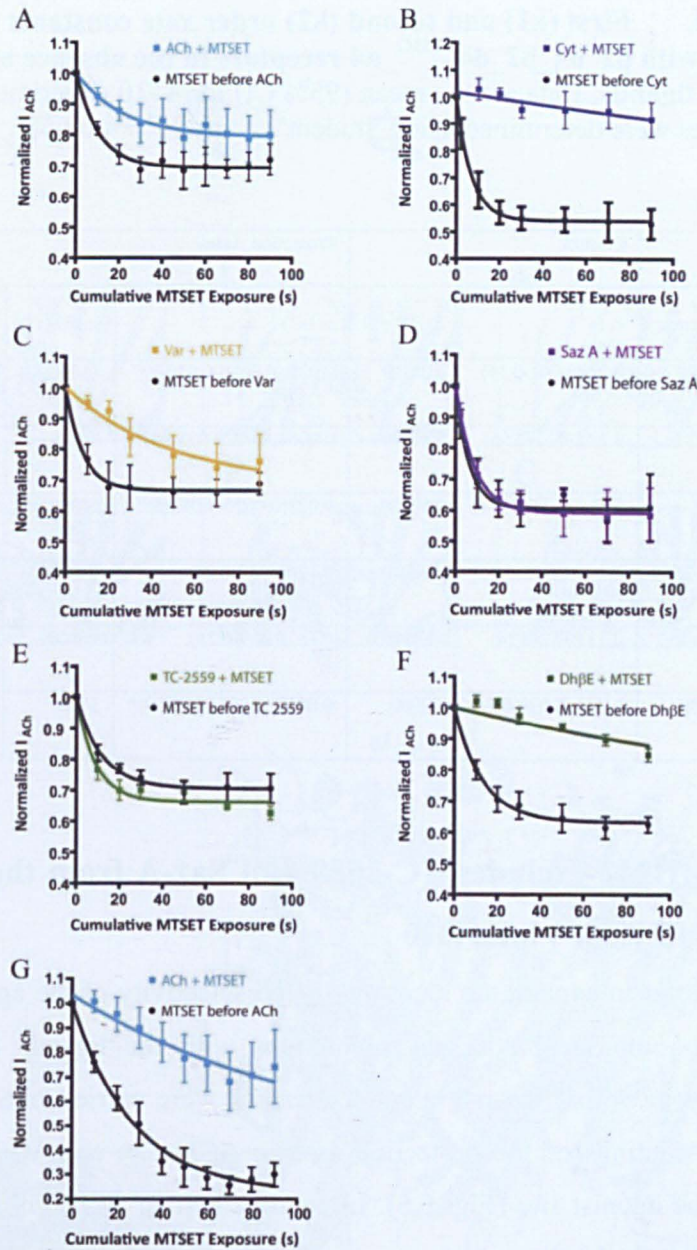
Figure 5.4. **Rates of MTSET modification of β2_α4_β2_α4T152C_α4 receptors in the presence and absence of nicotinic ligands.** Normalised ACh currents in the absence and presence of ACh **(A)**, Cyt **(B)**, Var **(C)**, Saz-A **(D)**, TC-2559 **(E)**, DhβE **(F)** were plotted versus cumulative time of MTSET (1 μM each 10 s) and fit with single exponential functions. Data were normalised to ACh current measured at time 0 and are the mean ± SEM of at least 4 independent experiments. For comparison the rate of MTSET modification of β2^{L146C}_α4_β2_α4_α4 receptors in the presence and absence of ACh is shown in **(G)**. Note the difference in the decay of β2^{L146C}_α4_β2_α4_α4 (k_1 0.032 s^{-1}) and β2_α4_β2_α4^{T152C}_α4 receptors ($k1$ 0.10 (0.061-0.14) s^{-1}). The exponential decay due to MTSET treatment was slower in the β2^{L146C}_α4_β2_α4_α4 than the β2_α4_β2_α4^{T152C}_α4 receptor, even using a concentration of MTSET 10 times higher in the β2^{L146C}_α4_β2_α4_α4 receptor (cumulative time of MTSET (10 μM each 10 s,)).

Table 5.5. **First (k1) and second (k2) order rate constants for reaction of MTSET with β2_α4_β2_α4^{T152C}_α4 receptors in the absence and presence of nicotinic ligands.** Data are the mean (95% CI) for 4 -10 experiments. Significant differences were determined using Student's t-tests. (*$p < 0.05$).

	Control		Protection Assay		
Ligands	k_1 (s^{-1})	k_2 (M^{-1}s^{-1})	k_1 (s^{-1})	k_2 (M^{-1}s^{-1})	$k_{2\text{-control}}/k_{2\text{-test}}$
ACh	0.10 (0.061-0.14)	100000	0.021 (0.0016-0.040)*	21000	4.8
Cyt	0.22 (-0.11-0.56)	220000	0.0064(0.0029-0.0099)*	6400	34.4
Var	0.16 (-0.027-0.34)	160000	0.027(0.0026-0.052)*	27000	5.9
TC-2559	0.10 (-0.052-0.26)	100000	0.12(-0.037-0.28)	120000	0.83
Saz-A	0.13 (0.12-0.14)	130000	0.15 (0.039-0.25)	150000	0.87
DhβE	0.087 (0.039-0.14)	87000	0.0037 (0.0015-0.0059)*	3700	23.5

5.2.5 α4H142 excludes TC-2559 and Saz-A from the agonist site at the α4(+)/α4(-) interface

In an attempt to explain the nicotinic ligand selectivity of the agonist site at the α4(+)/α4(-) interface, docking calculations with the ligands on a structural homology model of the α4(+)/α4(-) interface were carried out. As anticipated from the findings of the protection assays, ACh, Cyt and Var were found to occupy the agonist site **(Fig. 5.5)**. In contrast neither TC-2559 nor Saz-A were able to enter the binding site.
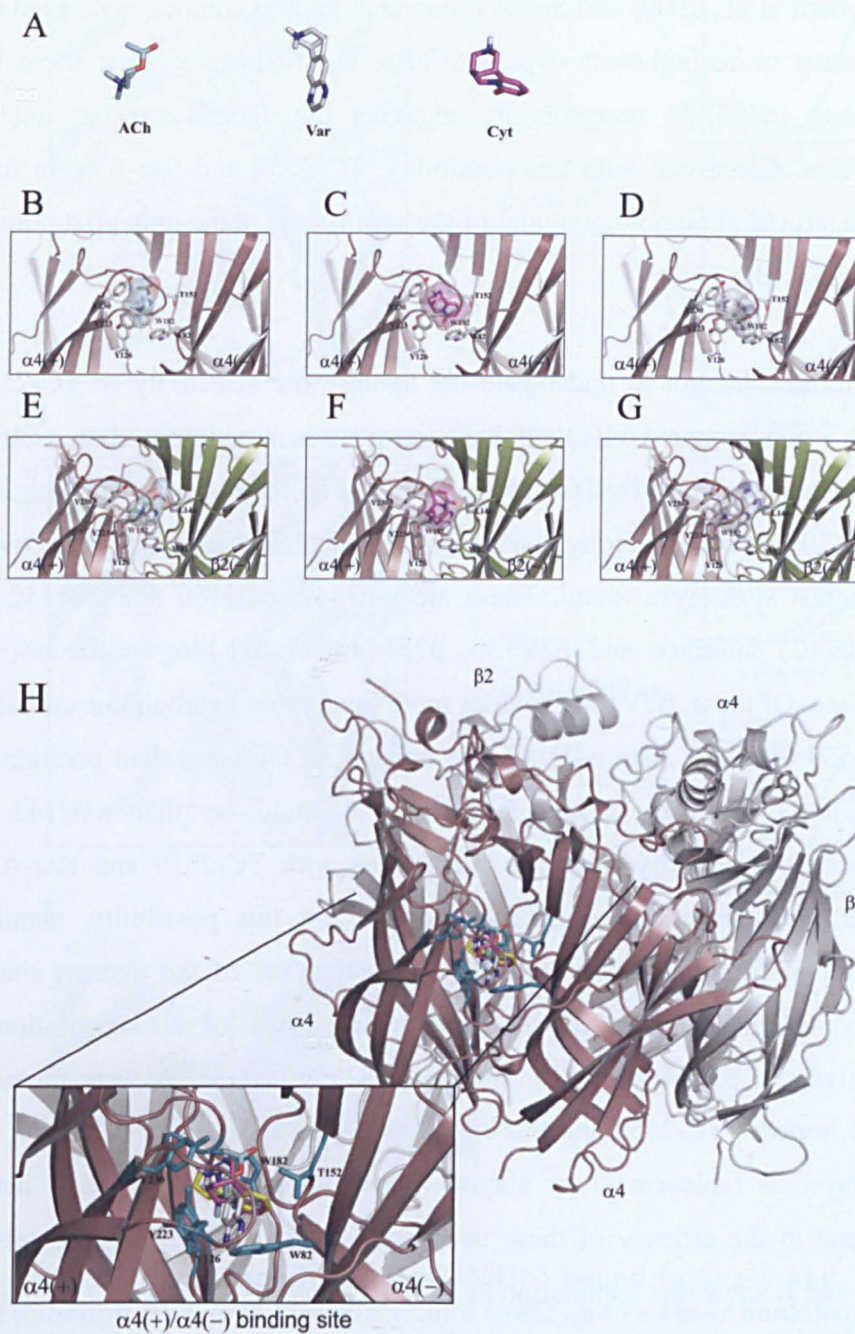
Figure 5.5. **Docking of nicotinic ligands to α4(+)/α4(-) and α4(+)/β2(-) interfaces in a (α4β2)2α4 receptor homology model.** (A) Stick representations of the ACh, Var and Cyt. Single docking of ACh, Cyt and Var, at the α4(+)/α4(-) (**B, C, D,** respectively) and α4(+)/β2(-) (**E, F, G,** respectively) interfaces. (**H**) Superimposition of ACh, Cyt and Var docking to α4(+)/α4(-) interface of the (α4β2)2α4 receptor homology model.

As previous radioligand binding studies have shown that both TC-2559 (Bencherif et al., 2000) and Saz-A (Xiao et al., 2006) compete with high affinity for native or recombinant α4β2 nAChRs, the findings suggest these ligands stimulate (α4β2)₂α4 receptors by engaging the agonist sites at α4(+)/β2(-) interfaces. Consistent with this possibility, TC-2559 and Saz-A were found to bind a structural homology model of the agonist site at the α4(+)/β2(-) interfaces **(Fig. 5.6A, B).**

In a further attempt to understand the agonist site selectivity of TC-2559 and Saz-A a non-occupied α4(+)/α4(-) agonist site was superimposed on a α4(+)/β2(-) agonist site engaged by TC-2559 or Saz-A **(Fig. 5.6A)**. In accord with Harpsøe et al., (2011), three differing residues in the complementary face of the two types of agonist sites were found. These are α4H142, α4Q150 and α4T152 on the α4(+)/α4(-) interface and β2V136, β2F144 and β2L146 on the α4(+)/β2(-) interface. Of these, β2V136 provides more favourable hydrophobic contacts with TC-2559 or Saz-A than α4H142, the residue on the equivalent position on the α4(+)/α4(-) interface, **(Figs. 5.6A, B)**. It could be that α4H142 causes unfavourable polar/hydrophobic interactions with TC-2559 and Saz-A which hinder them from occupying the site. To test this possibility, alanine was substituted for α4H142 in the complementary face of the agonist site at the α4(+)/α4(-) interface, and the functional consequences of this substitution on the sensitivity of $\beta2\_\beta4\_\beta2\_\alpha4^{H142A}\_\alpha4$ to TC-2559 and Saz-A were measured. If H142 impedes TC-2559 and Saz-A accessing the agonist site in the α4(+)/α4(-) interface, its replacement by alanine should allow occupancy, and hence, an increase in the efficacy of these two compounds at (α4β2)₂α4 receptors. **Figs. 5.6D** and **E** show that stimulation of $\beta2\_\beta4\_\beta2\_\alpha4^{H142A}\_\alpha4$ by TC-2559 and Saz-A produced maximal currents that were 6- and 12-fold greater than wild type, respectively **(Fig. 5.6D, E)**. Additionally, the activation effects of these compounds were monophasic and more potent than wild type.
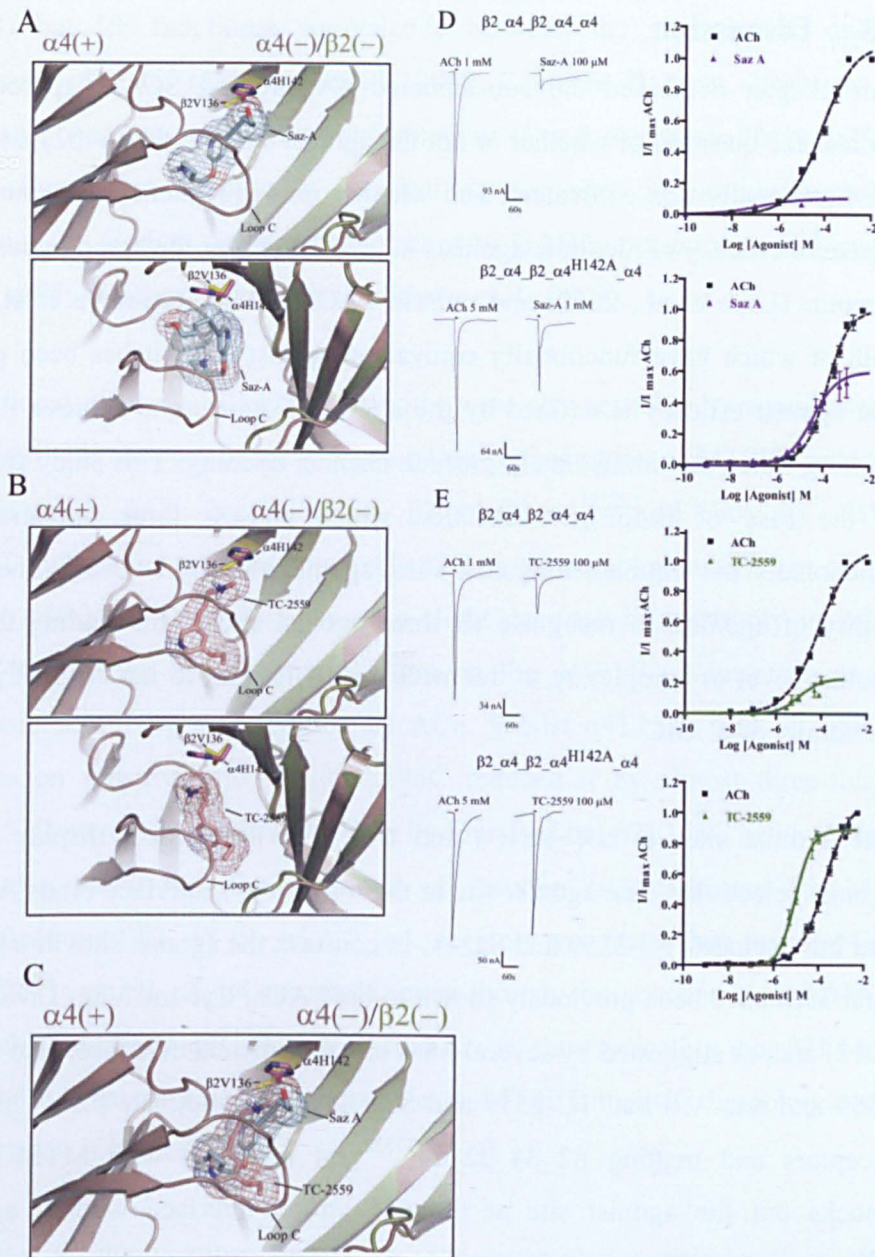
Figure 5.6. **Superimposition of α4(+)/β2(-) bound to Saz-A and TC-2559 and unbound α4(+)/α4(-) interfaces of a (α4β2)₂α4 receptor homology model.** Superimposition of structural homology models of non-occupied α4(+)/α4(-) interface with α4(+)/β2(-) interface engaged by Saz-A **(A)** or TC-2559 **(B)** shows that α4H142 is in lieu of β2V136 in the complementary face of the α4(+)/α4(-) interface. (In each view β2V136 and α4H142 are shown as sticks. **(C)** Simultaneous superimposition of the dockings of TC-2559 and Saz-A shows that both agonists occupy the same region of the α4(+)/β2(-) binding site. Functional effects of Saz-A **(D)** and TC-2559 **(E)** on wild type and β2_α4_β2_α4^H142A_α4 receptors. Representative traces are shown next to CRC. Alanine substitution of H142 in the complementary face of the agonist site at the α4(+)/α4(-) interface increases markedly the efficacy and potency of TC-2559 and Saz-A, compared to wild-type.

123

5.3 Discussion

This chapter combined the concatenated nAChR and SCAM approaches to address the question of whether or not the agonist sites on the $(\alpha4\beta2)_2\alpha4$ nAChR are functionally non-equivalent, and whether non-equivalency accounts for the signature efficacy of nicotinic agonists at $(\alpha4\beta2)_2\alpha4$. For the homologous glycine receptor (Lape et al., 2009) and muscle nAChR (Mukhtasimova et al., 2009), both of which have functionally equivalent agonist sites, it has been proposed that agonist efficacy is defined by the ability of agonists to achieve flipped or priming states that immediately precede channel opening. This study shows that in the case of $(\alpha4\beta2)_2\alpha4$ nAChRs, which possess three operational and functionally non-equivalent agonist sites, agonist efficacy is also defined by the ability of agonists to recognise all three agonist sites. This finding thus adds another level of complexity to the mechanisms leading to ion channel gating in the family of pLGIC

The agonist sites at $\alpha4(+)/\alpha4(-)$ and $\alpha4(+)/\beta2(-)$ interfaces display differing agonist selectivity. The agonist site at the $\alpha4(+)/\alpha4(-)$ interface binds ACh, Cyt, Var but excludes TC-2559 and Saz-A. In contrast, the agonist sites at $\alpha4(+)/\beta2(-)$ interfaces have been previously shown to bind ACh, Cyt and Var (Tavares et al., 2012) and, as suggested by several lines of experimental evidence, also bind TC-2559 and Saz-A. First, TC-2559 and Saz-A partially activate $\beta2\_\alpha4\_\beta2\_\alpha4\_\alpha4$ receptors and treating $\beta2\_\beta4\_\beta2\_\alpha4^{T152C}\_\alpha4$ receptors with MTSET, which knocks out the agonist site at the $\alpha4(+)/\alpha4(-)$ interface without apparently affecting $\alpha4(+)/\beta2(-)$ interfaces, did not abolish the agonist effects of these compounds. This is in accord with previous findings that have shown that the ion channel in $(\alpha4\beta2)_2\alpha4$ receptors can open efficiently when only the sites at $\alpha4(+)/\beta2(-)$ interfaces are occupied (Mazzaferro et al., 2011). Second, radioligand binding studies have shown that both TC-2559 (M Bencherif et al., 2000) and Saz-A (Xiao et al., 2006) compete with high affinity for native or recombinant $\alpha4\beta2$ nAChRs, indicating that these agonists recognise the agonist sites at $\alpha4(+)/\beta2(-)$ interfaces. In the homologous muscle nAChR, there is evidence for differences between the two agonist sites in the resting closed state (Blount & Merlie, 1989; Sine et al., 1990; Edelstein et al., 1997; Prince & Sine,

1998) but for functional equivalency between the sites in the open and desensitised states (Martinez et al., 2000; Tantama & Licht, 2009) or in the resting closed and open active conformations (Jha & Auerbach, 2010). It has also been found that structurally identical agonist sites in another homologous protein, the $GABA_A$ receptor, interact with GABA, muscimol and bicuculline with subtly different selectivity (Baumann et al., 2003).

Functional differences between the sites were also revealed by agonists capable of entering both types of sites. A saturating concentration of MTSET reduced the efficacy of ACh by 43% in $\beta2\_\alpha4\_\beta2\_\alpha4^{T152C}\_\alpha4$ but by 71% in $\beta2^{L146C}\_\alpha4\_\beta2\_\alpha4\_\alpha4$ receptors. $\alpha4T152C$ on the complementary face of the site at the $\alpha4(+)/\alpha4(-)$ interface caused a slight decrease in sensitivity to ACh but $\beta2L146C$ on the homologous position on the $\alpha4(+)/\beta2(-)$ interface produced biphasic sensitivity to activation by ACh. Whilst $\alpha4T152C$ had no significant effects on sensitivity to Cyt, $\beta2L146C$ reduced it by almost three-fold, and $\alpha4T152C$ increased sensitivity to Var by four-fold but $\beta2L146C$ had no effects. It was also found that the first rate of reaction (k_1) estimated for MTSET modification of $\beta2\_\alpha4\_\beta2\_\alpha4^{T152C}\_\alpha4$ receptors was faster than for modification of $\beta2^{L146C}\_\alpha4\_\beta2\_\alpha4\_\alpha4$ receptors, even though the concentration of MTSET used for modifying $\alpha4^{T152C}$ was 10-fold lower, thus indicating that $\beta2L146C$ on $\alpha4(+)/\beta2(-)$ interface is less accessible to MTSET than its homologue on the $\alpha4(+)/\alpha4(-)$ interface.

Residues on the complementary face of the sites play a critical role in defining the ligand selectivity of the agonist sites in $\beta2\_\alpha4\_\beta2\_\alpha4\_\alpha4$ receptors. Because the principal face is formed by $\alpha4$ subunits at both types of agonist sites, binding interactions between agonist-binding residues and the agonists are expected to be similar for both types of agonist sites. In contrast, the complementary site is formed by an $\alpha4$ subunit at the site on the $\alpha4(+)/\alpha4(-)$ interface and a $\beta2$ subunit at the site on $\alpha4(+)/\beta2(-)$ interfaces. Accordingly, the complementary face contributes to define agonist efficacy by selecting the type of $(\alpha4\beta2)_2\alpha4$ agonists that can enter the site. Comparison of the maximum compounds length (MCL) and accessible surface area (ASA) of the nicotinic agonists studied suggests that the site at the $\alpha4(+)/\alpha4(-)$ interface is readily occupied by small ligands such as

Cyt (MCL 5.6 Å; - ASA 262.39) and Var (MCL 7.5 Å; ASA 298.87). Larger compounds such as TC-2559 (MCL 10.4 Å; ASA 353.9) and Saz-A (MCL 14 Å; 413.6) cannot enter the site, thus reducing agonists efficacy **(Fig 5.7)**. Taken together the findings suggest that α4H142 on the complementary face at the α4(+)/α4(-) interface acts as a gate-keeper occluding entry to agonists with a critical large/long size and that this is most likely due to steric rather than electrostatic effects.
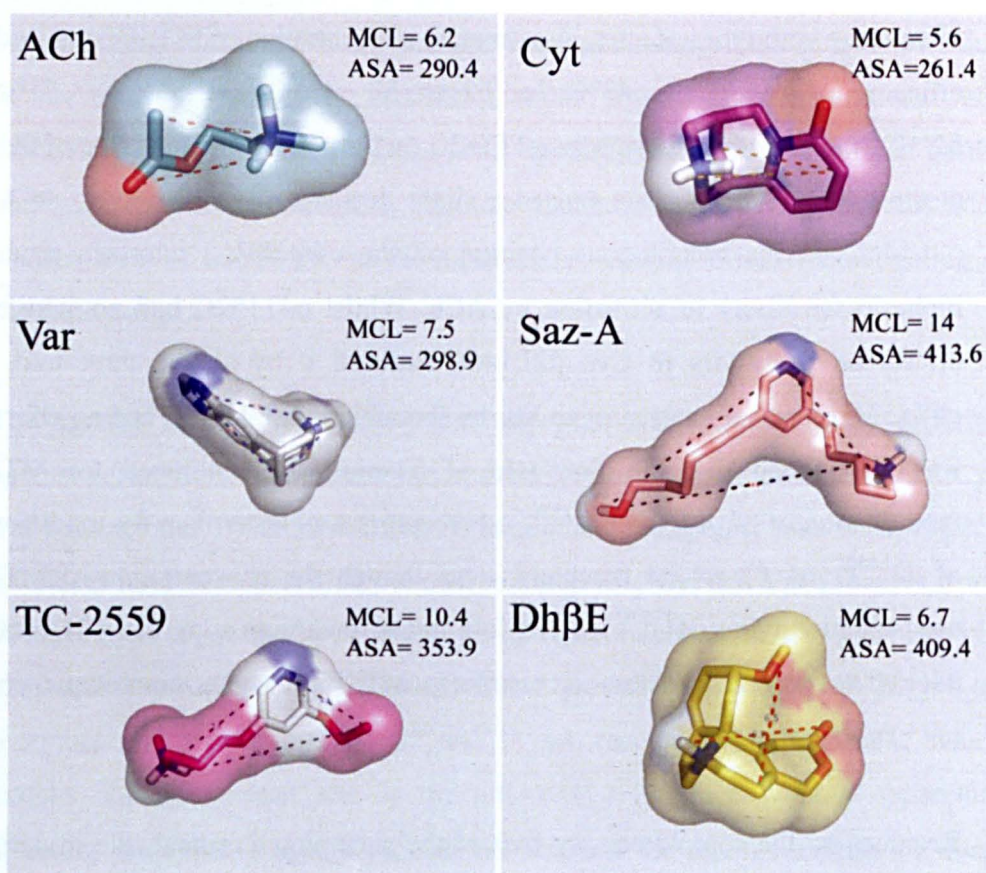
Figure, 5.7. Maximum compound length (MCL) and accessible surface area (ASA) for ACh, Cyt, Var, TC-2559, Saz-A and DhβE. ASA values were calculated using the server at http://www.chemicalize.org/, whereas MCL (Å) for each compound was measured in ligands after energy minimization using spartan'08 software.

The complementary face also contributes to defining the sensitivity of the agonists sites for ligands able to bind sites at the α4(+)/α4(-) and α4(+)/β2(-) interfaces, which intuitively indicates that agonist-specific interactions with residues on the complementary site are important for ligand efficacy. In accord with this possibility, it was observed that the extent agonists shielded the agonist site at the α4(+)/α4(-) interface from MTSET reactions depended on the nature of the protectant agonists. For example, Cyt protected more efficiently than ACh or Var. Furthermore, as noted above, cysteine substitutions on the complementary face of the two types of agonist sites, led to markedly different effects on the functional properties of ACh, depending on the subunit interface location of the agonist site. These findings are consistent with previous studies of α4β2 nAChRs that have shown that structurally diverse agonists activate nAChRs with agonist-specific efficacy by engaging into intermolecular interactions with residues on the complementary face (Rohde et al., 2012; Blum et al., 2013). Also, in the muscle nAChR several residues on the complementary face have been suggested as critical determinants of differential competitive ligand selectivity between the two agonist sites of muscle nAChRs (Akk & Auerbach, 1999; Martinez et al., 2000; Karlin, 2002). Early studies have shown that both α and β subunits define sensitivity to activation by agonists in neuronal nAChRs (Luetje & Patrick, 1991; Chavez-Noriega et al., 1997). It has also been shown that alanine or cysteine substitution of agonist binding aromatic residues on the principal face decreases ACh sensitivity regardless of the subunit interface location (Mazzaferro et al., 2011). These findings are consistent with the view that interactions with aromatic residues on the principal face are a pre-requisite for binding and define ligand affinity, whilst interactions with residues on the complementary face play a central role in defining ligand selectivity and efficacy (Rohde et al., 2012).

Regardless of the subunit interface location, obliteration of one agonist site by MTSET reactions produces receptors with two intact agonist sites that when occupied by ACh efficiently gate the intrinsic ion channel. Indeed, even agonists such as TC-2559 can gate the ion channel to produce measurable currents. If, as proposed by Mukhtasimova et al., (2009), each binding site communicates with the ion channel gate independently of the other binding sites, ligand efficacy would then represent the summation of the signals arriving to the gate, which

could explain why engagement of three sites increases agonist efficacy. Studies of the AChBP bound with agonists or antagonists have suggested that channel opening and, possibly, ligand selectivity may occur through a conformation induced by the ligand. The agonist site is inherently flexible, allowing it to conform to the structural characteristics of the ligand (Hansen et al., 2005). One important conformational change upon agonist binding is a capping motion of loop C, which has been proposed to initiate a clockwork sequence of domain motions leading to gating (Mukhtasimova et al., 2005; Mukhtasimova et al., 2009). This possibility is however not consistent with the observation that residues on the complementary face play an important role in defining agonist efficacy and with recent observations that structures of AChBP with partial agonist lobeline (Billen et al., 2012) and Var (Rucktooa et al., 2012) display full loop C closure. Indeed, the molecular pathway by which energy is transfer from the binding site to the ion pore is still an open question (Purohit & Auerbach, 2013).

Removal of the agonist site at the $\alpha4(+)/\alpha4(-)$ interface by exchange of the N-terminal domain of the auxiliary subunit $\alpha4$ with a $\beta2$ subunit produces receptors that display $(\alpha4\beta2)_2\beta2$-like sensitivity to activation by ACh, Cyt or Saz-A (Mazzaferro et al., 2011). However, occupancy of three intact agonist sites produces more efficacious ion channel gating, as indicated by a significant increase in the amplitude of maximal ACh responses (Harpsøe et al., 2011; Mazzaferro et al., 2011) and the maximal responses to Cyt and Var, compared to TC-2559 and Saz-A. In heteromeric receptors with only two agonist sites, single occupancy inefficiently opens the receptors (Auerbach, 2010). However, homomeric Cys-loop ion channels, which are endowed with five structurally identical agonist sites, are activated efficiently by double occupancy, although triple occupancy is required for maximal gating (Beato et al., 2004; Solt et al., 2007; Lape et al., 2008; Rayes et al., 2009). Thus, depending on agonist site selectivity $(\alpha4\beta2)_2\alpha4$ receptors can activate efficiently through occupation of either two or three sites. Furthermore, although the affinity of each agonist site for ACh has not been determined, the differing effects of alanine substitution of $\alpha4W182$ on ACh sensitivity on the two types of agonist sites, suggest that full agonists may activate the receptors through occupying just two agonist sites

producing functional effects more typical of $(\alpha4\beta2)_2\beta2$ nAChRs. Hence, $(\alpha4\beta2)_2\alpha4$ nAChRs represents two receptors in one.

An unexpected observation was that the efficacy of TC2559 and Saz-A at $(\alpha4\beta2)_2\alpha4$ receptors is not $(\alpha4\beta2)_2\beta2$–like, even though these agonist bind the agonist sites at $\alpha4(+)/\beta2(-)$ interfaces. At $(\alpha4\beta2)_2\beta2$ receptors, which have two operational agonist sites, one at each of the $\alpha4(+)/\beta2(-)$ interfaces, Saz-A behaves as a full agonist and TC-2559 as a super agonist (Moroni et al., 2006; Zwart et al., 2006; Carbone et al., 2009). A possible explanation is that the $\alpha4(+)/\alpha4(-)$ interface or the fifth subunit may allosterically influence the function of the agonist site at the adjacent $\alpha4(+)/\beta2(-)$ interface such that binding of agonist to $\alpha4(+)\beta2(-)$ interfaces differs from binding to $\alpha4(+)/\beta2(-)$ sites on $(\alpha4\beta2)_2\beta2$ receptors. In support of this possibility, a recent study that has compared the binding of agonist to the agonist sites on $\alpha4(+)/\beta2(-)$ interfaces in both $(\alpha4\beta2)_2\alpha4$ and $(\alpha4\beta2)_2\beta2$ receptors has suggested that ligands such as Cyt bind the agonist sites with different poses, depending on the receptor isoform (Tavares et al., 2009).

CHAPTER 6

Final discussion and future work

The aim of this study was to define the role of the $\alpha4(+)/\alpha4(-)$ interface on the shaping of the stoichiometry-specific functional properties of the $(\alpha4\beta2)_2\alpha4$ nAChR. $\alpha4\beta2$ nAChRs are the most abundant nAChR in the mammalian brain, and their role in brain behaviours and diseases is well documented (Cassels et al., 2005; Mantione et al., 2012; Gotti et al., 2009). It is well established that $\alpha4$ and $\beta2$ subunits assemble into alternate receptors $(\alpha4\beta2)_2\alpha4$ and $(\alpha4\beta2)_2\beta2$ that display 100-fold difference in sensitivity to activation by ACh (Nelson et al., 2003; Moroni et al., 2006; Carbone et al., 2009). The alternate receptors also differ in sensitivity to $\alpha4\beta2$-preferring ligands (Moroni et al., 2006; Carbone et al., 2009), unitary conductance (Nelson et al., 2003), calcium permeability (Tapia et al., 2007), sensitivity to modulation by Zn^{2+} (Moroni et al., 2008) and the allosteric compound NS9283 (Timmermann et al., 2012). Both receptor forms consist of two identical $\alpha4\beta2$ subunit pairs and a fifth auxiliary $\alpha4$ or $\beta2$ subunit, all arranged around a central cation pore (Moroni et al., 2006; Carbone et al., Mazzaferro et al., 2011). As mentioned elsewhere in this thesis, each $\alpha4\beta2$ subunit pair harbours a structural identical ACh binding site formed at the interface between the two adjacent subunits. The principal or (+) face of the binding site at $\alpha4(+)/\beta2(-)$ interfaces is contributed by the $\alpha4$ subunit, whilst the $\beta2$ subunit contributes the complementary or (-) face (Mazzaferro et al., 2011). Hence, structurally, the alternate $\alpha4\beta2$ receptors are identical except for the auxiliary subunit, which is $\alpha4$ in $(\alpha4\beta2)_2\alpha4$ nAChRs and $\beta2$ in $(\alpha4\beta2)_2\beta2$ nAChRs. That the auxiliary subunit can be either $\alpha4$ or $\beta2$ leads to stoichiometry-specific interfaces. In the $(\alpha4\beta2)_2\beta2$ receptor there is a $\beta2(+)/\beta2(-)$ interface, whereas in the $(\alpha4\beta2)_2\alpha4$ receptors there is a $\alpha4(+)/\alpha4(-)$ interface (**Fig. 3.1**). At the commencement of this study, the auxiliary $\alpha4$ subunit had been identified as key provider of structural determinants of functional signatures of $(\alpha4\beta2)_2\alpha4$ nAChRs such as sensitivity to potentiation by Zn^{2+} (Moroni et al., 2008) or Ca^{2+} permeability (Tapia et al., 2007). Thus, the view that drove the studies reported in this thesis was that the $\alpha4(+)/\alpha4(-)$ interface most likely additionally defines the response of $(\alpha4\beta2)_2\alpha4$ nAChRs to agonists, and that the elucidation of how this interface influences the function of the $(\alpha4\beta2)_2\alpha4$ nAChR should be prioritised, if we are to understand how, despite having identical agonist sites, the alternate $\alpha4\beta2$ nAChRs display differing sensitivity to agonists.

The study of individual subunit interfaces is challenged by the high conservation of the subunits of the nAChR family, which in heterologous systems typically leads to one subunit substituting for any other leading to the expression of a vast assortment of possible pentameric arrangements. To circumvent this problem, this thesis used fully concatenated $(\alpha4\beta2)_2\alpha4$ nAChRs. Concatenated $(\alpha4\beta2)_2\alpha4$ nAChRs had been previously shown to be stable and reproduce the functional properties of $(\alpha4\beta2)_2\alpha4$ nAChRs assembled from loose $\alpha4$ and $\beta2$ subunits (Carbone et al., 2009). In terms of the development of experimental strategies with which to address the study of specific regions of pLGIC, an important achievement of this thesis has been to successfully combine the concatenated receptor technology with the SCAM method to address the role of the $\alpha4(+)/\alpha4(-)$ interface on the stoichiometry-specific properties of the $(\alpha4\beta2)_2\alpha4$ receptor. By combining these two approaches, this thesis identified a third operational agonist site at the $\alpha4(+)/\alpha4(-)$ interface whose functional properties differ from those of the classical agonist sites found on the $\alpha4(+)/\beta2(-)$ interfaces. To my knowledge, this is the first time that it has been shown that the agonist sites in a heteromeric pLGIC are both structurally and functionally different. Of course, the SCAM approach has been used previoulsy to address fundamental issues on the structure, function and dynamics of LGIC (for a comprehensive review see Baker et al., 2007 pages 439-452), however this is the first time that it has been combined with the concatenated receptor approach to study individual and identified subunits in a pLGIC. The tool, as shown by the achievements of this thesis, is powerful and can potentially illuminate the role of each subunit interface on the function of other concatenated pLGICs. Hopefully, the approach will lead to important insights in other members of the pLGIC family.

Using the approaches discussed above, this study identified a third operational agonist site at the $\alpha4(+)/\alpha4(-)$ interface of $(\alpha4\beta2)_2\alpha4$ nAChRs **(Chapter 3)**; Mazzaferro et al., 2011). The site is fully operational and plays a cardinal role in the shaping of the functional properties of the $(\alpha4\beta2)_2\alpha4$ nAChRs. The findings of **Chapter 3** to **5** provided remarkable new insights into roles of the two types of ACh binding sites in both activation and desensitisation and revealed dominance of the site at the $\alpha4(+)/\alpha4(-)$ interface. Some of the findings are highly surprising. For example, in the context of homomeric $\alpha7$ nAChRs or

chimeric 5HT-3-α7, which have been shown to be maximally activated by occupation of three non-consecutive agonist binding sites (Rayes et al., 2009; Dacosta & Sine, 2013), occupation of the three agonist sites of the $(\alpha4\beta2)_2\alpha4$ nAChR would be expected to increase sensitivity to activation and the desensitisation kinetics of this receptor would be expected to be determined by the fastest desensitising sites at the α4(+)/β2(-) interfaces. One possible explanation for these differences is that the α4(+)/α4(-) interface not only harbours an operational agonist site but also exerts a modulatory influence on the agonist sites at the α4(+)/β2(-) interfaces. Some of the findings of this thesis support this view. For example, the effects of the incorporation of α4W182A into the α4(+)/α4(-) interface on the function of the agonist sites at the α4(+)/β2(-) interfaces were different than the effects of the mutation incorporated into the α4(+)/β2(-) interfaces on the function of agonist site at the α4(+)/α4(-) interface. Moreover, the effects of the agonists Saz-A and TC-2559, compared to their effects on $(\alpha4\beta2)_2\beta2$ nAChRs, could be explained if the α4(+)/α4(-) interface influenced the interaction of these agonists with the binding sites at the α4(+)/β2(-) interfaces or with the gating signals generated by these agonists.

Besides the identification of an additional operational agonist site at the α4(+)/α4(-) interface, a key finding of this thesis is that full receptor occupancy increases maximal agonist responses. Given that occupation of the agonist sites at α4(+)/β2(-) interfaces produces efficacious gating, additional occupation of the site at the α4(+)/α4(-) interface increases the efficacy of the gating even if the agonist is a partial agonist. Another key finding that could have profound implications for drug discovery programs is that the agonist sites at the α4(+)/α4(-) and α4(+)/β2(-) interfaces have different agonist selectivity. It was found that large agonists are excluded from the agonist site at the α4(+)/α4(-) interface, leading to partial agonism, even for agonists that are full or super agonists at the $(\alpha4\beta2)_2\beta2$ receptor, the receptor isoform endowed with only two agonist sites, both located at the α4(+)/β2(-) interfaces. Examples of this type of agonist are TC-2559 and Saz-A. Agonists that bind the three sites display higher efficacy than ligands excluded fom the site at the α4(+)/α4(-) interface, regardless of their efficacy relative to the full agonist ACh. In the case of pLGICs with functionally equivalent agonist sites, agonist efficacy seems to be

determined by the ability of agonists to achieve flipped (Lape et al., 2009) states, which are shut states immediately preceding ion channel gating. In the context of current views on agonist efficacy at pLGIC (Lape et al., 2009), the finding that relative agonist efficacy in $(\alpha4\beta2)_2\alpha4$ is first determined by the ability of agonists to bind all three sites adds another layer of complexity to the mechanisms by which agonists gate pLGIC.

Because of the unavailability of single channel data, it is not possible to propose an adequate kinetic scheme for the activation/desensitisation cycle of the $(\alpha4\beta2)_2\alpha4$ nAChR, and the possible existence of flipped or primed states provides additional difficulties. Although it was found that two agonist binding sites desensitise with higher sensitivity than three, it is not known whether the two desensitised states are connected. Similarly, it is not known whether the activation state achieved by engagement of two $\alpha4(+)/\beta2(-)$ binding sites by agonists not selected by the site at the $\alpha4(+)/\alpha4(-)$ interface is the same as the active state achieved by occupation of two sites by agonists able to bind all three sites. It seems likely, however, that there are two pathways for the activation/desensitisation of the $(\alpha4\beta2)_2\alpha4$ receptor **(Fig. 6.1)**, with each pathway following a cyclic model similar to those proposed for the muscle nAChR by Cachelin & Colquhoun, (1989). The model proposed in **Fig 6.1** shows that activation through pathway 1 (red), which leads to engagement of all three agonist sites by a full agonsit such as ACh, produces maximal activation (A3RO), whilst activation via pathway 2 (green), which involves occupation of the sites at $\alpha4(+)/\beta2(-)$ interfaces by agonist excluded from the $\alpha4(+)/\alpha4(-)$ site also leads to gating, albeit with reduced efficacy. Incorporation of $\alpha4W182A$ into any of the agonist sites produced biphasic concentration response curves showing that binding of two intact agonist sites produced effective receptor activation **(Chapters 3 and 4)**, which, together with the finding that some agonists such as TC-2559 and Saz-A activate the receptor by binding only to the agonist sites at the $\alpha4(+)/\beta2(-)$ interfaces, suggest that state A2R may be common both pathways.

R ⟷ A2R ⟷ A3R ⟷ A3RO ⟷ A3RD

A2RO

A2RD
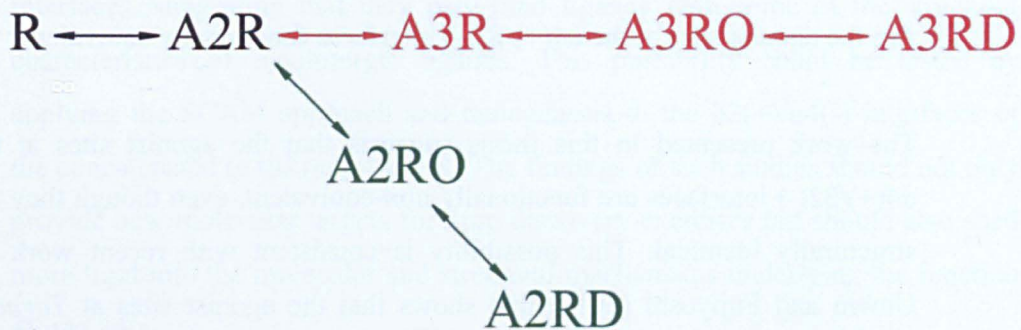
Figure. 6.1.   A scheme for the activation and desensitisation of ($\alpha4\beta2$)2$\alpha4$ nAChRs. The resting receptor is shown by R, a receptor with an open channel by O, an agonist molecule by A, desensitised state of a receptor occupied by two agonist sites by D, and the desensitised state of a receptor occupied by three agonists molecules by D.

In summary, this study has allowed an insight into a complex receptor behaviour that was not anticipated from current views on the function of nAChRs. There is still much to learn about this receptor and most certainly new advances will be made by studying the concatenated receptors at the single channel level. Finally, the finding that ($\alpha4\beta2$)$_2\alpha4$ nAChRs can be effectively activated and desensitised through two pathways depending on the concentration of the agonist or the agonist site selectivity may have important consequences for our understanding and control of $\alpha4\beta2$-signalling in brain pathologies. One of these pathways leads to active and desensitised receptors that resemble those of the isoform ($\alpha4\beta2$)$_2\beta2$ nAChR, suggesting that at low concentrations of agonist, $\alpha4\beta2$ signalling in neurones may be essentially of the high-sensitivity type, whilst ($\alpha4\beta2$)$_2\alpha4$ nAChRs signalling may occur at higher concentrations of agonist and when ($\alpha4\beta2$)$_2\beta2$ nAChRs receptors are desensitised.

Future work

1) Are the agonist sites at the $\alpha4(+)/\beta2(-)$ interfaces functionally equivalent?

The work presented in this thesis suggests that the agonist sites at the $\alpha4(+)/\beta2(-)$ interfaces are functionally non-equivalent, even though they are structurally identical. This possibility is consistent with recent work by Unwin and Fujiyoshi (2012) that shows that the agonist sites at *Torpedo* nAChRs contribute asymmetrically to gating. Asymmetry in gating appears to occur because the auxiliary subunit adjacent to the α/γ, interface is displaced outwardly upon agonist binding, suggesting the pseudosymmetric arrangement of subunits around the ion channel in heteromeric pLGICs as an important structural element of receptor function. Thus, because the position of the fifth subunit in $(\alpha4\beta2)_2\alpha4$ nAChRs is similar to that of the $\beta1$ subunit in the *Torpedo* nAChR, it would be of interest to determine whether the agonist sites at the $\alpha4(+)/\beta2(-)$ interfaces function asymmetrically.

Specifically, the following aspect should be interesting to address:

- Knocking out one $\alpha4(+)/\beta2(-)$ site at time using MTS reagents and mutagenesis in order to unveil if the two sites have the same or different function in the activation of the $(\alpha4\beta2)_2\alpha4$ nAChR.
- To determine whether, and how, the $\alpha4(+)/\alpha4(-)$ site is connected allosterically to the $\alpha4(+)/\beta2(-)$ binding sites.

2) Define the role of the non-binding $\beta2(+)/\alpha4(-)$ interfaces in $(\alpha4\beta2)_2\alpha4$ nAChR activation.

In addition to the subunit interfaces that harbour the agonist sites, the $(\alpha4\beta2)_2\alpha4$ receptor is endowed with two $\beta2(+)/\alpha4(-)$ interface that up to now have been considered as non-binding interfaces. However the $\beta2(+)/\alpha4(-)$ interfaces host the inhibition binding site for Zn^{++} (Moroni et al., 2008) and the homologue interfaces $\beta2(+)/\alpha3(-)$ of the $\alpha3\beta2$ nAChR bind the positive allosteric modulator morantel (Seo et al., 2009).

Interestingly, agonist binding structural elements are conserved in $\beta2(+)/\alpha4(-)$ interfaces, suggesting that they may bind ligands with some of the structural characteristics of nicotinergic ligands. This possibility could be tested by applying the SCAM approach and mutagenesis to the $\beta2(+)/\alpha4(-)$ interfaces of the concatenated $(\alpha4\beta2)_2\alpha4$ nAChR. The findings of such studies should not only provide new molecular targets for drug discovery exercises but should also shed more light into the molecular and structural mechanisms underlying the function of nAChRs.

Acknowledgment

Bibliography

Absalom NL, Lewis TM, Kaplan W, Pierce KD and Schofield PR (2003) Role of charged residues in coupling ligand binding and channel activation in the extracellular domain of the glycine receptor. *The Journal of Biological Chemistry.* 278 (50), 50151–7.

Akk G and Auerbach A (1999) Activation of muscle nicotinic acetylcholine receptor channels by nicotinic and muscarinic agonists. *British Journal of Pharmacology.* 128 (7), 1467–76.

Akk G (2001) Aromatics at the murine nicotinic receptor agonist binding site: mutational analysis of the alphaY93 and alphaW149 residues. *The Journal of Physiology.* 535 (Pt 3), 729–40.

Albuquerque E X, Pereira EFR, Alkondon M and Rogers SW (2009) Mammalian nicotinic acetylcholine receptors: from structure to function. *Physiological reviews.* 89 (1), 73–120.

Alkondon M and Albuquerque E X (1993) Diversity of nicotinic acetylcholine receptors in rat hippocampal neurons. I. Pharmacological and functional evidence for distinct structural subtypes. *The Journal of Pharmacology and Experimental Therapeutics.* 265 (3), 1455–73.

Andreasen J T, Olsen GM, Wiborg O and Redrobe J P (2009) Antidepressant-like effects of nicotinic acetylcholine receptor antagonists, but not agonists, in the mouse forced swim and mouse tail suspension tests. *Journal of psychopharmacology (Oxford, England).* 23 (7), 797–804.

Andreasen J T, Nielsen EO and Redrobe John P (2009) Chronic oral nicotine increases brain [3H]epibatidine binding and responsiveness to antidepressant drugs, but not nicotine, in the mouse forced swim test. *Psychopharmacology.* 205 (3), 517–28.

Arevalo E, Chiara DC, Forman SA, Cohen J B and Miller K W (2005) Gating-enhanced accessibility of hydrophobic sites within the transmembrane region of the nicotinic acetylcholine receptor's {delta}-subunit. A time-resolved photolabeling study. *The Journal of Biological Chemistry.* 280 (14), 13631–40.

Arneric S P, Holladay M and Williams M (2007) Neuronal nicotinic receptors: a perspective on two decades of drug discovery research. *Biochemical Pharmacology.* 74 (8), 1092–101.

Auerbach A (2010) The gating isomerization of neuromuscular acetylcholine receptors. *The Journal of Physiology.* 588 (Pt 4), 573–86.

Azam L, Winzer-Serhan U and Leslie F M (2003) Co-expression of alpha7 and beta2 nicotinic acetylcholine receptor subunit mRNAs within rat brain cholinergic neurons. *Neuroscience.* 119 (4), 965–77.

Badio B and Daly J (1994) Epibatidine, a potent analgetic and nicotinic agonist. *Molecular. Pharmacology.* 45 (4), 563–569.

Baker G, Dunn S and Holt A (2007) *Handbook of Neurochemistry and Molecular Neurobiology Practical Neurochemistry Methods Volume Editors.* G. Baker, S. Dunn, & A. Holt eds. Springer Science + Business Media, LLC., 233 Spring Street, New York, NY 10013, USA)

Baumann SW, Baur R and Sigel E (2003) Individual properties of the two functional agonist sites in GABA(A) receptors. *The Journal of Neuroscience.* 23 (35), 11158–66.

Beato M, Groot-Kormelink PJ, Colquhoun D and Sivilotti LG (2004) The activation mechanism of alpha1 homomeric glycine receptors. *The Journal of Neuroscience.* 24 (4), 895–906.

Bencherif M, Bane AJ, Miller CH, Dull GM and Gatto G J (2000) TC-2559: a novel orally active ligand selective at neuronal acetylcholine receptors. *European journal of Pharmacology.* 409 (1), 45–55.

Berrettini W, Yuan X, Tozzi F, Song K, Francks C, Chilcoat H, Waterworth D, Muglia P and Mooser V (2008) Alpha-5/alpha-3 nicotinic receptor subunit alleles increase risk for heavy smoking. *Molecular Psychiatry.* 13 (4), 368–73.

Berrettini WH and Doyle GA (2012) The CHRNA5-A3-B4 gene cluster in nicotine addiction. *Molecular Psychiatry.* 17 (9), 856–66.

Bertrand D, Devillers-Thiéry A, Revah F, Galzi J, Hussy N, Mulle C, Bertrand S, Ballivet M and Changeux J (1992) Unconventional pharmacology of a neuronal nicotinic receptor mutated in the channel domain. *Proceedings of the National Academy of Sciences of the United States of America.* 89 (February), 1261–1265.

Bertrand D, Picard F, Le Hellard S, Weiland S, Favre I, Phillips H, Bertrand S, Berkovic SF, Malafosse A and Mulley J (2002) How mutations in the nAChRs can cause ADNFLE epilepsy. *Epilepsia.* 43 Suppl 5, 112–22.

Bertrand S, Weiland S, Berkovic S, Steinlein O and Bertrand D (1998) Properties of neuronal nicotinic acetylcholine receptor mutants from humans suffering from autosomal dominant nocturnal frontal lobe epilepsy. *British Journal of Pharmacology.*, 751–760.

De Biasi M and Dani J A (2011) Reward, addiction, withdrawal to nicotine. *Annual Review of Neuroscience.* 34, 105–30.

Billen B, Spurny R, Brams M, Van Elk R, Valera-Kummer S, Yakel JL, Voets T, Bertrand D, Smit August B and Ulens C (2012) Molecular actions of smoking cessation drugs at α4β2 nicotinic receptors defined in crystal structures of a homologous binding protein. *Proceedings of the National Academy of Sciences of the United States of America.* 109 (23), 9173–8.

Bloomenthal AB, Goldwater E, Pritchett DB and Harrison N L (1994) Biphasic modulation of the strychnine-sensitive glycine receptor by Zn2+. *Molecular Pharmacology.* 46 (6), 1156–9.

Blount P and Merlie JP (1989) Molecular basis of the two nonequivalent ligand binding sites of the muscle nicotinic acetylcholine receptor. *Neuron.* 3 (3), 349–57.

Blum AP, Van Arnam EB, German L a, Lester H a and Dougherty D a (2013) Binding interactions to the complementary subunit of nicotinic receptors. *The Journal of Biological Chemistry*, 1–15.

Bocquet N, Nury H, Baaden M, Le Poupon C, Changeux JP, Delarue M and Corringer P-J (2009) X-ray structure of a pentameric ligand-gated ion channel in an apparently open conformation. *Nature.* 457 (7225), 111–4.

Boileau AJ, Evers AR, Davis AF and Czajkowski C (1999) Mapping the Agonist Binding Site of the GABA A Receptor: Evidence for a beta-strand. *The Journal of Neuroscience.* 19 (12), 4847–4854.

Bouzat C, Gumilar F, Spitzmaul G, Wang H-L, Rayes D, Hansen SB, Taylor P and Sine S M (2004) Coupling of agonist binding to channel gating in an ACh-binding protein linked to an ion channel. *Nature.* 430 (7002), 896–900.

Brams M, Gay EA, Sáez JC, Guskov A, Van Elk R, Van der Schors RC, Peigneur S, Tytgat J, Strelkov S V, Smit August B, Yakel JL and Ulens C (2011) Crystal structures of a cysteine-modified mutant in loop D of acetylcholine-binding protein. *The Journal of Biological Chemistry.* 286 (6), 4420–8.

Brejc K, Van Dijk W J, Klaassen R V, Schuurmans M, Van Der Oost J, Smit A B and Sixma T K (2001) Crystal structure of an ACh-binding protein reveals the ligand-binding domain of nicotinic receptors. *Nature.* 411 (6835), 269–76.

Briggs CA and McKenna DG (1996) Effect of MK-801 at the human alpha 7 nicotinic acetylcholine receptor. *Neuropharmacology.* 35 (4), 407–14.

Brown RWB, Collins A C, Lindstrom J M and Whiteaker P (2007) Nicotinic alpha5 subunit deletion locally reduces high-affinity agonist activation without altering nicotinic receptor numbers. *Journal of Neurochemistry.* 103 (1), 204–15.

Buisson B and Bertrand D (1998a) Allosteric modulation of neuronal nicotinic acetylcholine receptors. *Journal of Physiology, Paris*. 92 (2), 89–100.

Buisson B and Bertrand D (1998b) Open-channel blockers at the human alpha4beta2 neuronal nicotinic acetylcholine receptor. *Molecular Pharmacology*. 53 (3), 555–63.

Buisson B and Bertrand D (2001) Chronic exposure to nicotine upregulates the human (alpha)4((beta)2 nicotinic acetylcholine receptor function. *The Journal of Neuroscience*. 21 (6), 1819–29.

Cachelin AB and Colquhoun D (1989) Desensitization of the acetylcholine receptor of frog end-plates measured in a Vaseline-gap voltage clamp. *The Journal of Physiology*. 415, 159–88.

Caggiula AR, Epstein LH, Antelman SM, Saylor SS, Perkins KA, Knopf S and Stiller R (1991) Conditioned tolerance to the anorectic and corticosterone-elevating effects of nicotine. *Pharmacology, Biochemistry, and Behavior*. 40 (1), 53–9.

Carbone AL, Moroni M, Groot-Kormelink P-J and Bermudez I (2009) Pentameric concatenated (alpha4)(2)(beta2)(3) and (alpha4)(3)(beta2)(2) nicotinic acetylcholine receptors: subunit arrangement determines functional expression. *British Journal of Pharmacology*. 156 (6), 970–81.

Cassels Bruce K, Bermúdez I, Dajas F, Abin-Carriquiry JA and Wonnacott S (2005) From ligand design to therapeutic efficacy: the challenge for nicotinic receptor research. *Drug Discovery Today*. 10(23-24):1657-65.

Celie PHN, Van Rossum-Fikkert SE, Van Dijk Willem J, Brejc Katjusa, Smit August B and Sixma Titia K (2004) Nicotine and carbamylcholine binding to nicotinic acetylcholine receptors as studied in AChBP crystal structures. *Neuron*. 41 (6), 907–14.

Cesa LC, Higgins CA, Sando SR, Kuo DW and Levandoski MM (2012) Specificity determinants of allosteric modulation in the neuronal nicotinic acetylcholine receptor: a fine line between inhibition and potentiation. *Molecular Pharmacology*. 81 (2), 239–49.

Chakrapani S, Bailey TD and Auerbach Anthony (2004) Gating dynamics of the acetylcholine receptor extracellular domain. *The Journal of General Physiology*. 123 (4), 341–56.

Chakrapani S and Auerbach A (2005) A speed limit for conformational change of an allosteric membrane protein. *Proceedings of the National Academy of Sciences of the United States of America*. 102 (1), 87–92.

Chavez-Noriega LE, Crona JH, Washburn MS, Urrutia A, Elliott KJ and Johnson EC (1997) Pharmacological characterization of recombinant human neuronal nicotinic acetylcholine receptors h alpha 2 beta 2, h alpha 2 beta 4, h alpha 3 beta 2, h alpha 3 beta 4, h alpha 4 beta 2, h alpha 4 beta 4 and h alpha 7 expressed in Xenopus oocytes. *The Journal of Pharmacology and Experimental Therapeutics*. 280 (1), 346–56.

Chen Y, Sharples TJW, Phillips KG, Benedetti G, Broad LM, Zwart R and Sher E (2003) The nicotinic alpha 4 beta 2 receptor selective agonist, TC-2559, increases dopamine neuronal activity in the ventral tegmental area of rat midbrain slices. *Neuropharmacology*. 45 (3), 334–44.

Coe JW, Brooks PR, Vetelino MG, Wirtz MC, Arnold EP, Huang J, Sands SB, Davis TI, Lebel LA, Fox CB, Shrikhande A, Heym JH, Schaeffer E, Rollema H, Lu Y, Mansbach RS, Chambers LK, Rovetti CC, Schulz DW, Tingley FD and O'Neill BT (2005) Varenicline: an alpha4beta2 nicotinic receptor partial agonist for smoking cessation. *Journal of Medicinal Chemistry*. 48 (10), 3474–7.

Corringer PJ, Bertrand S, Bohler S, Edelstein SJ, Changeux JP and Bertrand D (1998) Critical elements determining diversity in agonist binding and desensitization of neuronal nicotinic acetylcholine receptors. *The Journal of Neuroscience*. 18 (2), 648–57.

Corringer PJ, Nove N Le and Changeux JP (2000) Nicotinic receptors at the amino acid level. *Annual Review of Pharmacology and Toxicology*. 40:431-58.

Covernton PJ and Connolly JG (2000) Multiple components in the agonist concentration-response relationships of neuronal nicotinic acetylcholine receptors. *Journal of Neuroscience Methods*. 96 (1), 63–70.

Covey LS, Glassman AH and Stetner F (1998) Cigarette smoking and major depression. *Journal of Addictive Diseases*. 17 (1), 35–46.

Cymes GD, Ni Y and Grosman C (2005) Probing ion-channel pores one proton at a time. *Nature*. 438 (7070), 975–80.

Dacosta CJB and Sine S M (2013) Stoichiometry for drug potentiation of a pentameric ion channel. *Proceedings of the National Academy of Sciences of the United States of America*. 110 (16), 6595–600.

Dajas-Bailador F and Wonnacott S (2004) Nicotinic acetylcholine receptors and the regulation of neuronal signalling. *Trends in Pharmacological Sciences*. 25 (6), 317–24.

Daly JW, Garraffo HM, Spande TF, Decker MW, Sullivan JP and Williams M (2000) Alkaloids from frog skin: the discovery of epibatidine and the potential for developing novel non-opioid analgesics. *Natural Product Reports.* 17 (2), 131–5.

Dani J A (2001) Overview of nicotinic receptors and their roles in the central nervous system. *Biological Psychiatry.* 49 (3), 166–74.

Dellisanti CD, Yao Y, Stroud JC, Wang Z and Chen L (2007). Crystal structure of the extracellular domain of nAChR alpha1 bound to alpha-bungarotoxin at 1.94 Å resolution. *Nature Neuroscience.* 10(8):953-62.

Dutertre S and Lewis RJ (2006) Toxin insights into nicotinic acetylcholine receptors. *Biochemical Pharmacology.* 72 (6), 661–70.

Edelstein SJ, Schaad O and Changeux JP (1997) Single binding versus single channel recordings: a new approach to study ionotropic receptors. *Biochemistry.* 36 (45), 13755–60.

Elgoyhen AB, Vetter DE, Katz E, Rothlin C V, Heinemann SF and Boulter J (2001) alpha10: a determinant of nicotinic cholinergic receptor function in mammalian vestibular and cochlear mechanosensory hair cells. *Proceedings of the National Academy of Sciences of the United States of America.* 98 (6), 3501–6.

Exley R, Moroni M, Sasdelli F, Houlihan Lee M, Lukas Ronald J, Sher E, Zwart R and Bermudez I (2006) Chaperone protein 14-3-3 and protein kinase A increase the relative abundance of low agonist sensitivity human alpha 4 beta 2 nicotinic acetylcholine receptors in Xenopus oocytes. *Journal of Neurochemistry.* 98 (3), 876–85.

Fenster CP, Rains MF, Noerager B, Quick MW and Lester RAJ (1997) Influence of Subunit Composition on Desensitization of Neuronal Acetylcholine Receptors at Low Concentrations of Nicotine. *The Journal of Neuroscience.* 17 (15), 5747–5759.

Fucile S (2004) Ca2+ permeability of nicotinic acetylcholine receptors. *Cell Calcium.* 35 (1), 1–8.

Galzi JL, Devillers-Thiéry A, Hussy N, Bertrand S, Changeux JP and Bertrand D (1992) Mutations in the channel domain of a neuronal nicotinic receptor convert ion selectivity from cationic to anionic. *Nature.* 359 (6395), 500–5.

Galzi JL and Changeux JP (1994) Neurotransmitter-gated ion channels as unconventional allosteric proteins. *Current Opinion in Structural Biology.* 4 (4), 554–565.

Gao M, Jin Y, Yang K, Zhang Die, Lukas R J and Wu J (2010) Mechanisms involved in systemic nicotine-induced glutamatergic synaptic plasticity on dopamine neurons in the ventral tegmental area. *The Journal of Neuroscience*. 30 (41), 13814–25.

Gatto G J, Bohme GA, Caldwell WS, Letchworth SR, Traina VM, Obinu MC, Laville M, Reibaud M, Pradier L, Dunbar G and Bencherif Merouane (2004) TC-1734: an orally active neuronal nicotinic acetylcholine receptor modulator with antidepressant, neuroprotective and long-lasting cognitive effects. *CNS Drug Reviews*. 10 (2), 147–66.

Giniatullin R, Nistri A and Yakel JL (2005) Desensitization of nicotinic ACh receptors: shaping cholinergic signaling. *Trends in Neurosciences*. 28 (7), 371–8.

Gopalakrishnan M, Monteggia LM, Anderson DJ, Molinari EJ, Piattoni-Kaplan M, Donnelly-Roberts D, Americ S P and Sullivan JP (1996) Stable expression, pharmacologic properties and regulation of the human neuronal nicotinic acetylcholine alpha 4 beta 2 receptor. *The Journal of Pharmacology and Experimental Therapeutics*. 276 (1), 289–97.

Gotti C, Zoli M and Clementi F (2006) Brain nicotinic acetylcholine receptors: native subtypes and their relevance. *Trends in Pharmacological Sciences*. 27 (9), 482–91.

Gotti C, Moretti M, Meinerz NM, Clementi F, Gaimarri A, Collins Allan C and Marks Michael J (2008) Partial deletion of the nicotinic cholinergic receptor alpha 4 or beta 2 subunit geneschanges the acetylcholine sensitivity of receptor-mediated 86Rb+ efflux in cortex andthalamus and alters relative expression of alpha 4 and beta 2 subunits. *Molecular Pharmacology*. 73 (6), 1796–1807.

Gotti C, Clementi F, Fornari A, Gaimarri A, Guiducci S, Manfredi I, Moretti M, Pedrazzi P, Pucci L and Zoli Michele (2009) Structural and functional diversity of native brain neuronal nicotinic receptors. *Biochemical Pharmacology*. 78 (7), 703–11.

Grady Sharon R, Salminen O, Laverty DC, Whiteaker P, McIntosh JM, Collins A C and Marks M J (2007) The subtypes of nicotinic acetylcholine receptors on dopaminergic terminals of mouse striatum. *Biochemical Pharmacology*. 74 (8), 1235–46.

Grady S R, Salminen O, McIntosh JM, Marks Michael J and Collins A C (2010) Mouse striatal dopamine nerve terminals express alpha4alpha5beta2 and two stoichiometric forms of alpha4beta2*-nicotinic acetylcholine receptors. *Journal of Molecular Neuroscience : MN*. 40 (1-2), 91–5.

Grady S R, Wageman CR, Patzlaff NE and Marks M J (2012) Low concentrations of nicotine differentially desensitize nicotinic acetylcholine receptors that include α5 or α6 subunits and that mediate synaptosomal neurotransmitter release. *Neuropharmacology.* 62 (5-6), 1935–43.

Groot-Kormelink PJ, Broadbent SD, Boorman JP and Sivilotti LG (2004) Incomplete incorporation of tandem subunits in recombinant neuronal nicotinic receptors. *The Journal of General Physiology.* 123 (6), 697–708.

Grosman C, Salamone FN, Sine S M and Auerbach a (2000) The extracellular linker of muscle acetylcholine receptor channels is a gating control element. *The Journal of General Physiology.* 116 (3), 327–40.

Grucza RA, Wang JC, Stitzel JA, Hinrichs AL, Saccone SF, Saccone NL, Bucholz KK, Cloninger CR, Neuman RJ, Budde JP, Fox L, Bertelsen S, Kramer J, Hesselbrock V, Tischfield J, Nurnberger JI, Almasy L, Porjesz B, Kuperman S, Schuckit MA, Edenberg HJ, Rice JP, Goate AM and Bierut LJ (2008) A risk allele for nicotine dependence in CHRNA5 is a protective allele for cocaine dependence. *Biological Psychiatry.* 64 (11), 922–9.

Hahn B, Shoaib M and Stolerman IP (2003) Involvement of the prefrontal cortex but not the dorsal hippocampus in the attention-enhancing effects of nicotine in rats. *Psychopharmacology.* 168 (3), 271–9.

Hansen SB, Sulzenbacher G, Huxford T, Marchot P, Taylor P and Bourne Y (2005) Structures of Aplysia AChBP complexes with nicotinic agonists and antagonists reveal distinctive binding interfaces and conformations. *The EMBO Journal.* 24 (20), 3635–46.

Hansen SB and Taylor P (2007) Galanthamine and non-competitive inhibitor binding to ACh-binding protein: evidence for a binding site on non-alpha-subunit interfaces of heteromeric neuronal nicotinic receptors. *Journal of Molecular Biology.* 369 (4), 895–901.

Harpsøe K, Ahring P K, Christensen J K, Jensen M L, Peters Dan and Balle T (2011) Unraveling the high- and low-sensitivity agonist responses of nicotinic acetylcholine receptors. *The Journal of Neuroscience.* 31 (30), 10759–66.

Harvey SC, Maddox FN and Luetje C W (1996) Multiple determinants of dihydro-beta-erythroidine sensitivity on rat neuronal nicotinic receptor alpha subunits. *Journal of Neurochemistry.* 67 (5), 1953–9.

Henderson BJ, Pavlovicz RE, Allen JD, González-Cestari TF, Orac CM, Bonnell AB, Zhu MX, Boyd RT, Li Chenglong, Bergmeier SC and McKay DB (2010) Negative allosteric modulators that target human alpha4beta2 neuronal nicotinic receptors. *The Journal of Pharmacology and Experimental Therapeutics.* 334 (3), 761–74.

Hibbs RE and Gouaux E (2011) Principles of activation and permeation in an anion-selective Cys-loop receptor. *Nature.* 474 (7349), 54–60.

Hilf RJC and Dutzler R (2008) Hilf 2008.X-ray structure of a prokaryotic pentameric ligand-gated ion channel. *Nature.* 452 (7185), 375–9.

Hilf RJC and Dutzler R (2009) Structure of a potentially open state of a proton-activated pentameric ligand-gated ion channel. *Nature.* 457 (7225), 115–8.

Holden JH and Czajkowski C (2002) Different residues in the GABA(A) receptor alpha 1T60-alpha 1K70 region mediate GABA and SR-95531 actions. *The Journal of Biological Chemistry.* 277 (21), 18785–92.

Houlihan L M, Slater Y, Guerra DL, Peng JH, Kuo YP, Lukas R J, Cassels B K and Bermudez I (2001) Activity of cytisine and its brominated isosteres on recombinant human alpha7, alpha4beta2 and alpha4beta4 nicotinic acetylcholine receptors. *Journal of Neurochemistry.* 78 (5), 1029–43.

Hsiao B, Mihalak KB, Magleby KL and Luetje C W (2008) Zinc potentiates neuronal nicotinic receptors by increasing burst duration. *Journal of Neurophysiology.* 99 (2), 999–1007.

Hurst R, Rollema H and Bertrand D (2013) Nicotinic acetylcholine receptors: From basic science to therapeutics. *Pharmacology & Therapeutics.* 137 (1), 22–54.

Ikemoto S (2007) Dopamine reward circuitry: two projection systems from the ventral midbrain to the nucleus accumbens-olfactory tubercle complex. *Brain Research Reviews.* 56 (1), 27–78.

Imoto K, Busch C, Sakmann B, Mishina M, Konno T, Nakai J, Bujo H, Mori Y, Fukuda K and Numa S (1988) Rings of negatively charged amino acids determine the acetylcholine receptor channel conductance. *Nature.* 335 (6191), 645–8.

Iturriaga-Vásquez P, Carbone A L, García-Beltrán O, Livingstone PD, Biggin PC, Cassels Bruce K, Wonnacott S, Zapata-Torres G and Bermudez I (2010) Molecular determinants for competitive inhibition of alpha4beta2 nicotinic acetylcholine receptors. *Molecular Pharmacology.* 78 (3), 366–75.

Jackson KJ, Marks M J, Vann RE, Chen X, Gamage TF, Warner JA and Damaj MI (2010) Role of alpha5 nicotinic acetylcholine receptors in pharmacological and behavioral effects of nicotine in mice. *The Journal of Pharmacology and Experimental Therapeutics.* 334 (1), 137–46.

Jensen AA, Frølund B, Liljefors T and Krogsgaard-Larsen P (2005) Neuronal nicotinic acetylcholine receptors: structural revelations, target identifications, and therapeutic inspirations. *Journal of Medicinal Chemistry.* 48 (15), 4705–45.

Jha A and Auerbach A (2010) Acetylcholine receptor channels activated by a single agonist molecule. *Biophysical Journal.* 98 (9), 1840–6.

Karlin A and Akabas MH (1998) Substituted-cysteine accessibility method. *Methods in Enzymology.* 293, 123–45.

Karlin A (2002) Emerging structure of the nicotinic acetylcholine receptors. *Nature reviews. Neuroscience.* 3 (2), 102–14.

Kash TL, Jenkins A, Kelley JC, Trudell JR and Harrison Neil L (2003) Coupling of agonist binding to channel gating in the GABA(A) receptor. *Nature.* 421 (6920), 272–5.

Kenny PJ and Markou A (2006) Nicotine self-administration acutely activates brain reward systems and induces a long-lasting increase in reward sensitivity. *Neuropsychopharmacology.* 31 (6), 1203–11.

Khiroug SS, Harkness PC, Lamb PW, Sudweeks SN, Khiroug L, Millar NS and Yakel JL (2002) Rat nicotinic ACh receptor alpha7 and beta2 subunits co-assemble to form functional heteromeric nicotinic receptor channels. *The Journal of Physiology.* 540 (Pt 2), 425–34.

Kim H, Flanagin B a, Qin C, Macdonald R L and Stitzel J A (2003) The mouse Chrna4 A529T polymorphism alters the ratio of high to low affinity $\alpha4\beta2$ nAChRs. *Neuropharmacology.* 45 (3), 345–354.

Kummer W, Lips KS and Pfeil U (2008) The epithelial cholinergic system of the airways. *Histochemistry and Cell Biology.* 130 (2), 219–34.

Kuryatov A, Olale FA, Choi C and Lindstrom J (2000) Acetylcholine receptor extracellular domain determines sensitivity to nicotine-induced inactivation. *European Journal of Pharmacology.* 393 (1-3), 11–21.

Kuryatov A, Luo J, Cooper J and Lindstrom J (2005) Nicotine Acts as a Pharmacological Chaperone to Up-Regulate Human alpha4beta2 Acetylcholine Receptors. *Molecular Pharmacology.* 68 (6), 1839–1851.

Kuryatov A, Jennifer O and Lindstrom J (2008) Roles of auxiliary subunits in alpha4beta2(*) nicotinic receptors. *Molecular Pharmacology.* 74 (1), 132–143.

Labarca C, Schwarz J, Deshpande P, Schwarz S, Nowak MW, Fonck C, Nashmi R, Kofuji P, Dang H, Shi W, Fidan M, Khakh BS, Chen Z, Bowers BJ, Boulter J, Wehner JM and Lester H A (2001) Point mutant mice with hypersensitive alpha 4 nicotinic receptors show dopaminergic deficits and increased anxiety. *Proceedings of the National Academy of Sciences of the United States of America.* 98 (5), 2786–91.

Lape R, Colquhoun D and Sivilotti LG (2008) On the nature of partial agonism in the nicotinic receptor superfamily. *Nature*. 454 (7205), 722–7.

Laviolette SR and Van der Kooy D (2004) The neurobiology of nicotine addiction: bridging the gap from molecules to behaviour. *Nature reviews. Neuroscience*. 5 (1), 55–65.).

Lee C-H, Zhu C, Malysz J, Campbell T, Shaughnessy T, Honore P, Polakowski J and Gopalakrishnan M (2011) α4β2 neuronal nicotinic receptor positive allosteric modulation: an approach for improving the therapeutic index of α4β2 nAChR agonists in pain. *Biochemical pharmacology*. 82 (8), 959–66.

Lee WY and Sine S M (2005) Principal pathway coupling agonist binding to channel gating in nicotinic receptors. *Nature*. 438 (7065), 243–7.

Lester H A, Dibas MI, Dahan DS, Leite JF and Dougherty Dennis A (2004) Cys-loop receptors: new twists and turns. *Trends in Neurosciences*. 27 (6), 329–36.

Lester RAJ (2004) Activation and desensitization of heteromeric neuronal nicotinic receptors: implications for non-synaptic transmission. *Bioorganic & Medicinal Chemistry Letters*. 14 (8), 1897–900.

Levin ED and Simon BB (1998) Nicotinic acetylcholine involvement in cognitive function in animals. *Psychopharmacology*. 138 (3-4), 217–30.

Li S-X, Huang S, Bren N, Noridomi K, Dellisanti CD, Sine S M and Chen L (2011) Ligand-binding domain of an α7-nicotinic receptor chimera and its complex with agonist. *Nature Neuroscience*. 14 (10), 1253–9.

Lips KS, Pfeil U and Kummer W (2002) Coexpression of alpha 9 and alpha 10 nicotinic acetylcholine receptors in rat dorsal root ganglion neurons. *Neuroscience*. 115 (1), 1–5.

Liu L, Zhao-Shea R, McIntosh JM, Gardner PD and Tapper AR (2012) Nicotine persistently activates ventral tegmental area dopaminergic neurons via nicotinic acetylcholine receptors containing α4 and α6 subunits. *Molecular Pharmacology*. 81 (4), 541–8.

Luetje C W and Patrick J (1991) Both alpha- and beta-subunits contribute to the agonist sensitivity of neuronal nicotinic acetylcholine receptors. *The Journal of Neuroscience*. 11 (3), 837–45.

Lukas R J, Changeux JP, Le Novère N, Albuquerque E X, Balfour DJ, Berg DK, Bertrand D, Chiappinelli VA, Clarke PB, Collins A C, Dani J A, Grady S R, Kellar K J, Lindstrom J M, Marks M J, Quik M, Taylor PW and Wonnacott S (1999) International Union of Pharmacology. XX. Current status of the nomenclature for nicotinic acetylcholine receptors and their subunits. *Pharmacological Reviews*. 51 (2), 397–401.

Lummis SCR, Beene DL, Lee LW, Lester Henry A, Broadhurst RW and Dougherty Dennis A (2005) Cis-trans isomerization at a proline opens the pore of a neurotransmitter-gated ion channel. *Nature*. 438 (7065), 248–52.

Mansvelder HD and McGehee DS (2002) Cellular and synaptic mechanisms of nicotine addiction. *Journal of Neurobiology*. 53 (4), 606–17.

Mantione E, Micheloni S, Alcaino C, New K, Mazzaferro S and Bermudez I (2012) Allosteric modulators of α4β2 nicotinic acetylcholine receptors: a new direction for antidepressant drug discovery. *Future Medicinal Chemistry*. 4 (17), 2217–30.

Mao D, Perry DC, Yasuda RP, Wolfe BB and Kellar K J (2008) The alpha4beta2alpha5 nicotinic cholinergic receptor in rat brain is resistant to up-regulation by nicotine in vivo. *Journal of Neurochemistry*. 104 (2), 446–56.

Markett S, Montag C and Reuter M (2011) The nicotinic acetylcholine receptor gene CHRNA4 is associated with negative emotionality. *Emotion (Washington, D.C.)*. 11 (2), 450–5.

Marks M J, Whiteaker P, Calcaterra J, Stitzel J a, Bullock a E, Grady S R, Picciotto M R, Changeux JP and Collins a C (1999) Two pharmacologically distinct components of nicotinic receptor-mediated rubidium efflux in mouse brain require the beta2 subunit. *The Journal of Pharmacology and Experimental Therapeutics*. 289 (2), 1090–103.

Marks M J, Meinerz NM, Drago J and Collins A C (2008) Gene targeting demonstrates that alpha4 nicotinic acetylcholine receptor subunits contribute to expression of diverse [3H] epibatidine binding sites and components of biphasic 86Rb+ efflux with high and low sensitivity to stimulation by acetylcholine. *Neuropharmacology*. 53 (3), 390–405.

Marks Michael J, Meinerz NM, Brown RWB and Collins A C (2010) 86Rb+ efflux mediated by alpha4beta2*-nicotinic acetylcholine receptors with high and low-sensitivity to stimulation by acetylcholine display similar agonist-induced desensitization. *Biochemical Pharmacology*. 80 (8), 1238–51.

Martinez KL, Corringer PJ, Edelstein SJ, Changeux JP and Mérola F (2000) Structural differences in the two agonist binding sites of the Torpedo nicotinic acetylcholine receptor revealed by time-resolved fluorescence spectroscopy. *Biochemistry*. 39 (23), 6979–90.

Maskos U, Molles BE, Pons S, Besson M, Guiard BP, Guilloux J-P, Evrard A, Cazala P, Cormier A, Mameli-Engvall M, Dufour N, Cloëz-Tayarani I, Bemelmans AP, Mallet J, Gardier AM, David V, Faure P, Granon S and Changeux JP (2005) Nicotine reinforcement and cognition restored by targeted expression of nicotinic receptors. *Nature*. 436 (7047), 103–7.

Maskos U (2010) Role of endogenous acetylcholine in the control of the dopaminergic system via nicotinic receptors. *Journal of Neurochemistry.* 114 (3), 641–6.

Matsushima N, Hirose S, Iwata H, Fukuma G, Yonetani M, Nagayama C, Hamanaka W, Matsunaka Y, Ito M, Kaneko S, Mitsudome A and Sugiyama H (2002) Mutation (Ser284Leu) of neuronal nicotinic acetylcholine receptor alpha 4 subunit associated with frontal lobe epilepsy causes faster desensitization of the rat receptor expressed in oocytes. *Epilepsy Research.* 48 (3), 181–6.

Mazzaferro S, Benallegue N, Carbone A L, Gasparri F, Vijayan R, Biggin PC, Moroni M and Bermudez I (2011) Additional acetylcholine (ACh) binding site at alpha4/alpha4 interface of (alpha4beta2)2alpha4 nicotinic receptor influences agonist sensitivity. *The Journal of Biological Chemistry.* 286 (35), 31043–54.

McKee SA, Sinha R, Weinberger AH, Sofuoglu M, Harrison ELR, Lavery M and Wanzer J (2011) Stress decreases the ability to resist smoking and potentiates smoking intensity and reward. *Journal of Psychopharmacology (Oxford, England).* 25 (4), 490–502.

Miller PS, Beato M, Harvey RJ and Smart T G (2005) Molecular determinants of glycine receptor alphabeta subunit sensitivities to Zn2+-mediated inhibition. *The Journal of Physiology.* 566 (Pt 3), 657–70.

Miller PS and Smart T G (2010) Binding, activation and modulation of Cys-loop receptors. *Trends in Pharmacological Sciences.* 31 (4), 161–74.

Mineur YS and Picciotto M R (2010) Nicotine receptors and depression: revisiting and revising the cholinergic hypothesis. *Trends in Pharmacological Sciences.* 31 (12), 580–6.

Miyazawa A, Fujiyoshi Y and Unwin N (2003) Structure and gating mechanism of the acetylcholine receptor pore. *Nature.* 423 (6943), 949–55.

Mogg AJ, Jones F a, Pullar I a, Sharples CG V and Wonnacott S (2004) Functional responses and subunit composition of presynaptic nicotinic receptor subtypes explored using the novel agonist 5-iodo-A-85380. *Neuropharmacology.* 47 (6), 848–59.

Moroni M, Zwart R, Sher E, Cassels Bruce K and Bermudez I (2006) Alpha4beta2 Nicotinic Receptors with High and Low Acetylcholine Sensitivity: Pharmacology, Stoichiometry, and Sensitivity to Long-Term Exposure to Nicotine. *Molecular Pharmacology.* 70 (2), 755–768.

Moroni M, Vijayan R, Carbone A L, Zwart R, Biggin PC and Bermudez I (2008) Non-agonist-binding subunit interfaces confer distinct functional signatures to the alternate stoichiometries of the alpha4beta2 nicotinic receptor: an alpha4-alpha4 interface is required for Zn2+ potentiation. *The Journal of Neuroscience.* 28 (27), 6884–94.

Morris GM, Goodsell DS, Halliday RS, Huey R, Hart WE, Belew RK and Olson AJ (1998) Automated docking using a Lamarckian genetic algorithm and an empirical binding free energy function. *Journal of Computational Chemistry.* 19 (14), 1639–1662.

Mukhin AG, Gündisch D, Horti AG, Koren AO, Tamagnan G, Kimes AS, Chambers J, Vaupel DB, King SL, Picciotto M R, Innis RB and London ED (2000) 5-Iodo-A-85380, an alpha4beta2 subtype-selective ligand for nicotinic acetylcholine receptors. *Molecular Pharmacology.* 57 (3), 642–9.

Mukhtasimova N, Free C and Sine S M (2005) Initial coupling of binding to gating mediated by conserved residues in the muscle nicotinic receptor. *The Journal of General Physiology.* 126 (1), 23–39.

Mukhtasimova N, Lee WY, Wang H-L and Sine S M (2009) Detection and trapping of intermediate states priming nicotinic receptor channel opening. *Nature.* 459 (7245), 451–4.

Murray TA, Bertrand D, Papke RL, George AA, Pantoja R, Srinivasan R, Liu Q, Wu J, Whiteaker P, Lester Henry A and Lukas R J (2012) α7β2 Nicotinic Acetylcholine Receptors Assemble , Function , and Are Activated Primarily via Their α7-α7 Interfaces. *Molecular Pharmacology.* 81(2):175-88.

Nelson ME, Kuryatov A, Choi CH, Zhou Yan and Lindstrom J (2003) Alternate stoichiometries of alpha4beta2 nicotinic acetylcholine receptors. *Molecular Pharmacology.* 63 (2), 332–41.

Newman MB, Nazian SJ, Sanberg PR, Diamond DM and Shytle RD (2001) Corticosterone-attenuating and anxiolytic properties of mecamylamine in the rat. *Progress in Neuro-Psychopharmacology & Biological Psychiatry.* 25 (3), 609–20.

Le Novère N, Corringer PJ and Changeux JP (2002) The diversity of subunit composition in nAChRs: evolutionary origins, physiologic and pharmacologic consequences. *Journal of Neurobiology.* 53 (4), 447–56.

Paas Y, Gibor G, Grailhe R, Savatier-Duclert N, Dufresne V, Sunesen M, De Carvalho LP, Changeux JP and Attali B (2005) Pore conformations and gating mechanism of a Cys-loop receptor. *Proceedings of the National Academy of Sciences of the United States of America.* 102 (44), 15877–82.

Pandya A and Yakel JL (2011) Allosteric modulator Desformylflustrabromine relieves the inhibition of α2β2 and α4β2 nicotinic acetylcholine receptors by β-amyloid(1-42) peptide. *Journal of Molecular Neuroscience : MN.* 45 (1), 42-7.

Papke RL, Williams Dustin K, Horenstein AN and Stokes C (2011) The effective opening of nicotinic acetylcholine receptors with single agonist binding sites. *The Journal of General Physiology.* 137 (4), 369–84.

Paradiso K, Zhang J and Steinbach J H (2001) The C terminus of the human nicotinic alpha4beta2 receptor forms a binding site required for potentiation by an estrogenic steroid. *The Journal of Neuroscience.* 21 (17), 6561–8.

Paradiso KG and Steinbach J H (2003) Nicotine is highly effective at producing desensitization of rat alpha4beta2 neuronal nicotinic receptors. *The Journal of Physiology.* 553 (Pt 3), 857–71.

Paterson D and Nordberg A (2000) Neuronal nicotinic receptors in the human brain. *Progress in Neurobiology.* 61 (1), 75–111.

Paulsen IM, Martin IL and Dunn SMJ (2009) Isomerization of the proline in the M2-M3 linker is not required for activation of the human 5-HT$_3$A receptor. *Journal of Neurochemistry.* 110 (3), 870–8.

Pavlovicz RE, Henderson BJ, Bonnell AB, Boyd RT, McKay DB and Li Chenglong (2011) Identification of a negative allosteric site on human α4β2 and α3β4 neuronal nicotinic acetylcholine receptors. *PloS One.* 6 (9), e24949.

Peto R, Lopez AD, Boreham J, Thun M, Heath C and Doll R (1996) Mortality from smoking worldwide. *British Medical Bulletin.* 52 (1), 12–21.

Picciotto M R, Zoli M and Changeux JP (1999) Use of knock-out mice to determine the molecular basis for the actions of nicotine. *Nicotine & Tobacco Research.* 1 Suppl 2, S121–5; discussion S139–40

Picciotto M R, Caldarone BJ, Brunzell DH, Zachariou V, Stevens TR and King SL (2001) Neuronal nicotinic acetylcholine receptor subunit knockout mice: physiological and behavioral phenotypes and possible clinical implications. *Pharmacology & Therapeutics.* 92 (2-3), 89–108.

Price KL, Millen KS and Lummis SCR (2007) Transducing agonist binding to channel gating involves different interactions in 5-HT$_3$ and GABAC receptors. *The Journal of Biological Chemistry.* 282 (35), 25623–30.

Prince RJ and Sine S M (1998) Epibatidine binds with unique site and state selectivity to muscle nicotinic acetylcholine receptors. *The Journal of Biological Chemistry.* 273 (14), 7843–9.

Purohit P and Auerbach A (2007) Acetylcholine receptor gating: movement in the alpha-subunit extracellular domain. *The Journal of General Physiology.* 130 (6), 569–79.

Purohit P and Auerbach A (2008) Unliganded gating of acetylcholine receptor channels. *Proceedings of the National Academy of Sciences of the United States of America.* 106(1):115-20.

Purohit P and Auerbach A (2013) Loop C and the mechanism of acetylcholine receptor-channel gating. *The Journal of General Physiology*, 1–12.

Rabenstein RL, Caldarone BJ and Picciotto M R (2006) The nicotinic antagonist mecamylamine has antidepressant-like effects in wild-type but not beta2- or alpha7-nicotinic acetylcholine receptor subunit knockout mice. *Psychopharmacology.* 189 (3), 395–401.

Raber J, Koob GF and Bloom FE (1995) Interleukin-2 (IL-2) induces corticotropin-releasing factor (CRF) release from the amygdala and involves a nitric oxide-mediated signaling; comparison with the hypothalamic response. *The Journal of Pharmacology and Experimental Therapeutics.* 272 (2), 815–24.

Ramirez-Latorre J, Yu CR, Qu X, Perin F, Karlin A and Role L (1996) Functional contributions of alpha5 subunit to neuronal acetylcholine receptor channels. *Nature.* 380 (6572), 347–51.

Rayes D, De Rosa MJ, Sine S M and Bouzat C (2009) Number and locations of agonist binding sites required to activate homomeric Cys-loop receptors. *The Journal of Neuroscience.* 29 (18), 6022–32.

Rode F, Munro G, Holst D, Nielsen E Ø, Troelsen KB, Timmermann DB, Rønn LCB and Grunnet M (2012) Positive allosteric modulation of α4β2 nAChR agonist induced behaviour. *Brain Research.* 1458 (null), 67–75.

Rodrigues-Pinguet NO, Pinguet TJ, Figl A, Lester Henry A and Cohen BN (2005) Mutations linked to autosomal dominant nocturnal frontal lobe epilepsy affect allosteric Ca2+ activation of the alpha 4 beta 2 nicotinic acetylcholine receptor. *Molecular Pharmacology.* 68 (2), 487–501.

Rogers CJ, Twyman RE and Macdonald R L (1994) Benzodiazepine and beta-carboline regulation of single GABAA receptor channels of mouse spinal neurones in culture. *The Journal of Physiology.* 475 (1), 69–82.

Rohde LAH, Ahring Philip Kiær, Jensen Marianne Lerbech, Nielsen Elsebet Østergaard, Peters Dan, Helgstrand C, Krintel C, Harpsøe K, Gajhede M, Kastrup JS and Balle T (2012) Intersubunit bridge formation governs agonist efficacy at nicotinic acetylcholine α4β2 receptors: unique role of halogen bonding revealed. *The Journal of Biological Chemistry.* 287 (6), 4248–59.

Rollema H, Guanowsky V, Mineur YS, Shrikhande A, Jotham W, Seymour PA and Picciotto M R (2010) Varenicline has antidepressant-like activity in the forced swim test and augments sertraline's effect. *European Journal of Pharmacology.* 605, 114–116.

Rucktooa P, Haseler C a, Van Elk R, Smit August B, Gallagher T and Sixma Titia K (2012) Structural Characterization of Binding Mode of Smoking Cessation Drugs to Nicotinic Acetylcholine Receptors through Study of Ligand Complexes with Acetylcholine-binding Protein. *The Journal of Biological Chemistry.* 287 (28), 23283–93.

Sallette J, Pons Stéphanie, Devillers-Thiery A, Soudant M, Prado de Carvalho L, Changeux JP and Corringer PJ (2005) Nicotine upregulates its own receptors through enhanced intracellular maturation. *Neuron.* 46 (4), 595–607.

Sambrook J, Fritsch EF and Maniatis T (1989) *Molecular cloning : a laboratory manual. J. Sambrook, E.F. Fritsch, T. Maniatis.*2nd ed. New York : *Cold Spring Harbor Laboratory Press,* 1989.

Samochocki M, Höffle A, Fehrenbacher A, Jostock R, Ludwig J, Christner C, Radina M, Zerlin M, Ullmer C, Pereira EFR, Lübbert H, Albuquerque E X and Maelicke A (2003) Galantamine is an allosterically potentiating ligand of neuronal nicotinic but not of muscarinic acetylcholine receptors. *The Journal of pharmacology and Experimental Therapeutics.* 305 (3), 1024–36.

Sarter M, Hasselmo ME, Bruno JP and Givens B (2005) Unraveling the attentional functions of cortical cholinergic inputs: interactions between signal-driven and cognitive modulation of signal detection. *Brain research. Brain Research Reviews.* 48 (1), 98–111.

Scheffer IE, Jones L, Pozzebon M, Howell RA, Saling MM and Berkovic SF (1995) Autosomal dominant rolandic epilepsy and speech dyspraxia: a new syndrome with anticipation. *Annals of Neurology.* 38 (4), 633–42.

Sgard F, Charpantier E, Bertrand S, Walker N, Caput D, Graham D, Bertrand D and Besnard F (2002) A novel human nicotinic receptor subunit, alpha10, that confers functionality to the alpha9-subunit. *Molecular Pharmacology.* 61 (1), 150–9.

Sigel E, Kaur KH, Lüscher BP and Baur R (2009) Use of concatamers to study GABAA receptor architecture and function: application to delta-subunit-containing receptors and possible pitfalls. *Biochemical Society Transactions.* 37 (Pt 6), 1338–42.

Sine S M, Claudio T and Sigworth FJ (1990) Activation of Torpedo acetylcholine receptors expressed in mouse fibroblasts. Single channel current kinetics reveal distinct agonist binding affinities. *The Journal of General Physiology.* 96 (2), 395–437.

Slater YE, A, B, Valdivia AC and C (2003) Halogenated cytisine derivatives as agonists at human neuronal nicotinic acetylcholine receptor subtypes. *Neuropharmacology.* 44 (4), 503–515.

Smart T G, Xie X and Krishek BJ (1994) Modulation of inhibitory and excitatory amino acid receptor ion channels by zinc. *Progress in Neurobiology.* 42 (3), 393–441.

Son CD, Moss FJ, Cohen BN and Lester H A (2009) Nicotine Normalizes Intracellular Subunit Stoichiometry of Nicotinic Receptors Carrying Mutations Linked to Autosomal Dominant Nocturnal Frontal Lobe Epilepsy. *Molecular Pharmacology.* 75 (5), 1137–1148.

Spitz MR, Amos CI, Dong Q, Lin J and Wu X (2008) The CHRNA5-A3 region on chromosome 15q24-25.1 is a risk factor both for nicotine dependence and for lung cancer. *Journal of the National Cancer Institute.* 100 (21), 1552–6.

Srinivasan R, Pantoja R, Moss FJ, Mackey EDW, Son CD, Miwa J and Lester H A (2011) Nicotine up-regulates alpha4beta2 nicotinic receptors and ER exit sites via stoichiometry-dependent chaperoning. *The Journal of General Physiology.* 137 (1), 59–79.

Srinivasan R, Richards CI, Xiao C, Rhee D, Pantoja R, Dougherty D a, Miwa JM and Lester H A (2012) Pharmacological chaperoning of nicotinic acetylcholine receptors reduces the endoplasmic reticulum stress response. *Molecular Pharmacology.* 81 (6), 759–69.

Steinbach J H (1990) Mechanism of action of the nicotinic acetylcholine receptor. *Ciba Foundation Symposium.* 152, 53–61; discussion 61–7.

Steinlein OK, Kaneko S and Hirose S (2012) Nicotinic acetylcholine receptor mutations. In: *In: Noebels JL, Avoli M, Rogawski MA, et al., editors. Jasper's Basic Mechanisms of the Epilepsies [Internet]. 4th edition. Bethesda (MD): National Center for Biotechnology Information (US); 2012.*

Sullivan JP, Donnelly-Roberts D, Briggs CA, Anderson DJ, Gopalakrishnan M, Piattoni-Kaplan M, Campbell JE, McKenna DG, Molinari E, Hettinger AM, Garvey DS, Wasicak JT, Holladay MW, Williams M and Arneric S P (1996) A-85380 [3-(2(S)-azetidinylmethoxy) pyridine]: in vitro pharmacological properties of a novel, high affinity alpha 4 beta 2 nicotinic acetylcholine receptor ligand. *Neuropharmacology.* 35 (6), 725–34.

Taly A, Corringer PJ, Guedin D, Lestage P and Changeux JP (2009) Nicotinic receptors: allosteric transitions and therapeutic targets in the nervous system. *Nature reviews. Drug Discovery.* 8 (9), 733–50.

Tantama M and Licht S (2009) Functional equivalence of the nicotinic acetylcholine receptor transmitter binding sites in the open state. *Biochimica et Biophysica Acta.* 1788 (5), 936–44.

Tapia L, Kuryatov A and Lindstrom J (2007) Ca2+ permeability of the (alpha4)3(beta2)2 stoichiometry greatly exceeds that of (alpha4)2(beta2)3 human acetylcholine receptors. *Molecular Pharmacology.* 71 (3), 769–76.

Tapper AR, McKinney SL, Nashmi Raad, Schwarz Johannes, Deshpande Purnima, Labarca Cesar, Whiteaker Paul, Marks Michael J, Collins Allan C and Lester H A (2004) Nicotine activation of alpha4* receptors: sufficient for reward, tolerance, and sensitization. *Science (New York, N.Y.).* 306 (5698), 1029–32.

Tavares XDS, Blum AP, Nakamura DT, Puskar NL, Shanata J a P, Lester H A and Dougherty D a (2012) Variations in Binding Among Several Agonists at Two Stoichiometries of the Neuronal, α4β2 Nicotinic Receptor. *Journal of the American Chemical Society.* 134 (28), 11474–80.

Timmermann DB, Sandager-Nielsen K, Dyhring T, Smith M, Jacobsen A-M, Nielsen E Ø, Grunnet M, Christensen J K, Peters D, Kohlhaas K, Olsen GM and Ahring P K (2012) Augmentation of cognitive function by NS9283, a stoichiometry-dependent positive allosteric modulator of α2- and α4-containing nicotinic acetylcholine receptors. *British Journal of Pharmacology.* 167 (1), 164–82.

Ulens C, Hogg RC, Celie PH, Bertrand D, Tsetlin V, Smit August B and Sixma Titia K (2006) Structural determinants of selective alpha-conotoxin binding to a nicotinic acetylcholine receptor homolog AChBP. *Proceedings of the National Academy of Sciences of the United States of America.* 103 (10), 3615–20.

Unwin N (2005) Refined Structure of the Nicotinic Acetylcholine Receptor at 4A Resolution. *Journal of Molecular Biology.* 346(4):967-89

Unwin N, Fujiyoshi Y (2012). Gating movement of acetylcholine receptor caught by plunge-freezing. *Journal of Molecular Biology.* 422(5):617-34.

Venkatachalan SP and Czajkowski C (2008) A conserved salt bridge critical for GABA(A) receptor function and loop C dynamics. *Proceedings of the National Academy of Sciences of the United States of America.* 105 (36), 13604–9.

Verbitsky M, Rothlin C V, Katz E and Elgoyhen AB (2000) Mixed nicotinic-muscarinic properties of the alpha9 nicotinic cholinergic receptor. *Neuropharmacology.* 39 (13), 2515–24.

Vincler M and Eisenach JC (2004) Plasticity of spinal nicotinic acetylcholine receptors following spinal nerve ligation. *Neuroscience Research.* 48 (2), 139–45.

Wang H-L, Toghraee R, Papke D, Cheng X-L, McCammon JA, Ravaioli U and Sine S M (2009) Single-channel current through nicotinic receptor produced by closure of binding site C-loop. *Biophysical Journal.* 96 (9), 3582–90.

Weiland S, Bertrand D and Leonard S (2000) Neuronal nicotinic acetylcholine receptors: from the gene to the disease. *Behavioural Brain Research.* 113 (1-2), 43–56.

Weiss RB, Baker TB, Cannon DS, Von Niederhausern A, Dunn DM, Matsunami N, Singh NA, Baird L, Coon H, McMahon WM, Piper ME, Fiore MC, Scholand MB, Connett JE, Kanner RE, Gahring LC, Rogers SW, Hoidal JR and Leppert MF (2008) A candidate gene approach identifies the CHRNA5-A3-B4 region as a risk factor for age-dependent nicotine addiction. *PLoS Genetics.* 4 (7), e1000125.

Weltzin MM and Schulte MK (2010) Pharmacological characterization of the allosteric modulator desformylflustrabromine and its Interaction with alpha4beta2 Neuronal nicotinic acetylcholine aeceptor orthosteric ligands. *The Journal of Pharmacology and Experimental Terapeutics.* 334 (3), 917–926.

White BH and Cohen J B (1992) Agonist-induced changes in the structure of the acetylcholine receptor M2 regions revealed by photoincorporation of an uncharged nicotinic noncompetitive antagonist. *The Journal of Biological Chemistry.* 267 (22), 15770–83.

Wilkins JN, Carlson HE, Van Vunakis H, Hill MA, Gritz E and Jarvik ME (1982) Nicotine from cigarette smoking increases circulating levels of cortisol, growth hormone, and prolactin in male chronic smokers. *Psychopharmacology.* 78 (4), 305–8.

Williams DK, Stokes C, Horenstein NA and Papke RL (2009) Differential regulation of receptor activation and agonist selectivity by highly conserved tryptophans in the nicotinic acetylcholine receptor binding site. *The Journal of Pharmacology and Experimental Therapeutics.* 330 (1), 40–53.

Williamson PTF, Verhoeven a, Miller K W, Meier BH and Watts a (2007) The conformation of acetylcholine at its target site in the membrane-embedded nicotinic acetylcholine receptor. *Proceedings of the National Academy of Sciences of the United States of America.* 104 (46), 18031–6.

Wonnacott S (1997) Presynaptic nicotinic ACh receptors. *Trends in Neurosciences*. 20 (2), 92–8.

Wonnacott S, Barik J, Dickinson J and Jones IW (2006) Nicotinic receptors modulate transmitter cross talk in the CNS: nicotinic modulation of transmitters. *Journal of Molecular Neuroscience : MN*. 30 (1-2), 137–40.

Xiao Y, Fan H, Musachio JL, Wei Z-L, Chellappan SK, Kozikowski AP and Kellar Kenneth J (2006) Sazetidine-A, a novel ligand that desensitizes alpha4beta2 nicotinic acetylcholine receptors without activating them. *Molecular Pharmacology*. 70 (4), 1454–60.

Xiu X, Hanek AP, Wang J, Lester H A and Dougherty D A (2005) A unified view of the role of electrostatic interactions in modulating the gating of Cys loop receptors. *The Journal of Biological Chemistry*. 280 (50), 41655–66.

Xiu X, Puskar NL, Shanata JAP, Lester Henry A and Dougherty D A (2009) Nicotine binding to brain receptors requires a strong cation – p interaction. *Nature*. 458 (7237), 534–537.

Yakel JL (2010) Gating of nicotinic ACh receptors: latest insights into ligand binding and function. *The Journal of Physiology*. 588 (Pt 4), 597–602.

Yoshimura RF, Hogenkamp DJ, Li WY, Tran MB, Belluzzi JD, Whittemore ER, Leslie Frances M and Gee KW (2007) Negative allosteric modulation of nicotinic acetylcholine receptors blocks nicotine self-administration in rats. *The Journal of Pharmacology and Experimental Therapeutics*. 323 (3), 907–15.

Zanardi A, Leo G, Biagini G and Zoli M (2002) Nicotine and neurodegeneration in ageing. *Toxicology Letters*. 127 (1-3), 207–15.

Zhang H and Karlin A (1997) Identification of acetylcholine receptor channel-lining residues in the M1 segment of the beta-subunit. *Biochemistry*. 36 (50), 15856–64.

Zhang J, Xiao Y-D, Jordan KG, Hammond PS, Van Dyke KM, Mazurov AA, Speake JD, Lippiello PM, James JW, Letchworth SR, Bencherif Merouane and Hauser TA (2012) Analgesic effects mediated by neuronal nicotinic acetylcholine receptor agonists: correlation with desensitization of α4β2* receptors. *European Journal of Pharmaceutical Sciences*. 47 (5), 813–23.

Zhang J, Xue F, Whiteaker P, Li Chaokun, Wu W, Shen B, Huang Y, Lukas Ronald J and Chang Y (2011) Desensitization of alpha7 nicotinic receptor is governed by coupling strength relative to gate tightness. *The Journal of Biological Chemistry*. 286 (28), 25331–40.

Zhao-Shea R, Liu L, Soll LG, Improgo MR, Meyers EE, McIntosh JM, Grady S R, Marks M J, Gardner PD and Tapper AR (2011) Nicotine-mediated activation of dopaminergic neurons in distinct regions of the ventral tegmental area. *Neuropsychopharmacology.* 36 (5), 1021–32..

Zhong W, Gallivan JP, Zhang Y, Li L, Lester H A and Dougherty D A (1998) From ab initio quantum mechanics to molecular neurobiology: a cation-pi binding site in the nicotinic receptor. *Proceedings of the National Academy of Sciences of the United States of America.* 95 (21), 12088–93.

Zhou Yu, Pearson JE and Auerbach A (2005) Phi-value analysis of a linear, sequential reaction mechanism: theory and application to ion channel gating. *Biophysical Journal.* 89 (6), 3680–5.

Ziedonis D, Hitsman B, Beckham JC, Zvolensky M, Adler LE, Audrain-McGovern J, Breslau N, Brown RA, George TP, Williams J, Calhoun PS and Riley WT (2008) Tobacco use and cessation in psychiatric disorders: National Institute of Mental Health report. *Nicotine & Tobacco Research.* 10 (12), 1691–715.

Zwart R, Broad LM, Xi Q, Lee M, Moroni M, Bermudez I and Sher E (2006) 5-I A-85380 and TC-2559 differentially activate heterologously expressed alpha4beta2 nicotinic receptors. *European Journal of Pharmacology.* 539 (1-2), 10–7.

Zwart R, Carbone A L, Moroni M, Bermudez I, Mogg AJ, Folly EA, Broad LM, Williams AC, Zhang Deyi, Ding C, Heinz BA and Sher E (2008) Sazetidine-Ais a potent and selective agonist at native and recombinant alpha 4 beta 2 nicotinic acetylcholine receptors. *Molecular Pharmacology.* 73 (6), 1838–1843.

Publications

Carbone AL, Moroni M, Groot-Kormelink PJ, Bermudez I (2009). Pentameric concatenated (α4)$_2$(β2)$_3$ and (α4)$_3$(β2)$_2$ nicotinic acetylcholine receptors: subunit arrangement determines functional expression. Br J Pharmacol 156: 970–981.

Chavez-Noriega LE, Crona JH, Washburn MS, Urrutia A, Elliott KJ, Johnson EC (1997). Pharmacological characterization of recombinant human neuronal nicotinic acetylcholine receptors hα2β2, hα2β4, hα3β2, hα3β4, hα4β2, hα4β4 and hα7 expressed in *Xenopus* oocytes. J Pharmacol Exp Ther 280: 346–356.

Corringer PJ, Bertrand S, Bohler S, Edelstein SJ, Changeux JP, Bertrand D (1998). Critical elements determining diversity in agonist binding and desensitisation of neuronal nicotinic acetylcholine receptors. J Neurosci 18: 648–657.

daCosta CJB, Sine SM (2013). Stoichiometry for drug potentiation of a pentameric ion channel. Proc Natl Acad Sci U S A 110: 6595–6600.

Fenster CP, Rains MF, Noerager B, Quick MW, Lester RAJ (1997). Influence of subunit composition on desensitization of neuronal acetylcholine receptors at low concentrations of nicotine. J Neurosci 17: 5747–5759.

Giniatullin R, Nistri A, Yakel JL (2005). Desensitization of nicotinic ACh receptors: shaping cholinergic signaling. Trends Neurosci 28: 371–378.

Gopalakrishnan M, Monteggia LM, Anderson DJ, Molinari EJ, Piattoni-Kaplan M, Donnelly Roberts D et al. (1996). Stable expression, pharmacologic properties and regulation of the human neuronal nicotinic acetylcholine α4β2 receptor. J Pharmacol Exp Ther 276: 289–297.

Gotti C, Moretti M, Meinerz NM, Clementi F, Gainarri A, Collins AC et al. (2008). Partial deletion of the nicotinic cholinergic receptor α4 or β2 subunit genes changes the acetylcholine sensitivity of receptors mediated ^{86}Rb$^+$ efflux in cortex and thalamus and alters relative expression of α4 and β2 subunits. Mol Pharmacol 73: 1796–1807.

Grady SR, Wageman CR, Patzlaff NE, Marks MJ (2012). Low concentration of nicotine differentially desensitize nicotinic acetylcholine receptors that include α5 or α6 subunits and that mediate synaptosomal neurotransmitter release. Neuropharmacology 62: 1935–1943.

Harpsøe K, Ahring PK, Christensen JK, Jensen ML, Peters D, Balle T (2011). Unraveling the high- and low-sensitivity agonist responses of nicotinic acetylcholine receptors. J Neurosci 31: 10759–10766.

Jha A, Auerbach A (2010). Acetylcholine receptor channels activated by a single agonist molecule. Biophys J 98: 1840–1846.

Kuryatov A, Olale FA, Choi C, Lindstrom J (2000). Acetylcholine receptor extracellular domain determines sensitivity to nicotine-induced inactivation. Eur J Pharmacol 393: 11–21.

Lester RAJ (2004). Activation and desensitisation of heteromeric neuronal nicotinic receptors: implications for non-synaptic transmission. Bioorg Med Chem Lett 14: 1897–1900.

Mantione E, Micheloni S, Alcaino C, New K, Mazzaferro S, Bermudez I (2012). Allosteric modulators of α4β2 nicotinic acetylcholine receptors: a new direction for antidepressant drug discovery. Future Med Chem 4: 2217–2230.

Marks MJ, Whiteaker P, Calcaterra J, Stitzel JA, Bullock AE, Grady S et al. (1999). Two pharmacologically distinct components of

nicotinic receptor-mediated rubidium efflux in mouse brain require the β2 Subunit. J Pharmacol Exp Ther 289: 1090–1103.

Marks MJ, Meinerz NM, Brown RW, Collins AC (2010). ^{86}Rb$^+$ efflux mediated by α4β2*-nicotinic acetylcholine receptors with high and low-sensitivity to stimulation by acetylcholine display similar agonist-induced desensitisation. Biochem Pharmacol 15: 1238–1251.

Matsushima N, Hirose S, Iwata H, Fukuma G, Yonetani M, Nagayama C et al. (2002). Mutation (ser28Leu of neuronal nicotinic acetylcholine receptor α4 subunit associated with frontal lobe epilepsy causes faster desensitization of the rat receptor expressed in oocytes. Epilepsy Res 48: 181–186.

Mazzaferro S, Benallegue N, Carbone A, Gasparri F, Vijayan R, Biggin PC et al. (2011). Additional acetylcholine (ACh) binding site at α4(+)/α4(–) interface of (α4β2)$_2\alpha$4 nicotinic receptor influences agonist sensitivity. J Biol Chem 286: 31043–31054.

Moroni M, Zwart R, Sher E, Cassels BK, Bermudez I (2006). α4β2 nicotinic receptors with high and low acetylcholine sensitivity: pharmacology, stoichiometry, and sensitivity to long-term exposure to nicotine. Mol Pharmacol 70: 755–768.

Moroni M, Vijayan R, Carbone A, Zwart R, Biggin PC, Bermudez I (2008). Non-agonist-binding subunit interfaces confer distinct functional signatures to the alternate stoichiometries of the α4β2 nicotinic receptor: an alpha4-alpha4 interface is required for Zn^{2+} potentiation. J Neurosci 28: 6884–6894.

Nelson ME, Kuryatov A, Choi CH, Zhou Y, Lindstrom J (2003). Alternate stoichiometries of α4β2 nicotinic acetylcholine receptors. Mol Pharmacol 63: 332–341.

Paradiso KG, Steinbach JH (2003). Nicotine is highly effective at producing desensitisation of rat α4β2 neuronal nicotinic receptors. J Physiol 553: 857–871.

Rayes D, De Rosa MJ, Sine S, Bouzat C (2009). Number and locations of agonist binding sites required to activate homomeric Cys-loop receptors. J Neurosci 29: 6022–6032.

Rode F, Munro G, Holst D, Nielsen EØ, Troelsen KB, Timmermann DB et al. (2012). Positive allosteric modulation of α4β2 nAChR agonist induced behaviour. Brain Res 1458: 67–75.

Steinbach JH (1990). Mechanism of action of the nicotinic acetylcholine receptor. Ciba Found Symp 152: 53–67.

Taly A, Corringer P-J, Guedin D, Lestage P, Changeux J-P (2009). Nicotinic receptors: allosteric transitions and therapeutic targets in the nervous system. Nat Rev Drug Discov 8: 733–750.

Tapia L, Kuryatov A, Lindstrom J (2007). Ca^{2+} permeability of the (α4)$_3$(β2)$_2$ stoichiometry exceeds that of (α4)$_2$(β2)$_3$ human acetylcholine receptors. Mol Pharmacol 71: 769–776.

Timmermann DB, Sandager-Nielsen K, Dyhring T, Smith M, Jacobsen AM, Nielsen EO et al. (2012). Augmentation of cognitive function by NS9283, a stoichiometry-dependent positive allosteric modulator of α2- and α4-containing nicotinic acetylcholine receptors. Br J Pharmacol 167: 164–182.

Xiu X, Puskar NL, Shanata JA, Lester HA, Dougherty DA (2009). Nicotine binding to brain receptors requires a strong cation-pi interaction. Nature 458: 534–537.

Zhang J, Xue P, Whiteaker P, Li C, Wu W, Shen B et al. (2011). Desensitisation of α7 nicotinic receptors is governed by coupling strength relative to gate tighness. J Biol Chem 286: 25331–25340.